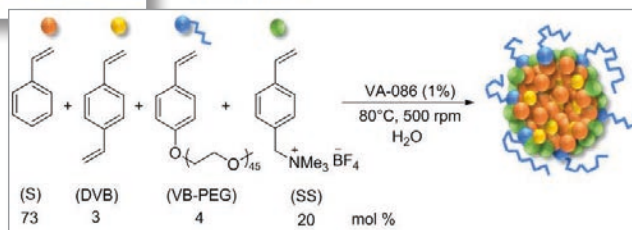
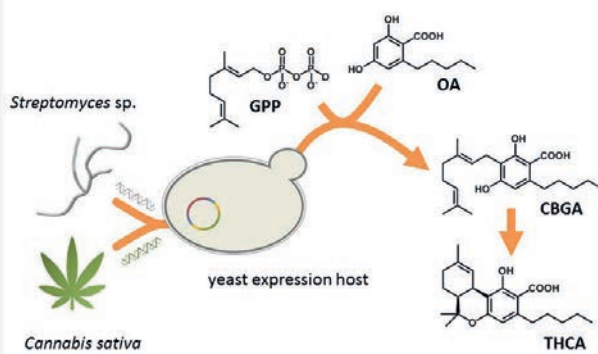
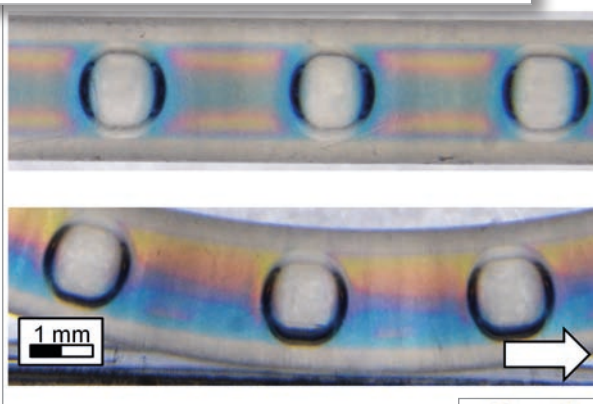
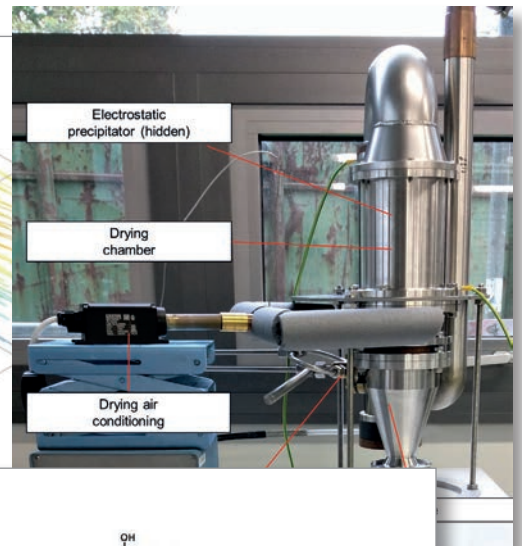
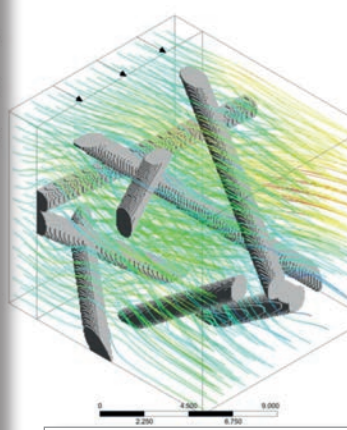
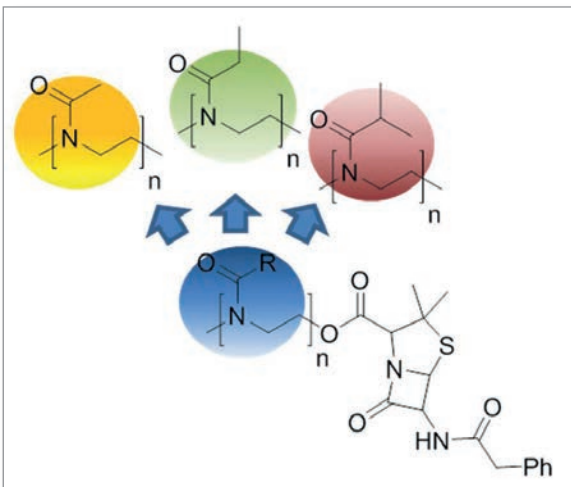


2017

SCIENTIFIC HIGHLIGHTS Annual Report



Content

Department of BCI	4
Preface	5
Equipment Design (AD)	6
Process Intensification of Catalytic Processes and Multiphase Flow Devices	7
Optimal Micronozzle Design for Energy Effective Bubble Breakup	8
Local Gas-Liquid Mass Transfer in Straight and Coiled Capillaries	9
Gas-liquid-solid flow in Coiled Flow Inverters CFI	10
Hydrodynamics and Mass Transfer in DN32 Stirred-Pulsed Extraction Column	11
Modular Equipment and Module-Based Process Design	12
Publications 2017 - 2015	13
Plant and Process Design (APT)	16
Generation of an Equipment Module Database for Heat Exchangers by Cluster Analysis of Industrial Applications	17
Discrimination of Single Particles, Agglomerates, and Air Bubbles using a Linear and Non-Linear Classifier	18
Publications 2017 - 2015	19
Biomaterials and Polymer Science (BMP)	22
Ultrafast-Swelling, Superabsorbing, Antimicrobial Hydrogels	23
Telechelic, Antimicrobial Hydrophilic Poly(ethylene imines)	24
Penicillin with a Polymer Tail for Combating Resistant Mechanism	25
Entropically driven Polymeric Enzyme Inhibitors by End-Group Conjugation	26
Biaxial Orientation upon Uniaxial Stretching	27
Publications 2017 - 2015	28
Bioprocess Engineering (BPT)	30
<i>In vitro</i> Protein Synthesis for Biocatalyst Development	31
Publications 2017 - 2015	32
Biochemical Engineering (BVT)	34
Process Improvement of fermentative Fusicoccadiene Production	35
Foam Adsorption as a new Generation unit Operation for recovery of Amphiphilic Compounds	36
Publications 2017 - 2015	37
Chemical Reaction Engineering (CVT)	38
Flexible Adjustment of liquid-liquid slug length in Micro-Channels	39
Selective Partial Oxidation of Hydrogen Sulfide via BrOx Cycle	40
Theoretical and Experimental Studies on Reactors for the high Temperature Methane Pyrolysis	41
Publications 2017 - 2015	42
Process Dynamics and Operations (DYN)	44
Application of Iterative Real-time Optimization in an Industrial Pilot Plant	45
Real-time Optimization of Chemical Processes under Uncertainty - Proof of Concept in a Miniplant	46
Economics Optimizing Control of a Pilot-Scale Reactive Distillation Process	47
Publications 2017 - 2015	48

Content

Solids Process Engineering (FSV)	54
Scaling Strategies for Twin Screw Extrusion	55
Influence of Slicing Parameters on Properties of 3D Printed Products	56
Preparation of Submicron Particles by Spray Drying	57
Publications 2017 - 2015	58
Fluid Separations (FVT)	60
Additive Manufacturing of Packings for Rotating Packed Bed	61
A Systematic Approach towards Synthesis and Design of Pervaporation-Assisted Separation Processes	62
Publications 2017 - 2015	63
Fluid Mechanics (SM)	66
Filling Flow into thin Porous Media	67
Pressure Drop in Fibrous Filters	68
Experimental Analysis of Bubble-Entrapment during Droplet Impact on solid Walls	69
Publications 2017 - 2015	70
Technical Biochemistry (TB)	72
Engineering Yeasts as Platform Organisms for Cannabinoid Biosynthesis	73
Publications 2017 - 2015	74
Technical Biology (TBL)	76
Rewiring Natural Product Biosynthesis	77
Exploration of Novel Biological Resources	78
Publications 2017 - 2015	79
Technical Chemistry (TC)	80
Isomerizing Hydroformylation of Unsaturated Ester Compounds	81
Recycling of Homogeneous Catalysts in Reactive Ionic Liquids – Solvent-Free Aminofunctionalizations of Alkenes	82
Process Development of the Continuously Operated Synthesis of <i>N,N</i> -Dimethylformamide Based on Carbon Dioxide	83
Selective Product Crystallization for Sustainable Recycling of Homogeneous Catalyst	84
Micelle-Like Polymer Particles – Phase Transfer Agents in Aqueous Multiphasic Hydroformylation of 1-octene	85
Continuously Operated Hydroamination – Toward High Catalytic Performance <i>via</i> Organic Solvent Nanofiltration in a Membrane Reactor	86
Publications 2017 - 2015	87
Thermodynamics (TH)	90
Modeling Mixtures of Long-Chain Hydrocarbons and Water Using PC-SAFT	91
Selecting Best Polymeric Excipients for Amorphous Solid Dispersions	92
Crystallization Kinetics in Pharmaceutical Formulations	93
Excipients for High-Concentration Biopharmaceutical Formulations	94
Reaction Equilibria and Reaction Kinetics of an Enzyme-Catalyzed Reaction	95
New Experimental Melting Properties for Predicting Amino-Acid Solubility	96
Publications 2017 - 2015	97



Department of BCI

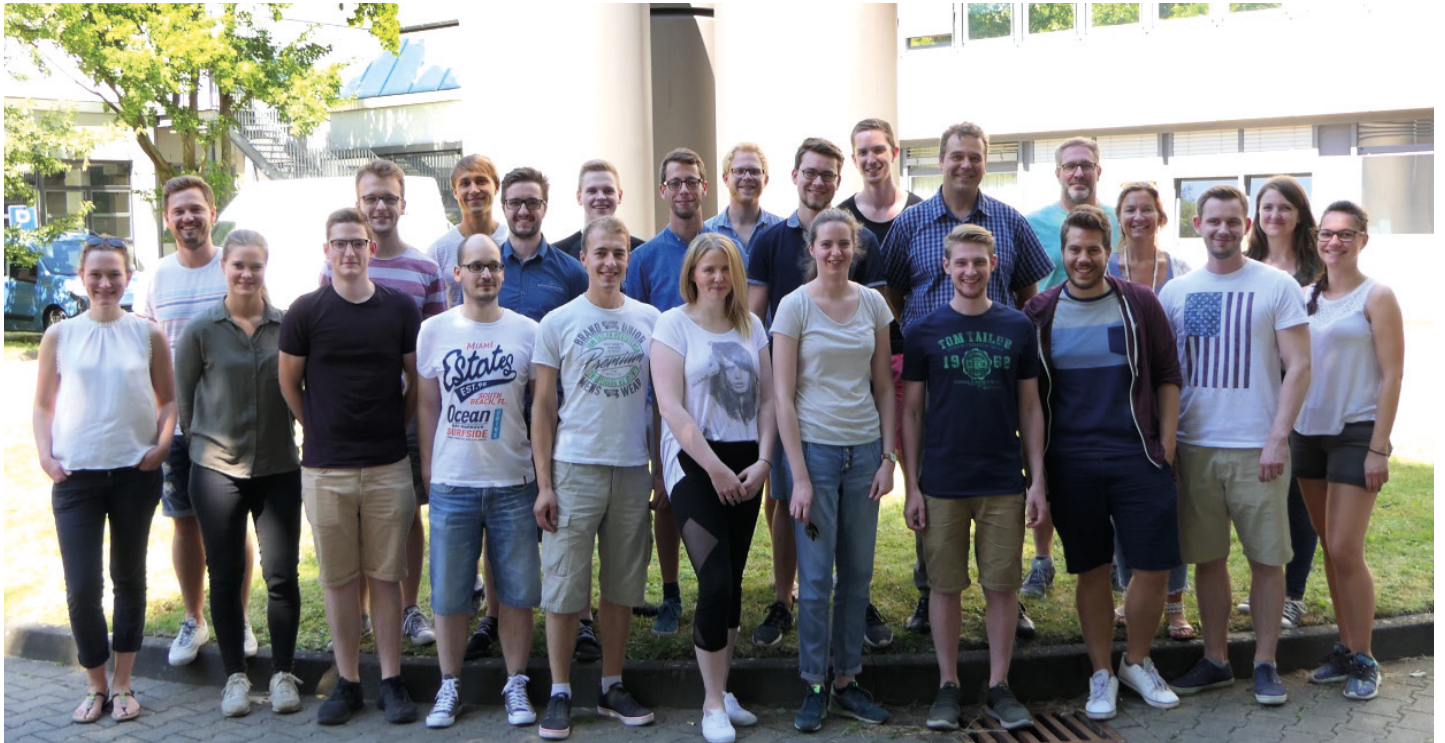
Preface

Dear Reader,

You will find the best off of the scientific work of the Department of Biochemical and Chemical Engineering (BCI) from the year 2017 on the following pages. The modern scientific methods, the broad faculty with mixed natural scientists and engineers, and the excellent equipment enable us to perform cutting edge research, which is one of the great benefits to our well educated Master and Bachelor absolvents, PhD students, and Postdocs. It is also a platform for collaborations with academic and industry partners, which are always welcome for joined research projects. Maybe you find some common interest in the following pages and join us in one way or another.

Enjoy the reading,

Joerg C. Tiller



Equipment Design (AD)

Process Intensification of Catalytic Processes and Multiphase Flow Devices

Catalytic processes as well as multiphase flow devices benefit from miniaturized equipment

Norbert Kockmann

Fluid dynamics, mixing, and heat transfer are very important for performing exothermic chemical reactions in microchannels under stable and robust conditions. However, the complex interplay of single and multiphase flow, residence time, mixing, and heat transfer with chemical kinetics has to be considered in chemical engineering tasks. Well-characterized, modular equipment can be described by short cut methods following the toolbox concept enabling consistent process development and scale up.

Research on transport phenomena in microstructured devices is increasing over the last 15 years. Profound understanding of fluid flow, residence time, mixing, and heat transfer is important for performing chemical reactions in small channels [1]. Well-characterized channel elements and coiled tubular devices are the basis for the toolbox and platform concept of a modular plant design on lab scale with consistent scale-up to higher flow rates with similar process performance. Experimental reference investigations guide the definition of dimensionless numbers, characteristic time scales, or temperature ratios for successful reactor design [2]. Similar approach is followed for separation units, e.g. a tubular device for cooling crystallization with 4 mm or a miniaturized extraction column with 15 mm inner diameter for intensified mass transfer and separation performance. Current work is focused on deeper understanding of the described phenomena regarding separation processes in miniaturized equipment [3]. The extraction column was scaled-up to a DN50 column, while the tubular device was tested with 4 mm inner diameter, then scaled up to 10 mm, and recently down to 1.6 mm.

Process Intensification (PI) aims at dramatic improvements, but also continuous improvement, in chemical processes leading to higher efficiency, lower production cost and safer, environmentally benign processes. Besides improved catalytic materials and processes, augmented transport processes, alternative energy sources, and integration/combination of various process steps are key tools of PI. Holistic design methods are required, including 'Conceive and Identify' the task, 'Design' various alternatives, 'Optimise' promising routes, 'Validate and Implement' the solution, and 'Operate' the improved plants [4]. Knowledge-based design, with help of a database and methods from process system engineering such as multiscale simulation or improved measurement and systems automation, assist the implementation into modern process design and production.

Contact:
norbert.kockmann@tu-dortmund.de

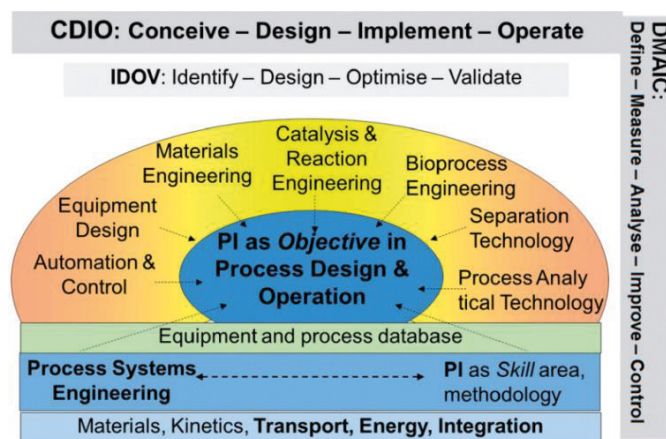


Figure 1: Process intensification as objective and methodical area integrating tools and methods. Design is facilitated with a database on equipment and processes in the framework of engineering design.

The future will bring more realised examples and success stories for process and equipment design and operation. It will be important to find the way from innovation to implementation by bridging the gap over the valley of death to innovation. As F. Keil already stated "In PI, the journey is the reward"; and so, let's proceed ...

Publications:

N. Kockmann, Transport phenomena and chemical reactions in modular microstructured devices, *Heat Transfer Engineering*, 38 (14-15), 1316-1330, 2017.

E. Mielke, P. Plouffe, N. Koushik, M. Eyholzer, M. Gottsponer, N. Kockmann, A. Macchi, D.M. Roberge, Investigation of Overall and Localized Heat Transfer in Curved Micro-Channel Reactor Systems, *Reac. Chem. & Eng.*, advance article, September 2017, DOI: 10.1039/C7RE00085E.

Vural-Gürsel, N. Kockmann, V. Hessel, Multiphase Flow in Microstructured Devices - Flow Separation Concepts and Their Integration into Process Flow Networks, *Chem. Eng. Sci.*, 169, 3-17, 2017.

S. Falß, M. Rieks, N. Kockmann, Process Intensification in Catalysis, Chap. 27 in P. Kamer, D. Vogt, J. Thybaut, (Eds), *Contemporary Catalysis*, RSC Publishing, June 2017.

Optimal Micronozzle Design for Energy Effective Bubble Breakup

Design-of-Experiment assisted evaluation of turbulent bubble flow redispersion in microchannels

Felix Reichmann, Fabian Varel, Norbert Kockmann

In recent years, gas–liquid flow in microchannels has drawn much attention in the research fields of analytics and applications, such as in oxidations or hydrogenations. Since surface forces are increasingly important on small scale, bubble coalescence is detrimental and leads to Taylor bubble flow in microchannels with relatively low surface-to-volume ratio. To overcome this limitation, the micronozzle induced bubble breakup was investigated. An optimal nozzle design for pressure drop-effective bubble breakup was found via Design-of-Experiment (DoE).

Gaseous reagents are often used in large stoichiometric excess due to insufficient interfacial mixing. Thus, extended reaction times and, consequently, prohibitively slow processes result. In microchannels, mainly Taylor bubble flow is achieved due to dominating surface forces. Here, refinement of gas–liquid dispersion using converging–diverging micronozzles has been found to be highly effective by breaking up larger bubbles into considerably smaller ones. Particularly, the turbulent bubble breakup regime, with characteristic high volumetric flow rates and Reynolds numbers in the continuous liquid phase, results into small daughter bubbles featuring a narrow size distribution (Figure 1). Bubbly flow regime presents highest interfacial area per unit volume compared to the other flow regimes existing in gas–liquid flow.

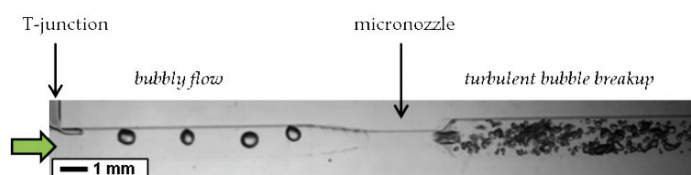


Figure 1: Turbulent mother bubble breakup into numerous daughter bubbles with narrow size distribution in a converging-diverging micronozzle, $Re_{nozzle} = 3732$.

Although high flow rates lead to small daughter bubbles, they also result in high pressure losses. In particular, the nozzle geometry takes influence on flow detachment and eddy generation in the diverging part. Thus, a compromise between pressure drop and bubble size has to be found and had been attended to in a DoE. Here, the hydraulic diameter of smallest cross section, the length of the smallest cross section, outlet angle, hydraulic diameter of the downstream channel, and the volumetric flow rate were implemented to find optimal parameter settings for an energy effective turbulent bubble breakup. The influence

of single parameters and their interactions on pressure drop and daughter bubble size were investigated regarding their significance in a Pareto diagram of effects. Highest impact on pressure drop and bubble size was found for the hydraulic diameter of the smallest cross section.

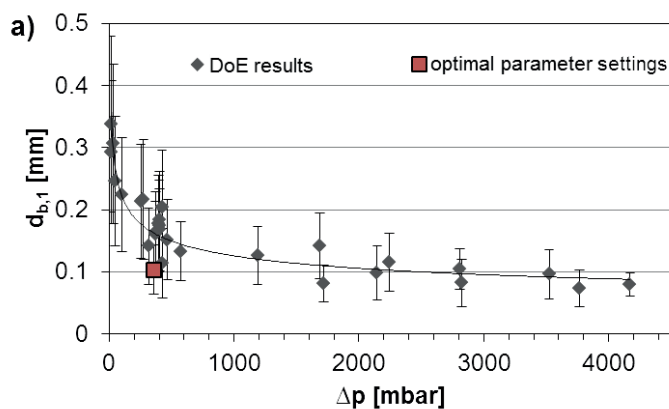


Figure 2: Daughter bubble size in dependence of the pressure drop from the Design of Experiment (grey diamond symbols). Experiment with optimal parameter setting is marked red.

After factor optimization regarding both output variables, an optimal nozzle design was obtained, manufactured, and tested. Figure 2 shows the results of all performed experiment within the DoE and the results from the experiment employing the optimal parameter setting. Obviously, small daughter bubble diameters are achieved at high pressure loss due to the asymptotic behavior of the trend line. The result of the optimal parameter setting experiment is right at the steep decline of the trend line. With a low pressure drop of 250 mbar, a daughter bubble diameter of 100 μm is obtained.

The optimal nozzle design can now be used for chemical gas–liquid reaction in order to attain high interfacial areas for intensified mass transfer and increased conversions.

Publications:

F. Reichmann, F. Varel, N. Kockmann, Processes, DOI:10.3390/pr5040057.

F. Reichmann, M.-J. Koch, S. Körner, N. Kockmann, Proceedings of the ASME2017 15th ICNMM, DOI:10.1115/ICNMM2017-5545.

F. Reichmann, M.-J. Koch, N. Kockmann, Proceedings of the ASME2017 15th ICNMM, DOI: 10.1115/ICNMM2017-5540.

Contact:

felix.reichmann@tu-dortmund.de

norbert.kockmann@tu-dortmund.de

Local Gas-Liquid Mass Transfer in Straight and Coiled Capillaries

Superposition of Taylor and Dean Flow and the Effect on Mass Transfer with Chemical Reaction

Waldemar Krieger, Norbert Kockmann

Microreactors are used to enhance heat and mass transfer overcoming mass transfer limitations in gas-liquid reactions. This influence can be further increased by employing coiled capillaries, which induce Dean vortices and improve radial mixing. In this work, a colorimetric technique is proposed in order to visualize local mass transfer phenomena and concentration distributions with high spatial and temporal resolution. Further, this method enables the local investigation of selectivity for gas-liquid reactions, which is a major topic in current research.

Mass transfer studies have been performed utilizing the consecutive oxidation of leuco-indigo carmine as colorimetric reaction with two distinct color changes (yellow-red-blue). This allows for comprehensive studies of local gas-liquid mass transfer and local chemical selectivity by using the information in the different color channels. Further, this technique was applied in straight and coiled capillary setups in order to study the differences in fluid dynamics, mass transfer and chemical selectivity. Slug flow was generated by means of a hypodermic needle, which was positioned at the center of an FEP tube through a T-junction ensuring stable bubble generation with low mass transfer contribution.

Higher conversions are achieved in coiled capillary due to enhanced radial mixing, which agrees with experimental investigations in coiled tubes from literature. On the other hand, selectivity related to the intermediate is higher in straight capillary, due to a lower degree of mixing compared to coiled capillaries (Figure 1).

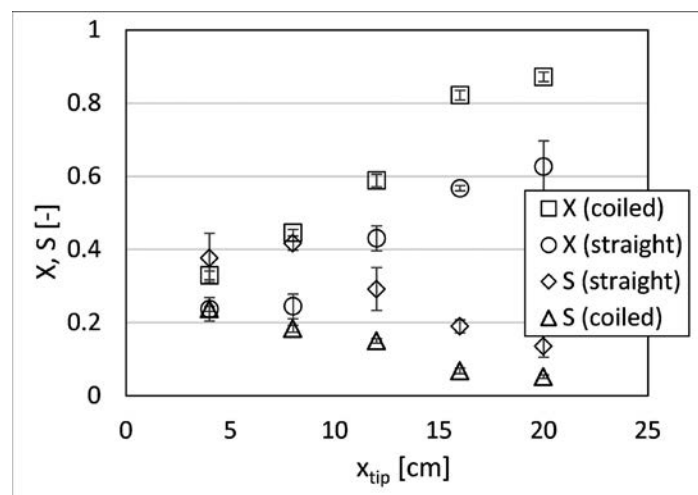


Figure 1: Comparison of conversion and selectivity of leuco-indigo carmine oxidation in straight and coiled capillary.

Very short reaction times in the order of a few milliseconds lead to fast oxidation of the intermediate in areas with increased oxygen concentration. Hence, elevated intermediate concentrations are only observed in areas of limited oxygen access (Figure 2). These areas occupy a larger volume fraction in the straight capillary, which results in a higher intermediate selectivity.

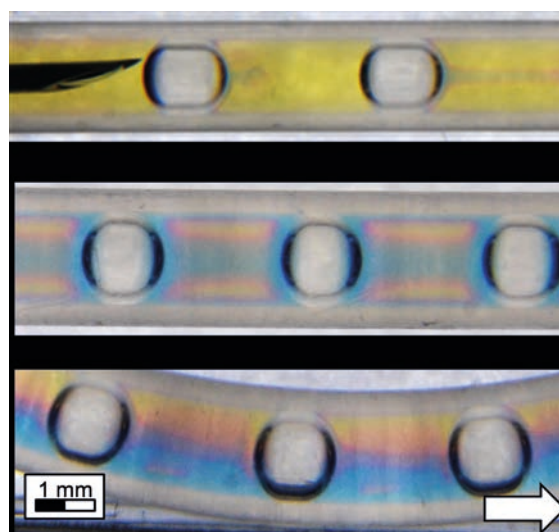


Figure 2: Oxidation of leuco-indigo carmine in straight and coiled capillary.

This work provides a non-invasive tool that can be used to characterize gas-liquid contactors in terms of mass transfer and chemical selectivity. Such information is valuable for the still challenging scale-up of gas-liquid processes and the development of theoretical models and numeric simulations. In future work, local quantitative mass transfer and selectivity studies will be carried out for varying process parameters in order to obtain a deeper understanding of flow structure and mass transfer in coiled capillaries and tubes.

Contact:

waldemar.krieger@tu-dortmund.de
norbert.kockmann@tu-dortmund.de

Publications:

W. Krieger, J. Lamsfuß, N. Kockmann, Method to visualize local mass transfer and chemical selectivity of gas-liquid reaction in coiled capillaries, ASME-ICNMM, 2017, DOI:10.1115/ICNMM2017-5538.
W. Krieger, J. Lamsfuß, W. Zhang, N. Kockmann, Local Mass, Transfer Phenomena and Chemical Selectivity of Gas-Liquid Reactions in Capillaries, Chem. Eng. & Technol., 40(11) 2134-2143, 2017, DOI 10.1002/ceat.201700420.

Gas-liquid-solid flow in Coiled Flow Inverters CFI

The helical structure enables multiphase flow processes under controlled conditions

Safa Kutup Kurt, Krishna D.P. Nigam, Norbert Kockmann

In various studies, a helically coiled tubular device with many 90° bends, called Coiled Flow Inverter CFI, was developed with robust and simple fabrication performing in multiphase reaction systems. The modular CFI is investigated in the production of uniform microscale particles with large throughput in continuous mode operation. A design method is proposed for narrow residence time distribution particularly for laminar flow conditions.

Curved microchannels and capillaries provide enhanced heat and mass transport due to their controllable flow patterns and high surface to volume ratio. Gas-liquid slug flow observations revealed that the Taylor vortices are influenced by secondary flow due to the centrifugal force acting perpendicular to the flow direction. Hence, mixing inside the liquid slug is enhanced by the combination of Dean and Taylor vortices in helically coiled tubular device (HCTD). The modular design of a specific type of HCTD, that is, the coiled flow inverter (CFI) is elucidated by the representation of a new design space diagram. Continuous precipitation of calcium carbonate (CaCO_3) was investigated for modular CFI made of polyvinyl chloride (PVC) tubes ($d_i = 3.2$ mm) with slug flow patterns. CaCO_3 was continuously precipitated along CFI with a conversion of ca. 90%. CFI provided a narrower particle size distribution with mean particle diameters around 28 μm and more uniform morphology in comparison to a batch reactor.

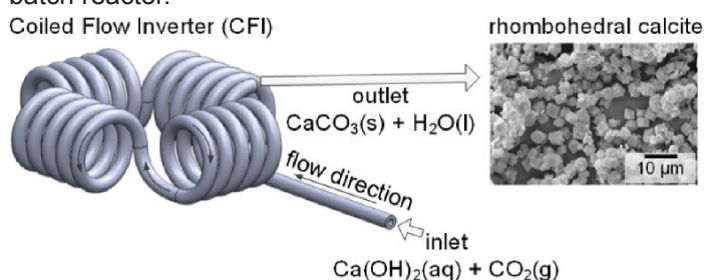


Figure 1: CFI setup with calcium carbonate formation.

A model for the simulation of mass transfer in a liquid/liquid plug flow in a microcapillary reactor is very useful for mass performance prediction. Starting from the interface tracking method, the modeling is carried out in separate form-adapted coupled computing areas on the basis of an imported interface topology. Experimental investigations are carried out with a standard reaction and extraction system.

Summarizing, the CFI device can provide enhanced radial mixing due to the secondary flow profiles and their inversion with 90° bends in the case of G-L slug flow patterns. The three main topics were studied for the first time in this work, that is, the particle tracking in a G-L slug flow within a HCTD, the design and implementation of a modular CFI reactor, and the continuous precipitation of the calcium carbonate.

A comprehensive way to design a modular CFI was developed providing a wide range of residence times displayed in a design space diagram (DSD) for the different volumetric flow rates. The DSD simplifies the selection of the geometrical design parameters of a CFI ensuring enhanced radial mixing by considering the process conditions and physical properties of the fluids.

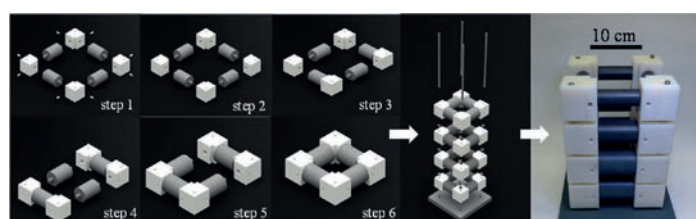


Figure 2: Modular CFI design for stack-wise setup.

Finally, a modular, continuously operated tubular reactor concept, that is, CFI with a robust and an easy fabrication was proposed in the content of this work for the multiphase reaction systems. Standard coil diameter enables rapid design on this flexible, multipurpose equipment for various process tasks.

Publications:

S.K. Kurt, M. Akhtar, K.D.P. Nigam, N. Kockmann, *Ind. Eng. Chem. & Res.*, 56 (39) 11320–11335, 2017.

C. Heckmann, S.K. Kurt, N. Kockmann, P. Ehrhard, *Chem. Ing. Technik*, 89 (12), 1642-1649, 2017.

S.K. Kurt, F. Warnebold, K.D.P. Nigam, N. Kockmann, *Chem. Eng. Sci.*, 169, 164-178, 2017.

Contact:

norbert.kockmann@tu-dortmund.de

Hydrodynamics and Mass Transfer in DN32 Stirred-Pulsed Extraction Column

Process intensification of counter-current extraction in columns through application of two energy inputs

Sebastian Soboll, Isabel Hagemann, Norbert Kockmann

In order to intensify extraction processes in extraction columns, a novel column type was designed, which combines two different energy inputs, stirring and pulsation. After successfully characterizing a stirred-pulsed column with 15 mm inner diameter, a 32 mm inner diameter (DN32) column was designed and investigated. Compared to conventional extraction columns, the DN32 stirred-pulsed column provides a much higher separation performance.

The DN32 column was investigated regarding hydrodynamic behavior and mass transfer performance. The flooding point is an important hydrodynamic parameter, because it limits the maximum throughput of the apparatus. In general, the term flooding denotes the breakdown of the counter-current flow, which occurs at too high flow rates. In the DN32 column, flooding is visually detected (Fig. 1).

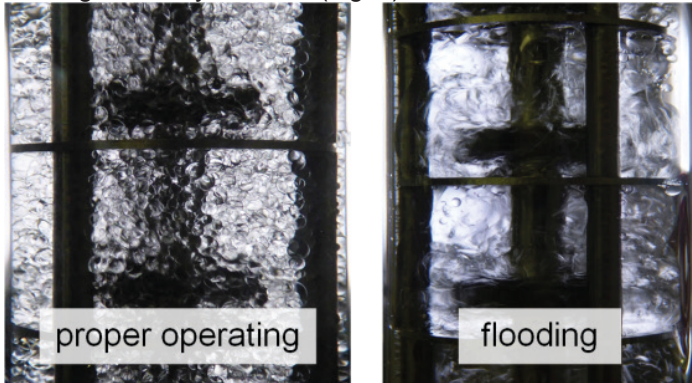


Figure 1: Pictures of the two-phase system inside the column during proper operating and during flooding.

During proper operation, the stirred cells in the column are filled with many small droplets, which are surrounded by the continuous phase. However, when the flooding point is reached, intense coalescence of the droplets at the column wall and column internals happens, leading to plugging of the column.

Determination of the flooding point is done by increasing the throughput stepwise at fixed stirrer speed and pulsation frequency until flooding behavior is visually detected. The throughput is given as loading B , which is the total ingoing volume flow rate divided by the cross sectional area of the column (Eq. 1).

$$B = \frac{\dot{V}_{in,total}}{A_{cross-section}} \quad 1$$

Flooding points B_{flood} were measured for different stirrer speeds and pulsation frequencies. As illustrated in Fig. 2, flooding occurs earlier at higher stirrer speeds, since the decreased droplet size leads to lower rising velocities of the droplets. In contrast, raising the pulsation frequency results

in higher flooding points, because pulsation helps to transport the droplets through the trays, which are mounted in the column.

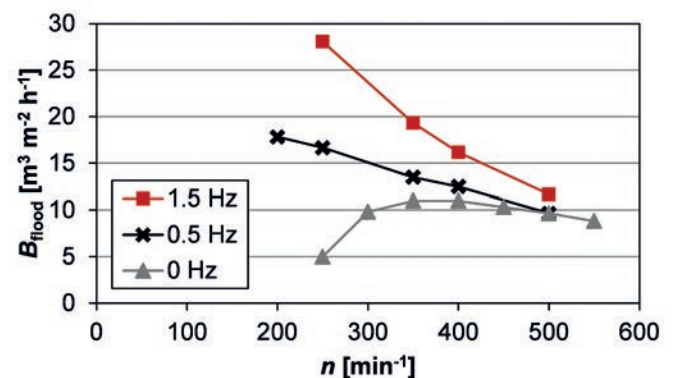


Figure 2: Flooding loading for different stirrer speeds and pulsation frequencies.

As a measure for the mass transfer performance, the number of theoretical stages per meter of column height is applied. The number of stages is determined via mass transfer experiments and a McCabe Thiele stage construction. Highest extraction performance is achieved with low or medium stirrer speeds at high pulsation frequencies (Fig. 3). In comparison with a conventional stirred extraction column of type Kühni, the stirred-pulsed column provides a much higher separation performance.

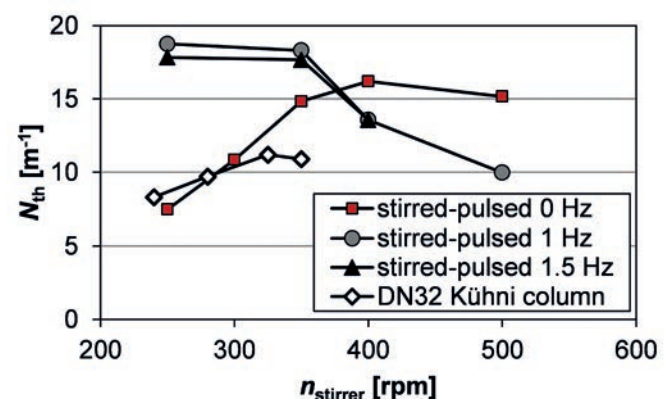


Figure 3: Extraction performance of stirred-pulsed column compared with performance of a comparable Kühni column (Kühni column data from P. Kolb, PhD Thesis, TU Kaiserslautern, 2004).

Contact:

sebastian.soboll@tu-dortmund.de
norbert.kockmann@tu-dortmund.de

Publications:

S. Soboll, I. Hagemann, N. Kockmann, Performance of Laboratory-Scale Stirred-Pulsed Extraction Columns with Different Diameters, Chem. Ing. Technik, 89 (12), 1611-1618, 2017.

Modular Equipment and Module-Based Process Design

Module-based plant design enables shorter time-to-market by reuse of engineering effort

Norbert Kockmann, Lukas Hohmann, Christoph Fleischer-Trebes, Gerhard Schembecker, Christian Bramsiepe

The database with modules and module-based methods are essential for rapid process development and market supply. Modular plant components with defined interfaces and performance are key components of multipurpose, small-scale, continuously operated processes. A toolbox of chemical equipment enables rapid process development and small-scale production. Examples demonstrated shorter development time up to 50% and 10% for energy or material consumption.

Modularly built production plants are considered for planning new chemical plants, in case they shall be designed quickly and transformable, flexible plants are required. This contribution summarizes the module based planning approach, which allows for structured planning of new modular plants in a time-efficient way. All required documents for building modules are stored in the Process Equipment Design PED documentation, which is available for re-use in future projects (Fig. 1).

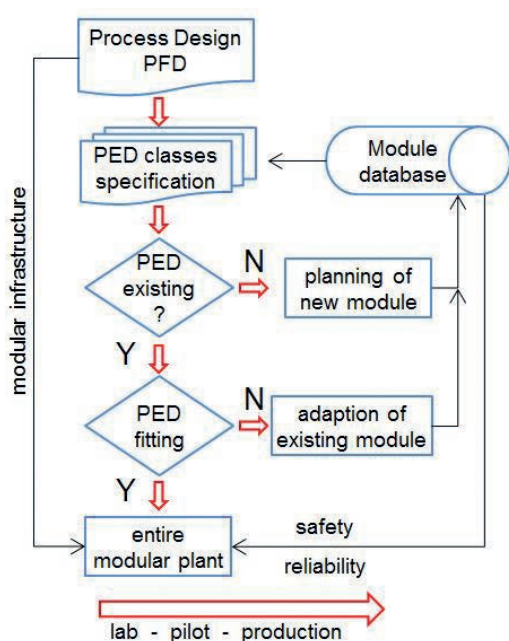


Figure 1: Module-based planning process from PFD to production plant with module database.

Stepwise process development with experience from module database starting from conceptual design and feasibility study, optimization study to long run studies for a robust process leading to production campaigns. A lot of information from two research groups at BCI, TU Dortmund University in close collaboration with INVITE in Leverkusen went into the DECHEMA white paper on Modular Plants (<http://dechema.de/2017+2+White+Paper+Modular+Plants.html>).

A process module has defined interfaces and well characterized, qualified operating range stored in an information data base. The modular toolbox of plate and tubular reactor, stirred vessel, and columns is the base of devices on different platform levels. This enables a flexible assembly for rapid continuous-flow process development with a wide range of throughput and application (Fig. 2).

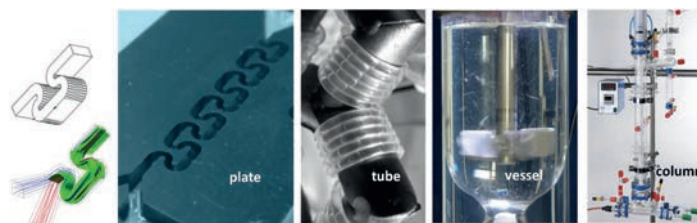


Figure 2: Equipment toolbox from channel element design with simulation results to geometrical realization of miniaturized channels on a plate; coiled tubes with internal bends; stirred vessels, counter-current flow column for separation purposes.

A stage-gate process including conceptual process design and basic engineering phase minimizes the risk of failure and development effort. Detail engineering effort leads to qualified module templates and devices serving a wide process window and enabling multipurpose plants. The development process is shown in Fig. 1. With this setup, the basic engineering happens in the early phase of process development, while detail engineering data is stored in the database. With the current setup, a continuously operating chemical process can be setup in the lab or pilot plant with existing modules in very short time. The scale-up process is quite straight forward with known characteristics of the equipment with their analogues on larger scale.

Publications:

C. Fleischer, N. Krasberg, C. Bramsiepe, N. Kockmann, Chemie Ingenieur Technik, 89 (6) 785-799, 2017.

L. Hohmann, K. Kössl, N. Kockmann, G. Schembecker, C. Bramsiepe, Chem. Eng. Proc.: PI, 111, 115-126, 2017.

N. Kockmann, Modular equipment and continuous process development for small-scale production plants, Chemistry Today, vol. 35 (4), 33-35, July/August 2017.

N. Kockmann, P. Thenée, C. Fleischer, G. Laudadio, T. Noel, Reaction Chemistry & Engineering, 2, 258-280, 2017, DOI: 10.1039/C7RE00021A.

Contact:
norbert.kockmann@tu-dortmund.de

Publications 2017 - 2015

2017

- S.K. Kurt, M. Akhtar, K.D.P. Nigam, N. Kockmann
Gas - Liquid - Solid Flow Profile and Reactive Particle Precipitation in a Modular Coiled Flow Inverter
Industrial & Engineering Chemistry Research 56 (39) 11320–11335 (2017)
- W. Krieger, J. Lamsfuß, W. Zhang, N. Kockmann
Local Mass Transfer Phenomena and Chemical Selectivity of Gas-Liquid Reactions in Capillaries
Chemical Engineering & Technology 40 (11) 2134-2143 (2017)
- F. Reichmann, S. Millhoff, Y. Jirmann, N. Kockmann
Reaction Calorimetry for Exothermic Reactions in Plate-Type Microreactors Using Seebeck Elements
Chemical Engineering & Technology 40 (11) 2144-2155 (2017)
- E. Mielke, P. Plouffe, N. Koushik, M. Eyholzer, M. Gottsponer, N. Kockmann, A. Macchi, D.M. Roberge
Investigation of Overall and Localized Heat Transfer in Curved Micro-Channel Reactor Systems
Reaction Chemistry & Engineering 2, 763-775 (2017)
- S. Soboll, I. Hagemann, N. Kockmann
Performance of Laboratory-Scale Stirred-Pulsed Extraction Columns with Different Diameters
Chemie Ingenieur Technik 89 (12), 1611-1618 (2017)
- C. Heckmann, S.K. Kurt, N. Kockmann, P. Ehrhard
Simulation und Validierung der Pfropfenströmung im Kanal mit Stofftransport
Chemie Ingenieur Technik 89 (12), 1642-1649 (2017)
- F. Reichmann, F. Varel, N. Kockmann
Energy Optimization of Gas-Liquid Dispersion in Micronozzles Assisted by Design of Experiment
Processes, 2017, paper 229828; DOI:10.3390/pr5040057
- N. Kockmann
Modular equipment and continuous process development for small-scale production plants
Chemistry Today 35 (4), 33-35 (2017)
- N. Kockmann, P. Thenée, C. Fleischer, G. Laudadio, T. Noel
Safety Assessment in Development and Operation of Modular Continuous-Flow Processes
Reaction Chemistry & Engineering 2, 258-280 (2017)
- I. Vural-Gürsel, N. Kockmann, V. Hessel
Multiphase Flow in Microstructured Devices - Flow Separation Concepts and Their Integration into Process Flow Networks
Chemical Engineering Science 169, 3-17 (2017)
- C. Fleischer, N. Krasberg, C. Bramsiepe, N. Kockmann
Modulbasierter Planungsansatz für kontinuierlich betriebene Kleinanlagen
Chemie Ingenieur Technik 89 (6), 785-799 (2017)
- S.K. Kurt, F. Warnebold, K.D.P. Nigam, N. Kockmann
Gas-Liquid Reaction and Mass Transfer in Microstructured Coiled Flow Inverter
Chemical Engineering Science 169, 164-178 (2017)
- L. Hohmann, K. Kössl, N. Kockmann, G. Schembecker, C. Bramsiepe
Modules in Process Industry - A life cycle definition
Chemical Engineering & Processing: Process Intensification 111, 115-126 (2017)
- F. Reichmann, A. Tollkötter, S. Körner, N. Kockmann
Gas-Liquid Dispersion in Micronozzles and Microreactor Design for High Interfacial Area
Chemical Engineering Science 169, 151-163 (2017)
- N. Kockmann
Transport phenomena and chemical reactions in modular microstructured devices
Heat Transfer Engineering 38 (14-15), 1316-1330 (2017)

Proceedings & Book Chapters

- F. Reichmann, M. Koch, S. Körner, N. Kockmann
Internal Jet Formation During Bubble Generation in Microchannels
Proc. ASME 2017 15th Intl. Conf. Nanochannels, Microchannels, and Minichannels, ASME-ICNMM2017-5545, Cambridge, USA, August 27-31 (2017)
- F. Reichmann, M. Koch, N. Kockmann
Investigation of Bubble Breakup in Laminar, Transient, and Turbulent Regime Behind Micronozzles
Proc. ASME 2017 15th Intl. Conf. Nanochannels, Microchannels, and Minichannels, ICNMM2017-5540, Cambridge, USA, August 27-31 (2017)
- F. Reichmann, S. Millhoff, N. Kockmann
Seebeck Calorimeter for the Characterization of Highly Exothermic Reactions in a Microreactor Made of PVDF-Foils
Proc. ASME 2017 15th Intl. Conf. Nanochannels, Microchannels, and Minichannels, ICNMM2017-5539, Cambridge, USA, August 27-31 (2017)
- W. Krieger, J. Lamsfuß, N. Kockmann
Method To Visualize Local Mass Transfer And Chemical Selectivity Of Gas-Liquid Reaction In Coiled Capillaries
Proc. ASME 2017 15th Intl. Conf. Nanochannels, Microchannels, and Minichannels, ICNMM2017-5538, Cambridge, USA, August 27-31 (2017)
- S. Falß, M. Rieks, N. Kockmann
Process Intensification in Catalysis
in P. Kamer, D. Vogt, J. Thybaut, (Eds), Contemporary Catalysis, RSC Publishing, June 2017

2016

- L. Hohmann, K. Kössl, N. Kockmann, G. Schembecker, C. Bramsiepe
Modules in Process Industry - A life cycle definition
Chemical Engineering & Processing: PI, DOI: 10.1016/j.cep.2016.09.017, (2016)
- F. Reichmann, A. Tollkötter, S. Körner, N. Kockmann
Gas-Liquid Dispersion in Micronozzles and Microreactor Design for High Interfacial Area
Chemical Engineering Science, DOI: 10.1016/j.ces.2016.10.028, (2016)
- F. Braun, S. Schwolow, J. Seltenreich, N. Kockmann, T. Röder, N. Gretz, M. Rädle
Highly sensitive Raman spectroscopy with low laser power for fast in-line reaction and multiphase flow monitoring
Analytical Chemistry, 88 (19), 9368-9374 (2016)
- L. Hohmann, S.K. Kurt, S. Soboll, N. Kockmann
Separation Units and Equipment for Lab-Scale Process Development
J. Flow Chemistry, 6 (3), 181-190 (2016)
- S. Schwolow, A. Neumüller, L. Abahmane, N. Kockmann, T. Röder
Design and application of a millistructured heat exchanger reactor for an energy-efficient process
Chemical Engineering & Processing: PI, 108, 109-116 (2016)
- L. Hohmann, R. Gorny, O. Klaas, J. Ahlert, K. Wohlgemuth, N. Kockmann
Design of a Continuous Tubular Cooling Crystallizer for Process Development on Lab-scale
Chemical Engineering & Technology, 39(7), 1268-1280 (2016)
- N. Kockmann
Modular Equipment for Chemical Process Development and Small-scale Production in Multipurpose Plants
ChemBioEng Reviews, 3 (1), 5-15 (2016)
- R. Trostorf, N. Kockmann
Methodik zur einfachen Standardisierung von Probenahmesystemen auf Basis der beteiligten Fluidphasen
Chemie - Ingenieur - Technik, 88 (1-2), 128-138 (2016)
- A. Tollkötter, F. Reichmann, J. Wesholowski, F. Schirmbeck, N. Kockmann
Gas-Liquid Flow Dispersion in Micro Offices and Bubble Coalescence with High Flow Rates
J. Electronics Packaging, 138(1):011013-011013-8, EP-15-1105 (2016)
- S. Schwolow, J.Y. Ko, N. Kockmann, T. Röder
Enhanced heat transfer by exothermic reactions in laminar flow capillary reactors
Chemical Engineering Science 141, 356-362 (2016)
- N. Kockmann, P. Lutze, A. Górak
Grand Challenges and Chemical Engineering Curriculum-Developments at TU Dortmund University
Universal Journal of Educational Research 4 (1), 200-204 (2016)
- E.C. Sindermann, A. Holbach, A. de Haan, N. Kockmann
Single stage and countercurrent extraction of 5-hydroxymethylfurfural from aqueous phase systems
Chemical Engineering Journal, 283 (1), 251-259 (2016)

- S.K. Kurt, I. Vural-Gürsel, V. Hessel, K.D.P. Nigam, N. Kockmann
Liquid-Liquid Extraction System with Microstructured Coiled Flow Inverter and Other Capillary Setups for Single-Stage Extraction Applications
Chemical Engineering Journal, 283 (1), 764-777 (2016)
- I. Vural-Gürsel, S.K. Kurt, Q. Wang, T. Noël, K.D.P. Nigam, N. Kockmann, V. Hessel
Utilization of Milli-scale Coiled Flow Inverter in Combination with Phase Separator for Continuous Flow Liquid-Liquid Extraction Processes
Chemical Engineering Journal, 283 (1), 855-868 (2016)

Peer-reviewed conference papers

2016

- L. Hohmann, S.K. Kurt, N. Pouya Far, D. Vieth, N. Kockmann
Micro-/Milli-Fluidic Heat-Exchanger Characterization by Non-Invasive Temperature Sensors
Proc. ASME 2016 14th Intl. Conf. Nanochannels, Microchannels and Minichannels ICNMM2016-8008, Washington, DC, July 10-14 (2016)
- F. Reichmann, A. Tollkötter, N. Kockmann
Investigation of Bubble Break-up in Microchannel Orifices
Proc. ASME 2016 14th Intl. Conf. Nanochannels, Microchannels and Minichannels, ICNMM2016-8048, Washington, DC, July 10-14 (2016)
- S.K. Kurt, M. Akhtar, K.D.P. Nigam, N. Kockmann
Modular Concept of a Smart Scale Helically Coiled Tubular Reactor for Continuous Operation of Multiphase Reaction Systems
Proc. ASME 2016 14th Intl. Conf. Nanochannels, Microchannels and Minichannels ICNMM2016-8004, Washington, DC, July 10-14 (2016)

2015

- S. Goicoechea, E. Kraveva, S. Sokolov, M.-M. Pohl, N. Kockmann, H. Ehrich
Support effect on structure and performance of Co and Ni catalysts for steam reforming of acetic acid
Appl. Cat. A, 514, 182-191 (2015)
- S. Liao, J. Sackmann, A. Tollkötter, M. Pasterny, N. Kockmann, W.K. Schomburg
Ultrasonic fabrication of PVDF micro nozzles for generating and characterizing liquid/liquid- and gas/liquid-dispersions
Microsystems Technology, DOI: 10.1007/s00542-015-2708-z (2016)
- M. Rieks, R. Bellinghausen, N. Kockmann, L. Mleczko
Experimental study of methane dry reforming in an electrically heated reactor
Int. J. Hydrogen Energy, 40 (46), 15940-15951 (2015)
- S. Schwolow, F. Braun, M. Rädle, N. Kockmann, T. Röder
Fast and efficient acquisition of kinetic data in microreactors using in-line Raman analysis
Org. Proc. R&D, 19 (9), 1286-1292 (2015)
- A. Holbach, S. Soboll, B. Schuur, N. Kockmann
Chiral Separation of 3,5-Dinitrobenzoyl-(R,S)-Leucine in Process Intensified Extraction Columns
Ind. & Eng. Chem. Res., 54 (33), 8266-8276 (2015)
- C. Fleischer, J. Wittmann, N. Kockmann, T. Bieringer, C. Bramsiepe
Sicherheitstechnische Aspekte bei der Planung und Bau modularer Produktionsanlagen
Chemie - Ingenieur - Technik, 87 (9), 1258-1269 (2015)
- N. Kockmann
Modulare chemische Reaktoren für die Prozessentwicklung und Produktion in kontinuierlichen Mehrzweckanlagen
Chemie - Ingenieur - Technik, 87 (9), 1173-1184 (2015)
- A. Tollkötter, J. Sackmann, T. Baldhoff, W.K. Schomburg, N. Kockmann
Ultrasonic hot embossed polymer micro reactors for the optical measurement of chemical reactions
Chemical Engineering & Technology, 38 (7), 1113-1121 (2015)
- S.K. Kurt, M.G. Gelhausen, N. Kockmann
Axial Dispersion and Heat Transfer in a Milli / Microstructured Coiled Flow Inverter for Narrow Residence Time Distribution at Laminar Flow
Chemical Engineering & Technology, 38 (7), 1122-1130 (2015)
- M.G. Gelhausen, S.K. Kurt, N. Kockmann
Parametrische Empfindlichkeit einer stark exothermen Reaktion im Kapillarwendelreaktor
Chemie - Ingenieur - Technik, 87 (6), 781-790 (2015)
- A. Tollkötter, J. Sackmann, T. Baldhoff, W.K. Schomburg, N. Kockmann
Modulares Mikoreaktorsystem aus ultraschallheißgeprägten Polymerfolien
Chemie - Ingenieur - Technik, 87 (6), 823-829 (2015)
- S. Klutz, S.K. Kurt, M. Lobedann, N. Kockmann
Narrow residence time distribution in tubular reactor concept for Reynolds number range of 10-100
Chem. Eng. R&D, 95, 22-33 (2015)
- S. Goicoechea, H. Ehrich, P.L. Arias, N. Kockmann
Thermodynamic analysis of acetic acid steam reforming for hydrogen production
J. Power Sources, 279, 312-322 (2015)
- A. Holbach, J. Godde, R. Mahendrarajah, N. Kockmann
Enantioseparation of Chiral Aromatic Acids in Process Intensified Liquid-Liquid Extraction Columns
AIChE J., 61 (1), 266-276 (2015)
- N. Kockmann, P. Lütze, A. Górak
Chemical engineering curricula and challenges resulting from global megatrends, World Congress on Engineering Education 2014
QScience Proceedings: Vol. (2015)
- A. Holbach, E. Caliskan, H.S. Lee, N. Kockmann
Process Intensification in Small Scale Extraction Columns for Counter-Current Operations
Chemical Engineering & Processing: PI, 80, 21-28 (2014)
- A. Holbach, D. Jaritsch, J. Godde, N. Kockmann
Prozessentwicklung der Enantioselektiven Extraktion in miniaturisierten Laborkolonnen
Chemie - Ingenieur - Technik, 86 (5), 621-629 (2014)
- N. Krasberg, L. Hohmann, Th. Bieringer, C. Bramsiepe, N. Kockmann
Selection of technical reactor equipment for modular, continuous small scale plants
MPDI Processes, 2, 265-292 (2014)
- A. Tollkötter, N. Kockmann
Absorption and Chemisorption of a Small Levitated, Single Bubbles in Aqueous Solutions
MPDI Processes, 2, 200-215 (2014)
- N. Kockmann
200 Years in Innovation of Continuous Distillation
ChemBioEng Reviews, 1, 40-49 (2014)

Peer-reviewed conference papers

2015

- A. Tollkötter, J. Wesholowski, F. Schirmbeck, N. Kockmann
High flow rate micro orifice dispersion of gas-liquid flow
Proc. ASME 2015 13th Intl. Conf. Nanochannels, Microchannels and Minichannels, ICNMM2015-48221, San Francisco, July 6-9 (2015)
- S.K. Kurt, K.D.P. Nigam, N. Kockmann
Two-Phase Flow and Mass Transfer in Helical Capillary Flow Reactors with Alternating Bends
Proc. ASME 2015 13th Intl. Conf. Nanochannels, Microchannels and Minichannels, ICNMM2015-48416, San Francisco, July 6-9 (2015)



Plant and Process Design (APT)

Generation of an Equipment Module Database for Heat Exchangers by Cluster Analysis of Industrial Applications

Martin Eilermann, Christian Post, Dorothea Schwarz, Stephan Leufke, Gerhard Schembecker, Christian Bramsiepe

Module-based plant design opens up the opportunity for the (bio-)chemical industry to reduce lead times, which is crucial for future competitiveness. The time-consuming equipment design step is replaced by selecting the most suitable equipment module from an equipment module database so that engineering work is reused. Although of central importance in module-based plant design, an applicable equipment module database has not been developed yet. Therefore, it is the aim of this work to develop a methodology for the generation of shell and tube heat exchanger modules for an equipment module database.

In conventional planning processes, the equipment is designed individually minimizing total cost with the aid of computer software and under consideration of functional requirements, operating constraints as well as industrial standards. This conventional design process involves several iteration steps. The question is, whether an individually designed apparatus is required for every application, or whether it is possible to cover a group of similar applications with one apparatus. This idea is embraced in the concept of module-based plant design. Equipment modules are designed once such that they can cover a wide range of process conditions and applications. The time-consuming design step is replaced by selecting the most suitable equipment module from an equipment module database. Thus, the lead time can be reduced, which may offer a substantial economic benefit. Overall, it becomes clear that promising approaches in module-based plant design already exist. However, there is a lack of an applicable equipment module database from which suitable equipment modules can be selected.

To consider applications with industrial relevance in the generation of the equipment module database, heat transfer applications provided by Evonik were considered within this work. The heat transfer applications were grouped in a hierarchical clustering analysis according to a set of defining features. For each of these groups a representative heat exchanger was selected. Therefore, a set of shell and tube heat exchangers was generated applying Sobol sampling. From this set a heat exchanger was selected to be the representative, which covers most of the applications inside the considered group of process applications. For that purpose thermodynamic as well hydrodynamic operating constraints were considered. The representative heat exchangers were stored in the equipment module database. Moreover, based on the simulation results the ratio of industrial applications that can be covered by the representative heat exchangers is determined in each step. The results of this work are presented in Figure 1 distinguishing between two cases of applied velocity constraints. If fouling risk is not an issue, the relaxed velocity constraints are adequate.

Contact:
martin.eilermann@tu-dortmund.de
christian.post@tu-dortmund.de

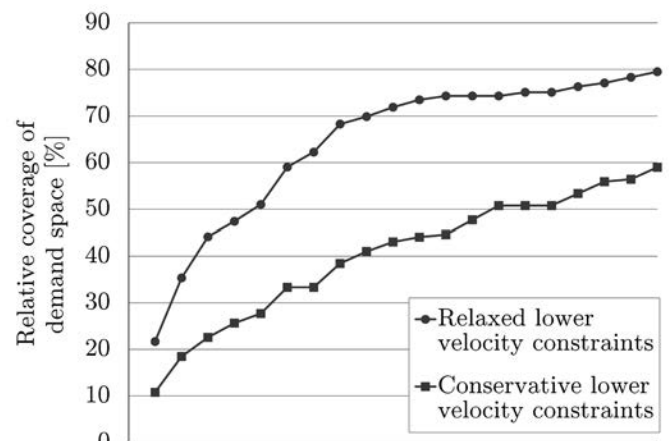


Figure 1: Coverage of the demand space over the number of clusters for conservative and relaxed lower velocity constraints.

With an increased number of clusters and hence an increased number of representative heat exchangers, also the coverage of the demand space increases. Considering the conservative constraints, 17 representative heat exchangers are required to cover 59% of the industrial applications. As can be seen from Table 1, the process and property data of the applications that can be covered show a great variety.

Process/property	Symbol	Unit	Minimum value	Maximum value
Mass flow rate	\dot{m}	[kg/h]	380	1 248 740
Heat flow rate	\dot{Q}	[kW]	5.8	10 987
Specific heat capacity	c_p	[kJ/kgK]	0.8	8.7
Density	ρ	[kg/m ³]	520	1770
Dynamic viscosity	η	[mPas]	0.07	10
Thermal conductivity	λ	[W/mK]	0.08	0.8

Table 1: Range of the process and property data for the industrial applications that can be covered by 17 representative heat exchangers considering the conservative lower velocity constraints.

Finally, the equipment module database should be integrated and applied in the module-based planning process.

Publications:

M. Eilermann, C. Post, D. Schwarz, S. Leufke, G. Schembecker, C. Bramsiepe, Generation of an equipment module database for heat exchangers by cluster analysis of industrial applications, Chem. Eng. Sci. 167 (2017) 278–287.

Discrimination of Single Particles, Agglomerates, and Air Bubbles using a Linear and Non-Linear Classifier

Variable selection with an easy-to-implement qualitative measure to rate image descriptors for classifier generation

Stefan Heisel, Tijana Kovačević, Heiko Briesen, Gerhard Schembecker, Kerstin Wohlgemuth

While particulate products are often characterized by their particle size distribution, no information is given about the agglomeration of particles. To obtain information on the agglomeration degree of a product, image analysis and sophisticated particle classification algorithms like discriminant factorial analysis (DFA) or artificial neural networks (ANN) can be used to discriminate single particles, agglomerates, and air bubbles. Latter have to be considered artifacts when measuring particle suspensions. The accuracy of the classification algorithm generated – the so-called classifier – is highly dependent on the input given like variable subset and training set design. The qualitative measure proportional similarity is used for variable selection for a linear and a non-linear classifier.

Using image analysis, each of the objects detected (Figure 1) can be characterized by a variety of image descriptors, describing qualities like size, roughness, or proportion. As crystalline systems adipic acid/water was used.



single particle

agglomerate

air bubble

Figure 1: Examples for an adipic acid single particle and agglomerate and an air bubble as detected by the imaging sensor.

The quantitative measure proportional similarity (PS, equation 1) is used to rate each of the 19 image descriptors available in terms of how well it can discriminate two populations.

$$PS = \sum_{i=1}^{20} \min(f_{U,i}, f_{V,i}) \quad (1)$$

As can be seen in Fig. 2, PS increases for populations whose similarity for a given image descriptor increases.

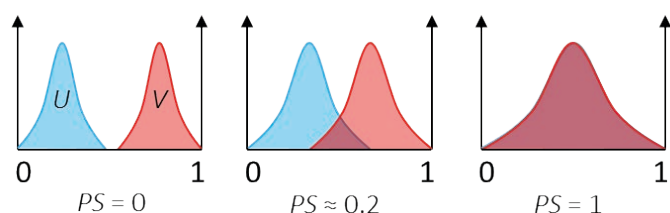


Figure 2: Schematic representation of the populations U and V for a given image descriptor and the resulting PS value.

For creation of a classifier, a set of manually classified objects (equal amount of single particles, agglomerates, and air bubbles) as well as a subset of variables is fed to the classification algorithm which tries to find the pattern within the data given. The accuracy is then tested using a separate test set of manually classified objects. To find a variable subset which results in a sufficiently high accuracy (> 0.9), the image descriptors were ranked according to

their PS value from best to worst. Successively, the image descriptors were added to the algorithms:

DFA was used to generate a linear classifier and ANN was used for non-linear classification. For adipic acid, the results can be found below:

For the linear classifier (Figure 3a) at least eight image descriptors and a training set size of 180 objects in total are necessary to reach an accuracy of 0.9 while for the non-linear classifier (Figure 3b) only three image descriptors and a training set size of 90 objects in total are necessary.

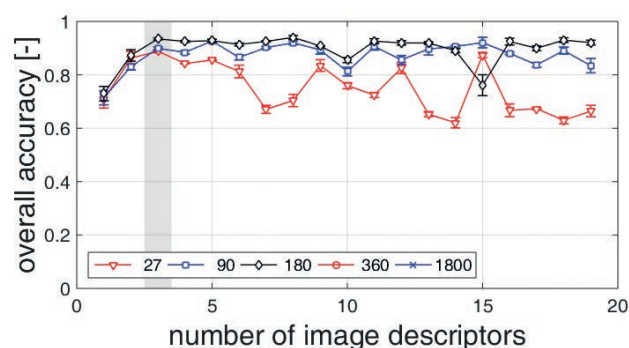
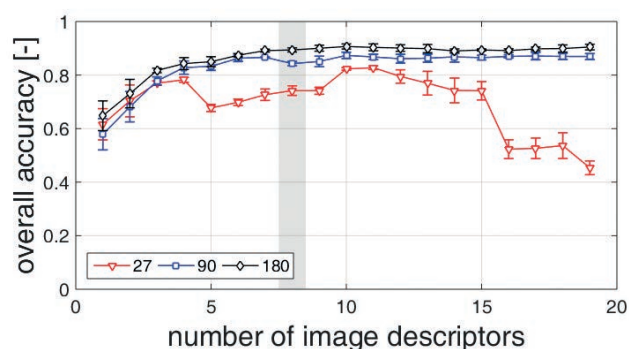


Figure 3a+b: Overall accuracies for the a) linear and b) non-linear classifier using training sets of different size.

In summary, the quantitative measure PS is capable of performing an easy-to-implement method for variable selection. Moreover, it was found that ANN is more accurate than DFA and needs less input in terms of manually classified objects and image descriptors, effectively simplifying the training process.

Publications:

S. Heisel, T. Kovačević, H. Briesen, G. Schembecker, K. Wohlgemuth, Chem. Eng. Sci. 173 (2017) 131-144.

Contact:

kerstin.wohlgemuth@tu-dortmund.de
stefan.heisel@tu-dortmund.de

Publications 2017 - 2015

Peer reviewed journal papers

2017

- M. Heitmann, G. Schembecker, C. Bramsiepe
Framework to decide for a volume flexible chemical plant during early phases of plant design
Chemical Engineering Research and Design 128, 85-95 (2017)
- L.-M. Terdenge, J. A. Kossuch, G. Schembecker, K. Wohlgemuth
Potential of gassing crystallization to control the agglomeration degree of crystalline products
Powder Technology 320, 386-396 (2017)
- S. Heisel; T. Kovačević; H. Briesen, G. Schembecker, K. Wohlgemuth
Variable Selection and Training Set Design for Particle Classification using a Linear and a Non-Linear Classifier
Chemical Engineering Science 173, 131-144 (2017)
- J. Krause, J. Merz
Hydrodynamic influences on the reaction performance of a crude yeast lysate in the CPC reactor
Biochemical Engineering Journal (2017), DOI: 10.1016/j.bej.2017.05.025
- J. Krause, J. Merz
Comparison of enzymatic hydrolysis in a centrifugal partition chromatograph and stirred tank reactor
Journal of Chromatography A 1504, 64-70 (2017)
- L.-M. Terdenge, K. Wohlgemuth
Effect of drying method on agglomeration degree of crystalline products
Chemical Engineering Science 167, 88-97 (2017)
- C. Schwienheer, J. Krause, G. Schembecker, J. Merz
Modelling centrifugal partition chromatography separation behavior to characterize influencing hydrodynamic effects on separation efficiency
Journal of Chromatography A 1492, 27-40 (2017)
- J. Sieberz, E. Cinar, K. Wohlgemuth, G. Schembecker
Clarification of a monoclonal antibody with cationic polyelectrolytes: analysis of influencing parameters
Biochemical Engineering Journal 122, 60-70 (2017)
- H. Radatz, J.M. Elischewski, M. Heitmann, G. Schembecker, C. Bramsiepe
Design of equipment modules for flexibility
Chemical Engineering Science 168, 271-288 (2017)
- L. Hohmann, K. Kössl, N. Kockmann, G. Schembecker, C. Bramsiepe
Modules in process industry - A life cycle definition
Chemical Engineering and Processing: Process Intensification 111, 115 - 126 (2017)
- T. Kleetz, G. Paetzold, G. Schembecker, K. Wohlgemuth
Gassing Crystallization at Different Scales: Potential to Control Nucleation and Product Properties
Crystal Growth & Design 17, 1028-1035 (2017)
- M. Eilermann, C. Post, D. Schwarz, (...), G. Schembecker, C. Bramsiepe
Generation of an equipment module database for heat exchangers by cluster analysis of industrial applications
Chemical Engineering Science 167, 278-287 (2017)
- M. Heitmann, T. Huhn, S. Sievers, G. Schembecker, C. Bramsiepe
Framework to decide for an expansion strategy of a small scale continuously operated modular multi-product plant
Chemical Engineering and Processing: Process Intensification 113, 74-85 (2017)
- S. Sievers, T. Seifert, M. Franzen, G. Schembecker, C. Bramsiepe
Fixed capital investment estimation for modular production plants
Chemical Engineering Science 158, 395-410 (2017)
- J. Krause, R. Krutz, G. Schembecker, J. Merz
Whole cell immobilization and catalysis in a Centrifugal Partition Chromatograph
Biochemical Engineering Journal 117 Part A, 188-197 (2017)

Proceedings & Book Chapters

- K. Wohlgemuth (editor)
BIWIC 2017 - 24th International Workshop on Industrial Crystallization
Verlag Dr. Hut, ISBN 978-3-8439-3247-9
- S. Heisel, L.-M. Terdenge, K. Wohlgemuth
Eine Strategie Zur Charakterisierung und dem Design organischer kristalliner Produkte
In: Produktgestaltung in der Partikeltechnologie, Band 8, pp. 33-40
Fraunhofer Verlag, ISBN 978-3-8396-1194-4
- S. Heisel, J. Schön, A.-L. Diekmann, G. Schembecker, K. Wohlgemuth
Evolution of the agglomeration degree over time during batch cooling crystallization
Proceedings of the 24th International Workshop on Industrial Crystallization "BIWIC" (2017) 60-65,
Verlag Dr. Hut, ISBN 978-3-8439-3247-9
- M.-C. Ostermann, M. Termühlen, J. Timmermann, G. Schembecker, K. Wohlgemuth
Nucleation and Growth Kinetic Measurements for the Design of a Novel MSMPR Cascade with Separated Zones of Crystallization Phenomena
Proceedings of the 24th International Workshop on Industrial Crystallization "BIWIC" (2017) 155-160,
Verlag Dr. Hut, ISBN 978-3-8439-3247-9

2016

- L. Hohmann, K. Kössl, N. Kockmann, G. Schembecker, C. Bramsiepe
Modules in process industry - A life cycle definition
Chemical Engineering and Processing: Process Intensification (2016) DOI: 10.1016/j.cep.2016.09.017
- M. Heitmann, T. Huhn, S. Sievers, G. Schembecker, C. Bramsiepe
Framework to decide for an expansion strategy of a small scale continuously operated modular multi-product plant
Chemical Engineering and Processing: Process Intensification (2016) DOI: 10.1016/j.cep.2016.09.004
- T. Kleetz, F. Funke, A. Sunderhaus, G. Schembecker, K. Wohlgemuth
Influence of Gassing Crystallization Parameters on Induction Time and Crystal Size Distribution
Crystal Growth & Design 16, 6797-6803 (2016)
- N. Wolters, C. Schabronath, G. Schembecker, J. Merz
Efficient conversion of pretreated brewer's spent grain and wheat bran by submerged cultivation of *Hericium erinaceus*
Bioresource Technology 222, 123-129 (2016)

- M. Lochmüller, G. Schembecker
Simultaneous optimization of scheduling, equipment dimensions and operating conditions of sequential multi-purpose batch plants
Computers and Chemical Engineering 94, 157-179 (2016)
 - S. Sievers, T. Seifert, G. Schembecker, C. Bramsiepe
Methodology for evaluating modular production concepts
Chemical Engineering Science 155, 153-166 (2016)
 - L. Holtmann, M. Lobedann, J. Magnus, G. Schembecker
Disposables for continuous viral clearance for the production of monoclonal antibodies
European Pharmaceutical Review 21 (2), 22-27 (2016)
 - L.-M. Terdenge, K. Wohlgemuth
Impact of agglomeration on crystalline product quality within the crystallization process chain
Crystal Research & Technology 51513-523 (2016)
 - L. Hohmann, R. Gorny, O. Klaas, J. Ahlert, K. Wohlgemuth, N. Kockmann
Design of a Continuous Tubular Cooling Crystallizer for Process Development on Lab-scale
Chemical Engineering & Technology 39, 1268-1280 (2016)
 - S. Klutz, L. Holtmann, M. Lobedann, G. Schembecker
Cost evaluation of antibody production processes in different operation modes
Chemical Engineering Science 141, 63-74 (2016)
 - S. Klutz, M. Lobedann, C. Bramsiepe, G. Schembecker
Continuous viral inactivation at low pH value in antibody manufacturing
Chemical Engineering and Processing: Process Intensification 102, 88-101 (2016)
 - T. Kleetz, F. Braak, N. Wehenkel, G. Schembecker, K. Wohlgemuth
Design of Median Crystal Diameter Using Gassing Crystallization and Different Process Concepts
Crystal Growth & Design 161320-1328 (2016)
 - C. Dowidat, M. Kalliski, G. Schembecker, C. Bramsiepe
Synthesis of batch heat exchanger networks utilizing a match ranking matrix
Applied Thermal Engineering 100, 78-83 (2016)
 - F. Thygs, J. Merz, G. Schembecker
Automation of Solubility Measurements on a Robotic Platform
Journal of Chemical and Engineering Technology 39 (6), 1049-1057 (2016)
 - B. Dreisewerd, J. Merz, G. Schembecker
Modeling the Quasi-Equilibrium of Multistage Phytoextractions
Industrial & Engineering Chemistry Research 55, 1808-1812 (2016)
 - K. Brandt, G. Schembecker
Production Rate-Dependent Key Performance Indicators for a Systematic Design of Biochemical Downstream Processes Plants
Chemical Engineering and Technology 39, 354-364 (2016)
 - S. Klutz, J. Magnus, M. Lobedann, M. Temming, G. Schembecker
Developing the biofacility of the future based on continuous processing and single-use technology
Source of the Document Journal of Biotechnology 213, 120-130 (2015)
- ## 2015
- C. Schwienheer, J. Merz, G. Schembecker
Investigation, comparison and design of chambers used in centrifugal partition chromatography on the basis of flow pattern and separation experiments
Journal of Chromatography A 1390, 39-49 (2015)
 - N. Wolters, G. Schembecker, J. Merz
Erinacine C: A Novel Approach to Produce the Secondary Metabolite by Submerged Cultivation of *Herichium erinaceus*
Fungal Biology 119, 1334-1344 (2015)
 - C. Schwienheer, A. Prinz, T. Zeiner, J. Merz
Separation of active laccases from *Pleurotus sapidus* culturesupernatant using aqueous two-phase systems in centrifugal partition chromatography
Journal of Chromatography B 1002, 1-7 (2015)
 - T. Seifert, J.M. Elischewski, S. Sievers, F. Stenger, B. Hamers, M. Priske, M. Becker, R. Franke, G. Schembecker, C. Bramsiepe
Multivariate risk analysis of an intensified modular hydroformylation process
Chemical Engineering and Processing: Process Intensification 95, 124-134 (2015)
 - J. Sieberz, K. Wohlgemuth, G. Schembecker
The influence of impurity proteins on the precipitation of a monoclonal antibody with an anionic polyelectrolyte
Separation and Purification Technology 146, 252-260 (2015)
 - A. Hofmann, G. Schembecker, J. Merz
Reply on "Comments on Role of bubble size for the performance of continuous foam fractionation in stripping mode"
Colloids and Surfaces A: Physicochemical and Engineering Aspects 474, 105-110 (2015)
 - L.-M. Terdenge, S. Heisel, G. Schembecker, K. Wohlgemuth
Agglomeration degree distribution as quality criterion to evaluate crystalline products
Chemical Engineering Science 133, 157-169 (2015)
 - B. Dreisewerd, J. Merz, G. Schembecker
Determining the Solute-Solid Interactions in Phytoextraction
Chemical Engineering Science 134, 287-296 (2015)
 - T. Seifert, H. Schreider, S. Sievers, G. Schembecker, C. Bramsiepe
Real Option Framework for Equipment Wise Expansion of Modular Plants applied to the design of a continuous multiproduct plant
Chemical Engineering Research and Design 93, 511-521 (2015)
 - K. Backhaus, M. Lochmüller, M. C. Arndt, O. Riechert, G. Schembecker
Knowledge-Based Conceptual Synthesis of Industrial-Scale Downstream Processes for Biochemical Products
Chemical Engineering Science 38, 537-546 (2015)
 - J. Krause, T. Oeldorf, G. Schembecker, J. Merz
Enzymatic hydrolysis in an aqueous organic two-phase system using Centrifugal Partition Chromatography
Journal of Chromatography A 1391, 72-79 (2015)

-
- C. Schwienheer, J. Merz, G. Schembecker
Selection and use of poly ethylene glycol and phosphate based aqueous two-phase systems for the separation of proteins by Centrifugal Partition Chromatography
Journal of Liquid Chromatography & Related Technologies 38, 929-941 (2015)
 - C. Fleischer, J. Wittmann, N. Kockmann, T. Bieringer, C. Bramsiepe
Safety Aspects in Planning and Construction of Modular Production Plans
Chemie Ingenieur Technik 87, 1258 – 1269 (2015)
 - C. Schwienheer, A. Prinz, T. Zeiner, J. Merz
Separation of active laccases from *Pleurotus sapidus* supernatant using aqueous two-phase systems in centrifugal partition chromatography
Journal of Chromatography B: Analytical Technologies in the Biomedical and Life Sciences 1002, 1-7 (2015)



Biomaterials and Polymer Science (BMP)

Ultrafast-Swelling, Superabsorbing, Antimicrobial Hydrogels

Cross-linked Ionomers towards interpenetration networks for long-term active antimicrobial coatings

Arne Strassburg, Christian Krumm, Monika Meuris, Joerg C. Tiller

Biocompatible materials with long lasting intrinsic antimicrobial properties are very important for modern medicine. Most antimicrobial materials, such as implants, catheters, and wound dressings contain biocides or antibiotics that are released into the surrounding and deplete eventually. Here, we report on a hydrogel material that is superior to previous coatings, because it can swell about 100 times faster than any other hydrogel and if converted into an interpenetrating polymer network (IPN) it shows antimicrobial properties that might last for a year.

A hemocompatible, antimicrobial 3,4-en-ionene (PBI) derived by polyaddition of trans-1,4-dibromo-2-butene and N,N,N',N'-tetramethyl-1,3-propanediamine was cross-linked via its bromine end groups using tris(2-aminoethyl)amine to form a fast-swelling, antimicrobial super absorber. This super absorber is taking up the 30-fold of its weight in 60 s and the powder is taking up the 96-fold of its weight forming a hydrogel (Figure 1).

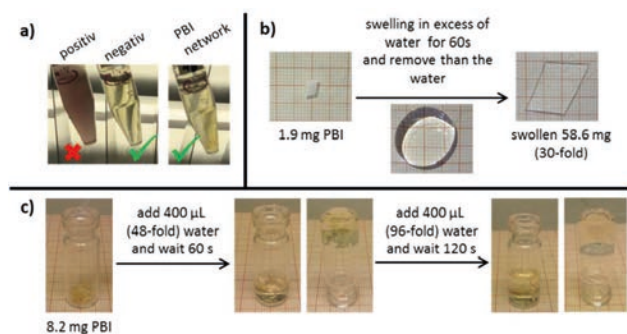


Figure 1: a) Photographs of 15 mL falcon tubes filled with 4 mL growth medium: left) inoculated with $2.5 \cdot 10^4$ *S. aureus* cells/mL incubated at 37 °C overnight, middle) incubated at 37 °C overnight without addition of bacterial cells, and right) 6 mg PBI network treated with 10 µL of *S. aureus* suspension in growth medium (10^7 *S. aureus* cells/mL) for 10 min added to growth medium, incubated at 37 °C overnight. The photographs were taken after 16 h incubation at 37 °C and staining with TTC. b+c) Photographs of the rapid swelling of a PBI network film (b) and in small pieces cut PBIN (c) in water.

It fully prevents growth of the bacterium *Staphylococcus aureus*. The PBI network was swollen with 2-hydroxyethyl acrylate and glycoldimethacrylate followed by photopolymerization to form an interpenetrating hydrogel (IPH) with varying PBI content in the range of 2.0 to 7.8 wt %. The nanophasic structure of the IPH was confirmed by atomic force microscopy and transmission electron microscopy. The bacterial cells of the nosocomial strains *S. aureus* (*S.a.*), *Escherichia coli* (*E.c.*) and *Pseudomonas aeruginosa* (*P.a.*) are killed on the IPH even at the lowest PBI concentration (Figure 1a). The number of the adhered bacterial cells is reduced by the 10^4 to 10^6 – fold after only 30 min of incubation.

Contact:

arne.strassburg@tu-dortmund.de
christian.krumm@tu-dortmund.de
monika.meuris@tu-dortmund.de
joerg.tiller@tu-dortmund.de

The IPHs show minor leaching of the PBI far below the MIC using a new quantitative test for PBI detection in solution. The leaching of PBI into the surrounding never reaches the MIC value of PBI, which is why the bacterial cells are only killed at the surface of the materials. Extrapolation of the determined PBI leaching rate over time suggests that the material is leaching a bacteria-toxic amount of PBI even after a year of washing.

The PBI leaching was shown to be not sufficient to form an inhibition zone and killing bacterial cells in the surroundings of the IPH (Figure 1b), suggesting a seemingly contact-active antimicrobial mechanism.

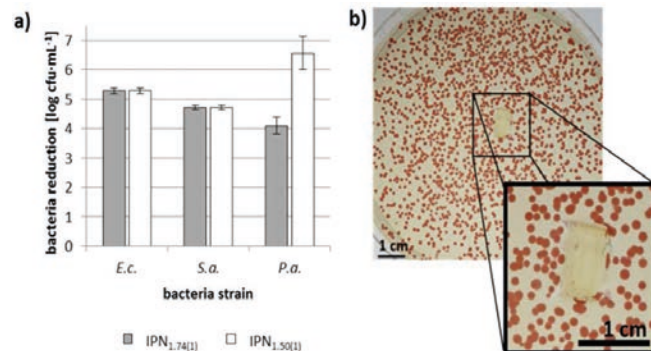


Figure 2: a) Reduction of bacterial cells on the surface of the in water-washed networks IPH_{1.74(1)} (12 d at 37 °C) and IPH_{1.50(1)} (27 d at 37 °C) after an incubation time of 3 h in PBS. b) Image *S. aureus* colonies formed after being sprayed on an agar plate with an embedded IPH_{1.50(1)} network (washed for 7 days with water), incubated at 37 °C overnight and stained with TTC.

The materials were washed for 4 weeks and still showed full antimicrobial activity. Such a hydrogel coating is a promising material as wound dressing, e.g. for burns or infected wounds.

Publications:

A. Strassburg, J. Petranowitsch, F. Paetzold, C. Krumm, E. Peter, M. Meuris, M. Köller, J. C. Tiller
ACS Applied Materials & Interfaces 9 (42), 36573-36582 (2017).

Telechelic, Antimicrobial Hydrophilic Poly(ethylene imines)

Combination of two modes of action in one biocidal macromolecule

Lena Richter, Montasser Hijazi, Christian Krumm, Joerg C. Tiller

Since the development of antimicrobial agents, such as biocides and antibiotics, lifetime and the state of health have continuously improved especially in affluent societies. The rise of immune and multi-resistant bacterial strains currently threatens this state that might end up in a post antibiotic era. In order to push antimicrobial polymeric biocides to the next level, we have combined two different antimicrobial modes of action in a single molecule.

The characteristics of two different classes of biocidal polymers were combined in one macromolecule by hydrolyzing Gram-positive-selective telechelic poly(2-methyl-2-oxazolines) (PMOx) with quaternary ammonium end groups to the hydrophilic polycation poly(ethyleneimine) (PEI) (Figure 1). The structures of the different PMOx and PEI were proven by ^1H NMR spectroscopy. The antimicrobial activity of these conjugates was tested against the Gram-positive bacterial strains *Staphylococcus aureus* and *Streptococcus mutans* as well as the Gram-negative strains *Escherichia coli*, *Pseudomonas aeruginosa* and *Klebsiella pneumoniae*.

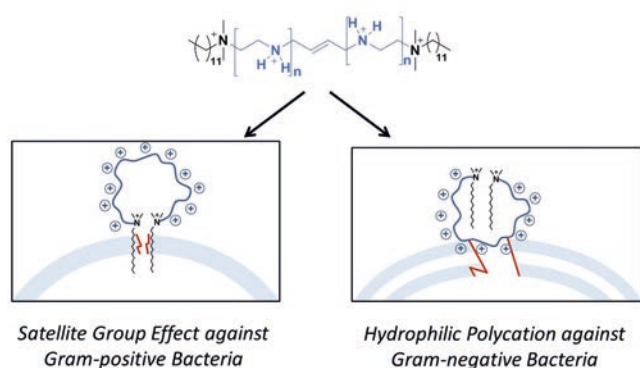


Figure 1: Modes of action of telechelic Poly(ethylene imine) against Gram-positive and Gram-negative bacterial strains.

By rendering the backbone of the telechelic PMOx to the hydrophilic polycation PEI, the antimicrobial activity against *E. coli* improved significantly from $2000 \mu\text{g}\cdot\text{mL}^{-1}$ to some $40\text{-}160 \mu\text{g}\cdot\text{mL}^{-1}$. The activity against the Gram-positive strain *S. aureus* also improved greatly with MIC values for the PEI of some $20\text{-}80 \mu\text{g}\cdot\text{mL}^{-1}$ (Figure 2). Since the characteristics of a telechelic biocidal polymer and a hydrophilic polycation are combined in one polymer, it was tested which mode of action dominates against the different bacterial strains. Since it is known to literature that PEI can be deactivated by Ca^{2+} ions, the MIC tests were repeated in the presence of 80 mM of CaCl_2 .

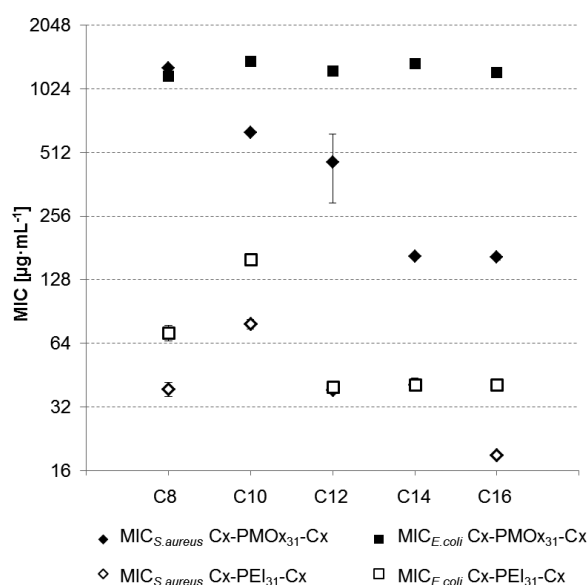


Figure 2: Antimicrobial activities (MIC) of end group functionalized Cx-PMOx₃₁-Cx and Cx-PEI₃₁-Cx against *S. aureus* and *E. coli* dependent on the length of the alkyl chain.

The activity of PEI with octyl and decyl carrying quaternary ammonium groups was deactivated against *E. coli*, while the PEI with longer alkyl chain end groups were less effected by Ca^{2+} ions. This shows that the backbone and the end groups act synergistically. In case of *S. aureus*, the polymers show no calcium-induced deactivation of PEI with longer alkyl chain end groups (C12-C16). This reveals that these telechelic PEIs indeed show a satellite group effect against this bacterial strain. PEIs with a higher molecular weight are dominated by the polycationic backbone. Thus, the polycationic backbone and the quaternary ammonium end groups act synergistically and the modes of action can be balanced by variation of the polymer chain length.

Penicillin with a Polymer Tail for Combating Resistant Mechanism

Polymer Penicillin conjugates with high activity

Martin Schmidt, Christian Krumm, Joerg C. Tiller

According to the World Health Organization antibiotic resistant bacterial strains are one of the greatest health threats to humankind in the 21st century. Today one of the most famous antibiotics, penicillin G is nearly useless because of distribution of resistant bacterial strains. In the most cases the resistant mechanism is based on penicillin hydrolyzing enzymes. Therefore, new methods of antibiotic design are strongly required to defeat bacterial resistance mechanisms. Here we covalently attached penicillin G to poly(2-methyl-2-oxazoline)s in order to achieve a higher stability against these Penicillin hydrolyzing enzymes. The polymer penicillin conjugates (PPC) are promising candidates for antibiotics with lower resistance potential.

The antibiotic penicillin G (PenG) was covalently attached to poly(2-methyl-2-oxazoline) (PMOx), poly(2-ethyl-2-oxazoline) (PEtOx) and poly(2-iso-propyl-2-oxazolin (PiPrOx) via direct termination of the living cationic polymer chain.

The different polymer antibiotic conjugates shown in Figure 1 were characterized by ¹H-NMR spectroscopy and electron spray ionization mass spectrometry.

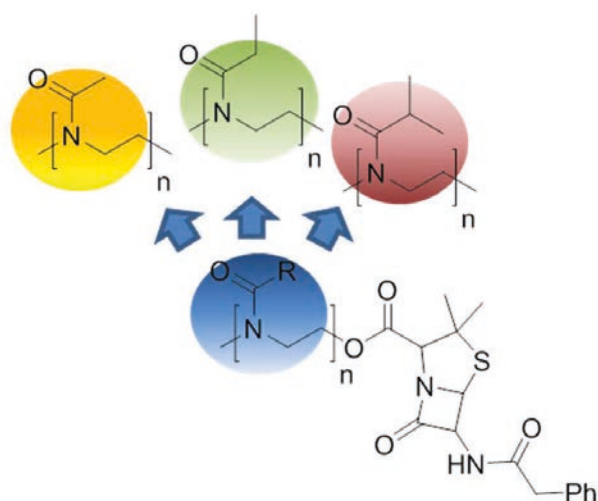


Figure 1: Chemical structure of polymer antibiotic conjugates.

The minimal inhibitory concentrations of these conjugates were determined against *Staphylococcus aureus* (*S. aureus*). As seen in Figure 2 (black bars), the activity of the different PPC is about 2 orders of magnitude lower than the free antibiotic. The MIC values of different poly(2-oxazoline) derivatives show that the most hydrophilic polymer PMOx affords the highest activity.

β -lactam hydrolyzing enzymes are the most common bacterial resistance mechanism against penicillin. MIC values against *S. aureus* in presence of the enzyme were determined, accordingly. The results are shown in Figure 2 (white bars). The presence of the enzyme renders the antibiotic PenG inactive, while the respective PPCs are still

exhibiting antimicrobial activity. The conjugates also lose their activity by 1 to 2 orders of magnitude in presence of the enzyme.

This indicates that the PPCs exhibit a 20-350-fold higher resistance against the enzyme compared to the free antibiotic.

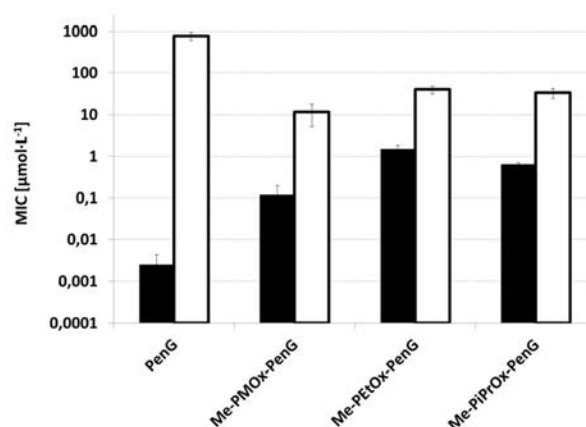


Figure 2: Molar MIC values for the different PPCs against *S. aureus* in comparison to the molar MIC value of PenG (white columns) full bars. The hatch bars present the MIC values of the PPCs and PenG against *S. aureus* in presence of a β -lactam hydrolyzing enzyme. All measurements were performed in triplicate and the bars are the standard deviation.

The results show that the conjugation of penicillin with poly(2-oxazoline)s is a promising method of modifying these antibiotics, making them more stable against hydrolyzing enzymes.

Entropically driven Polymeric Enzyme Inhibitors by End-Group Conjugation

A new generic concept for enzyme inhibitors

Montasser Hijazi, Christian Krumm, Joerg C.Tiller

Most pharmaceutically active compounds are enzyme inhibitors. These are typically binding at the active side of the respective biocatalyst. Non-competitive inhibitors do not bind at the active side and are therefore difficult to predict. Here, we present an unusual and new generic approach for the design of non-competitive enzyme inhibitors. To this end, poly(2-methyloxazoline)s are modified with specific not inhibitory functional end groups, which steer the polymers to the enzyme surface, resulting in non-competitive enzyme inhibition.

The concept for the novel enzyme inhibitors is based on a hydrophilic polymer that is driven onto the surface of an enzyme by a specific end group that is not an inhibitor by itself. The polymer is then collapsing on the protein changing the surface polarity, which inhibits the enzyme activity (Figure 1).

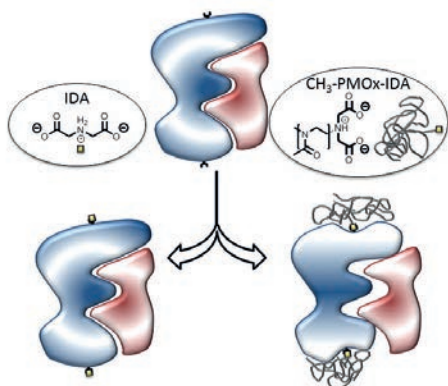


Figure 1: Schematic representation of the proposed generic concept for enzyme inhibition based on specifically binding anchor groups attached to an inert hydrophilic polymer.

Poly(2-methyloxazoline) (PMOx) was chosen as hydrophilic and biocompatible polymer that has only weak interactions with proteins. 2, 2'-Imino diacetate (IDA) has the potential of binding to bivalent metals that are often found in protein scaffolds. Due to this fact, IDA was selected as specific end group. The enzyme horse radish peroxidase (HRP) was chosen as model enzyme, because it contains two calcium ions in the protein structure and is not inhibited by IDA.

The activity of HRP was investigated by the oxidation of [2,2-azino-bis(3-ethylbenzothiazoline-6-sulfonic acid)] diammonium salt (ABTS) with H_2O_2 in the presence of different concentrations of IDA modified PMOx (Figure 2).

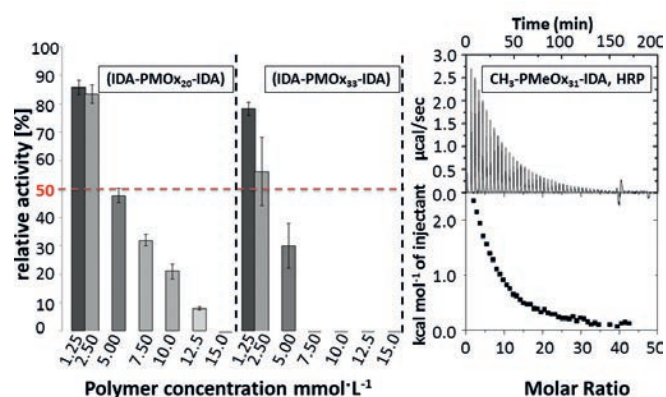


Figure 2: Left Inhibition of horseradish peroxidase (HRP) induced by mono- and bifunctional PMOx at varying concentrations (1.25, 2.5, 5, 7.5, 10, 12.5, and 15 mM). Right: Inhibition of HRP induced by 1 mM IDA-PMOx₃₃-IDA in different phosphate buffer concentrations. The inhibition was measured with ABTS substrate (10 mM) at pH 5.0 for all polymers.

The results show that the activity of HRP is fully inhibited at concentrations between 7.5 to 15 mM IDA modified PMOx (see Fig. 2, left). The polymer was found to be a non-competitive inhibitor. Furthermore the binding affinity and thermo-dynamic parameters of interactions of HRP with IDA terminated PMOx was investigated using Isothermal Titration Calorimetry (ITC) measurements (see Fig. 2, right). The titration showed that the addition of the polymer to HRP results in endothermic reaction. This might be caused by attachment of polymer to the enzyme surface, resulting in aggregation which also was confirmed by NMR spectroscopy. This endothermic effect is caused by an entropy-driven release of polymer- and enzyme-bound water molecules.

Publications:

M. Hijazi, C. Krumm, S. Cinar, L. Arns, W. Alachraf, W. Hiller, W. Schrader, R. Winter and J. Tiller, Chem. Eur. J. 24(18), 4523-4527 (2018).

Contact:

montasser.hijazi@tu-dortmund.de
joerg.tiller@tu-dortmund.de

Biaxial Orientation upon Uniaxial Stretching

T. Raidt, R. Hoehner, F. Katzenberg, Joerg C. Tiller

The development of biaxially oriented polypropylene (BOPP) was one of the most significant improvements in film technology. Nearly 90% of all polypropylene films are biaxially oriented and offer reinforcement in machine as well as transversal direction. Since polymers usually must be stretched simultaneously or successively along perpendicular directions to gain biaxial orientations, biaxial reinforcement is limited to sample geometries with large surface to distance ratios, such as thin films. Here we present a novel route for realizing multiaxial orientations in isotactic polypropylene (iPP) that needs drawing only along one direction and is also applicable for bulky samples.

For realizing multiaxial orientations upon uniaxial stretching we followed the idea to exploit the homoepitaxy of iPP. In the latter polymer specimens self-assembled cross-hatched textures were found, which consist of two sets of lamellae placed at an angle of 100° to each other. This effect is commonly entitled as homoepitaxy. Thus, the homoepitaxial crystallization from the oriented melt might be an appropriate way in order to gain a multiaxial orientation. Unfortunately, there is only a slight increase of the tensile properties upon melt drawing, because entropically driven relaxation of the macromolecules cannot be avoided completely. For this reason we cross-linked iPP to a very low degree (x-iPP) to allow crystallization under constraint conditions, but retain the homoepitaxy. Figure 1 shows the wide angle X-ray scattering (WAXS) of x-iPP crystallized under a strain of 600%.

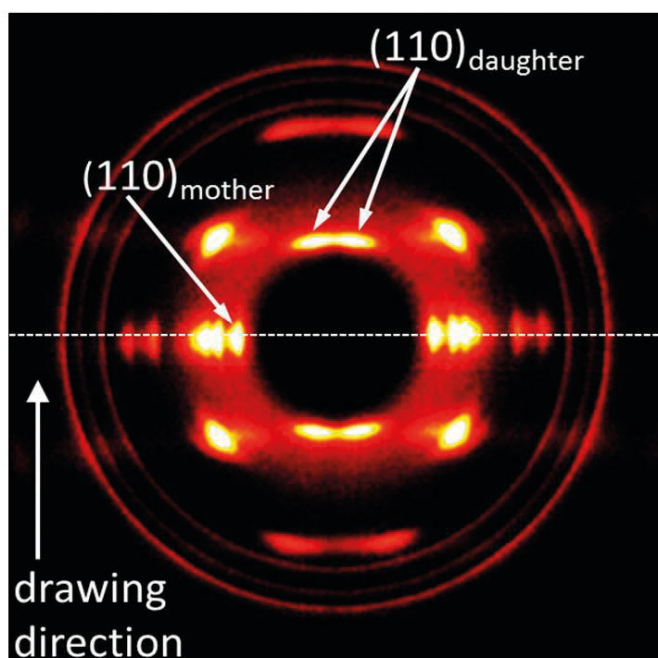


Figure 1: WAXS-pattern of x-iPP drawn to a strain of 600% with the annotation of the signals of the mother and daughter crystals.

The main orientation in drawing direction can be noticed by the crystal reflexes on the equatorial line (mother crystals), but there is also a significant amount of crystals oriented in an angle of 80° and 100° , which is contributed to the homoepitaxy (daughter crystals).

Finally, we investigated the impact of the obtained multiaxial crystal-orientations on the Young's modulus of the iPP-networks under different loading angles. The determined Young's moduli parallel, perpendicular and under 45° to the stretching direction, referred to as $E(0^\circ)$, $E(90^\circ)$, and $E(45^\circ)$, are displayed in Figure 2.

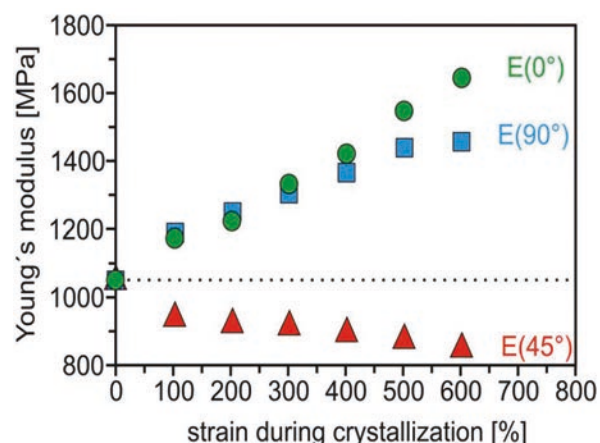


Figure 2: Young's modulus in dependence of the strain in drawing direction (0°), perpendicular (90°) and under an angle of 45° .

It is seen that the occurring multiaxial orientations cause significantly improved Young's moduli parallel (+60%) as well as perpendicular (+45%) to the stretching direction while that under an angle of 45° is slightly decreasing (-20%). Further, the multiaxial orientations and consequentially the Young's moduli can be adjusted within broad ranges by applying different strains during crystallization. In contrast to other techniques for multi or biaxial orienting iPP (e.g., BOPP) the here described method is not limited to thin films but can be efficiently applied also to bulky samples, because stretching is carried out in the molten state.

Contact:
 thomas.raidt@tu-dortmund.de
 frank.katzenberg@tu-dortmund.de
 joerg.tiller@tu-dortmund.de

Publications:
 T. Raidt, R. Hoehner, F. Katzenberg, J. C. Tiller, *Macromolecular Materials and Engineering* 302, 1600308 (2017).

Publications 2017 - 2015

2017

- A. Strassburg, J. Petranowitsch, F. Paetzold, C. Krumm, E. Peter, M. Meuris, M. Köller, J. C. Tiller
Cross-Linking of a Hydrophilic, Antimicrobial Polycation toward a Fast-Swelling, Antimicrobial Superabsorber and Interpenetrating Hydrogel Networks with Long Lasting Antimicrobial Properties
Applied Materials & Interfaces 9 (42), 36573-36582 (2017)
- M. Leurs, J. C. Tiller
Chapter 17 - Nanoarmored Enzymes for Organic Enzymology: Synthesis and Characterization of Poly(2-Alkyloxazoline)-Enzyme Conjugates
Methods in Enzymology 590, 413-444 (2017)
- C. Krumm, H. Montasser, S. Trump, S. Saal, L. Richter, G. G. F. K. Noschmann, T.-D. Nguyen, K. Preslikoska, T. Moll, J. C. Tiller
Highly active and selective telechelic antimicrobial poly(2-oxazoline) copolymers
Polymer 118, 107-115 (2017)
- N. Rauner, M. Meuris, M. Zoric, J. C. Tiller
Enzymatic mineralization generates ultrastiff and tough hydrogels with tunable mechanics
Nature 543, 407-410 (2017)
- R. Plothe, I. Sittko, F. Lanfer, M. Fortmann, M. Roth, V. Kolbach, J. C. Tiller
Poly(2-ethyloxazoline) as matrix for highly active electrospun enzymes in organic solvents
Biotechnology and Bioengineering 114 (1), 39-45 (2017)
- C. Krumm, J. C. Tiller
Chapter 15 Antimicrobial Polymers and Surfaces - Natural Mimics or Surpassing Nature?
Bio-inspired Polymers, The Royal Society of Chemistry, 490-522 (2017)
- T. Raidt, R. Hoeher, F. Katzenberg, J. C. Tiller
Multiaxial Reinforcement of Cross-Linked Isotactic Polypropylene upon Uniaxial Stretching
Macromolecular Materials and Engineering 302, 1600308 (2017)
- M. Schmidt, T. Raidt, S. Ring, S. Gielke, C. Gramse, S. Wilhelm, F. Katzenberg, C. Krumm, J. C. Tiller
Investigations on "near perfect" poly(2-oxazoline) based amphiphilic polymer conetworks with a crystallizable block
European Polymer Journal 88, 562-574 (2017)

2016

- T. Raidt, R. Hoeher, M. Meuris, F. Katzenberg, J. C. Tiller
Ionicallly Cross-Linked Shape Memory Polypropylene
Macromolecules 49 (18), 6918-6927 (2016)
- R. Plothe, I. Sittko, F. Lanfer, M. Fortmann, M. Roth, V. Kolbach, J. C. Tiller
Poly(2-ethyloxazoline) as matrix for highly active electrospun enzymes in organic solvents
Biotechnology and Bioengineering 114 (1), 39-45 (2016)
- R. Hoeher, T. Raidt, F. Katzenberg, J. C. Tiller
Heating Rate Sensitive Multi-Shape Memory Polypropylene: A Predictive Material
ACS Applied Materials & Interfaces 8, 13684-13687 (2016)
- F. Katzenberg, J. C. Tiller
Shape Memory Natural Rubber
Journal of Polymer Science Part B: Polymer Physics 54, 1381-1388 (2016)
- M. Leurs, P. S. Spiekermann, J. C. Tiller
Optimization of and Mechanistic Considerations for the Enantioselective Dihydroxylation of Styrene Catalyzed by Osmate-Laccase-Poly(2-Methyloxazoline) in Organic Solvents
ChemCatChem 8 (3), 593-599 (2016)
- N. Gushterov, F. Doghieri, D. Quitmann, E. Niesing, F. Katzenberg, J. C. Tiller, G. Sadowski
VOC Sorption in Stretched Cross-Linked Natural Rubber
Industrial & Engineering Chemistry Research 55 (26), 7191-7200 (2016)
- W. Tillmann, L. Hagen, F. Hoffmann, M. Dildrop, A. Wibbeke, V. Schöppner, V. Resonnek, M. Pohl, C. Krumm, J. C. Tiller, M. Paulus, C. Sternemann
The detachment behavior of polycarbonate on thin films above the glass transition temperature
Polymer Engineering & Science 56 (7), 786-797 (2016)
- S. Sommer, T. Raidt, B. M. Fischer, F. Katzenberg, J. C. Tiller, M. Koch
THz-Spectroscopy on High Density Polyethylene with Different Crystallinity
Journal of Infrared, Millimeter, and Terahertz Waves 37 (2), 189-197 (2016)
- A. Drahten, J. Reiber, C. Krumm, M. Meuris, J. C. Tiller, C. M. Niemeyer, S. Brakmann
Genetic Engineering of Silaffin-Like Peptides for Binding and Precipitating Siliceous Materials
Chemistry Select 1 (15), 4765-4771 (2016)

2015

- M. Schmidt, S. Harmuth, B. E. Barth, E. Wurm, R. Fobbe, A. Sickmann, C. Krumm, J. C. Tiller
Conjugation of Ciprofloxacin with Poly(2-oxazoline)s and Polyethylene Glycol via End Groups
Bioconjugate Chemistry 26 (9), 1950-1962 (2015)
- A. Strassburg, F. Kracke, J. Wenners, A. Jemeljanova, J. Kuepper, H. Petersen, J. C. Tiller
Nontoxic, Hydrophilic Cationic Polymers - Identified as Class of Antimicrobial Polymers
Macromolecular Bioscience 15 (12), 1710-1723 (2015)
- R. Hoeher, T. Raidt, N. Novak, F. Katzenberg, J.C. Tiller
Shape Memory PVDF Exhibiting Switchable Piezoelectricity
Molecular Rapid Communications 36 (23), 2042-2046 (2015)
- I. Sittko, K. Kremser, M. Roth, S. Kuehne, S. Stuhr, J. C. Tiller
Amphiphilic Polymer Conetworks With Defined Nanostructure and Tailored Swelling Behavior for Exploring the Activation of an Entrapped Lipase in Organic Solvents
Polymer 64, 122-129 (2015)
- F. Katzenberg, J.C. Tiller
Vielmehr als nur Gummi
Nachrichten aus der Chemie (6)623-626 (2015)
- T. Raidt, R. Hoeher, F. Katzenberg, J. C. Tiller
Chemical Cross-linking of Polypropylenes Towards New Shape Memory Polymers
Macromolecular Rapid Communications 36 (8), 744-749 (2015)
- D. Quitmann, F. M. Reinders, B. Heuwers, F. Katzenberg, J. C. Tiller
Programming of Shape Memory Natural Rubber for Near-Discrete Shape Transitions
ACS Applied Materials and Interfaces 7 (3), 1486-1490 (2015)
- S. Konieczny, M. Leurs, J. C. Tiller
Polymer Enzyme Conjugates as Chiral Ligands for Sharpless Dihydroxylation of Alkenes in Organic Solvents
ChemBioChem 16 (1), 83-90 (2015)
- N. Rauner, L. Buenger, S. Schuller, J. C. Tiller
Post-Polymerization of Urease-Induced Calcified, Polymer Hydrogels
Macromolecular Rapid Communications 36 (2), 224-230 (2015)
- D. Quitmann, M. Dibolik, F. Katzenberg, J.C. Tiller
Altering the Trigger-Behavior of Programmed SMNR by Solvent Vapor
Macromolecular Materials and Engineering 300 (1), 25-30 (2015)
- E. J. Kepola, L. Elena, C. S. Patrickios, L. Epameinondas, V. Chrysovalantis, S. Triantafyllos, R. Schweins, M. Gradzielski, C. Krumm, J. C. Tiller, M. Kushnir, C. Wesdemiotis
Amphiphilic Polymer Conetworks Based on End-Linked "Core-First" Star Block Copolymers: Structure Formation with Long-Range Order
ACS Macro Letters 4, 1163-1168 (2015)

Patents

- Tiller, J.C., Katzenberg, F., Hoeher, R., Raidt, T.
Method for producing an oriented polymer
Eur. Pat. Appl. (2016), EP 3098059 A1 20161130
- Tiller, J.C., Mueller, C., Rauner, N.
Derivatized silicon dioxide nanoparticles coated with quaternary ammonium salts contg. a silane group and long alkyl chain exhibiting biocidal action
Ger. Offen. (2015), DE 102014108278 A1 20151217
- Tiller, J.C., Quitmann, D., Katzenberg, F.
Polymer network comprising shape memory polymers used as a sensor or force element
Eur. Pat. Appl. (2014), EP 2783834 A1 20141001



Bioprocess Engineering (BPT)

In vitro Protein Synthesis for Biocatalyst Development

Jan Volmer, Lara J. Feliczak, Mattijs K. Julsing, Katrin Rosenthal, Stephan Lütz

In vitro protein synthesis is gene expression with the biological machinery without the use of cells. This cell-free method can be used to produce proteins in a very simple and rapid way. In vitro protein synthesis is especially advantageous in high-throughput applications to screen enzymes, e.g. derived from a gene library, in a short time and to study the influence of genetic modifications on protein activity, stability, substrate, and product specificity. The combination of in vitro protein synthesis with other modern molecular biology tools such as genome/transcriptome sequencing and gene synthesis will definitely increase the speed of biocatalyst development in industrial biotechnology.

The synthesis of proteins *in vitro* starting from DNA requires cell components such as ribosomes, enzymes, chaperones, amino acids, as well as energy sources (End et al., 2014). A defined composition of isolated, recombinant elements originating from the translation machinery of *Escherichia coli* turned out to result in the highest protein yields up to now (Kuruma und Ueda, 2015).

We used this protein synthesis system to synthesize a set of four homologous enzymes (cGAS) selected from genome sequences of different eukaryots. Fully synthetic genes were introduced in the *in vitro* protein synthesis system. Protein synthesis was confirmed by SDS-PAGE analyses. We also investigated *in vitro* protein synthesis in order to rapidly compare the activity of different trans-proline-4-hydroxylases with respect to biocatalytic performance. Trans-proline-4-hydroxylases catalyze the conversion of L-proline into trans-4-hydroxy-L-proline, which is an interesting building block in pharmaceutical industry and is also used in cosmetic and food industry. The trans-proline-4-hydroxylase P4H1of (Falcioni et al., 2013), an engineered P4H1of (P4Hkahof), and the isoenzyme P4H2 were compared.

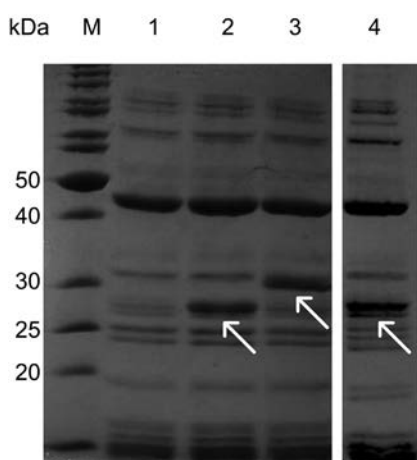


Figure 1: SDS-PAGE of *in vitro* synthesized proteins: M: marker, 1: reference reaction without DNA template, 2: P4Hkahof (29.7 kDa), 3: P4H2 (31.7 kDa), 4: P4H1of (31.7 kDa).

The enzymes were obtained in concentrations ranging from 0.30-0.59 mg mL⁻¹ (Figure 1). The amount of synthesized P4H1of was two-fold higher compared to the mutant and isoenzyme, which shows that *in vitro* expression is dependent on the gene sequence as is also the case for *in vivo* systems.

However, the three enzymes all showed activity in a subsequently performed activity assay (Figure 2). We showed that synthesis of active enzymes was possible in only 4 h based on the presence of the gene as a DNA molecule. The subsequent enzymatic reaction was performed in 15.5 h, which means that results were obtained within 24 h. In comparison, classical *in vivo* protein production including the strain construction and protein isolation takes at least several days.

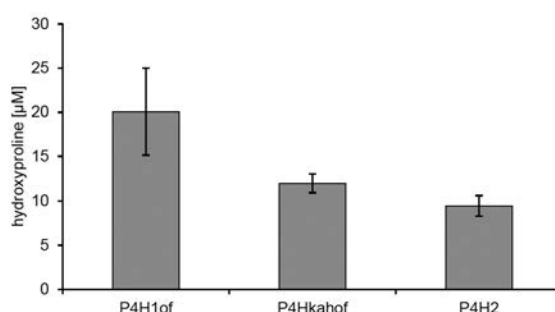


Figure 2: trans-4-hydroxy-L-proline concentrations after 15.5 h incubation with the *in vitro* synthesized trans-proline-4-hydroxylases P4H1of, P4Hkahof and P4H2 and 20 mM L-proline.

In conclusion, we showed the potential of *in vitro* protein synthesis as a tool for rapid production and screening of biocatalysts, which will definitely increase efficiency in biocatalyst development for biotechnological processes.

Contact:

stephan.luetz@tu-dortmund.de
katrin.rosenthal@tu-dortmund.de

Publications:

End, C., et al. (2014): *BIOspektrum* 20, p.70-72.
Kuruma, Y., Ueda, T. (2015): *Nature Protocols* 10, p. 1328-1344.
Falcioni, F., et al. (2013): *Applied and Environmental Microbiology* 79, p. 3091-3100.

Publications 2017 - 2015

In peer reviewed journal

2017

- S. Lütz
The First Biocatalytic Carbon-Silicon Bond Formation
Angewandte Chemie 56 (12), 3140-3141 (2017)
- C. Grumaz, Y. Vainshtein, P. Kirstahler, S. Lütz, M. Kittelmann, K. Schroer, F.K. Eggimann, R. Czaja, A. Vogel, T. Hilberath, A. Worsch, M. Girhard, V.B. Urlacher, M. Sandberg, Kai Sohn
Draft Genome Sequences of Three Actinobacteria Strains Presenting New Candidate Organisms with High Potentials for Specific P450 Cytochromes.
Genome Announcements 5 (28), e00532-17 (2017)
- K. Rosenthal, V. Oehling, C. Dusny, A. Schmid
Beyond the bulk: disclosing the life of single microbial cells
FEMS Microbiology Reviews 41 (6), 751-780 (2017)
- E. Theodosiou, M. Breisch, M.K. Julsing, F. Falcioni, B. Bühler, A. Schmid
An artificial TCA cycle selects for efficient α -ketoglutarate dependent hydroxylase catalysis in engineered *Escherichia coli*
Biotechnology and Bioengineering 114 (7), 1511-1520 (2017)
- R. Kourist, J. Gonzalez-Sabin, B. Siebers, M. Julsing
Editorial: Applied microbiology for chemical synthesis
Frontiers in Microbiology 8,1931 (2017)
- M. Kadisch, M.K. Julsing, M. Schrewe, N. Jehmlich, B. Scheer, M. von Bergen, A. Schmid, B. Bühler
Maximization of cell viability rather than biocatalyst activity determines whole-cell ω -oxyfunctionalization performance.
Biotechnology and Bioengineering 114 (4), 874-884 (2017)
- C. Willrodt, B. Halan, L. Karthaus, J. Rehdorf, M.K. Julsing, K. Bühler, A. Schmid
Continuous multistep synthesis of perillic acid from limonene by catalytic biofilms under segmented flow
Biotechnology and Bioengineering 114 (2), 281-290 (2017)
- J. Volmer, A. Schmid, B. Bühler
The application of constitutively solvent-tolerant *P. taiwanensis* VLB120 Δ C Δ ttgV for stereospecific epoxidation of toxic styrene alleviates carrier solvent use
Biotechnology Journal 12,1600558 (2017)

2016

- M. Antunes, F. Eggimann, M. Kittelmann, S. Lütz, S. P. Hanlon, B. Wirz, T. Bachler, M. Winkler
Human xanthine oxidase recombinant in *E. coli*: A whole cell catalyst for preparative drug metabolite synthesis
Journal of Biotechnology 235, 3-10 (2016)
- K. Lange, A. Schmid, M.K. Julsing
 Δ 9-Tetrahydrocannabinolic acid synthase: the application of a plant secondary metabolite enzyme in biocatalytic chemical synthesis
Journal of Biotechnology 233, 42-48 (2016)
- C. Willrodt, A. Hoschek, B. Bühler, A. Schmid, M.K. Julsing
Decoupling production from growth by magnesium sulfate limitation boosts de novo limonene production
Biotechnology and Bioengineering 113 (6), 1305-1314 (2016)
- N. Ladkau, M. Abmann, M. Schrewe, M.K. Julsing, A. Schmid, B. Bühler
Efficient production of the Nylon 12 monomer ω -aminododecanoic acid methyl ester from renewable dodecanoic acid methyl ester with engineered *Escherichia coli*
Metabolic Engineering, 36, 1-9 (2016)

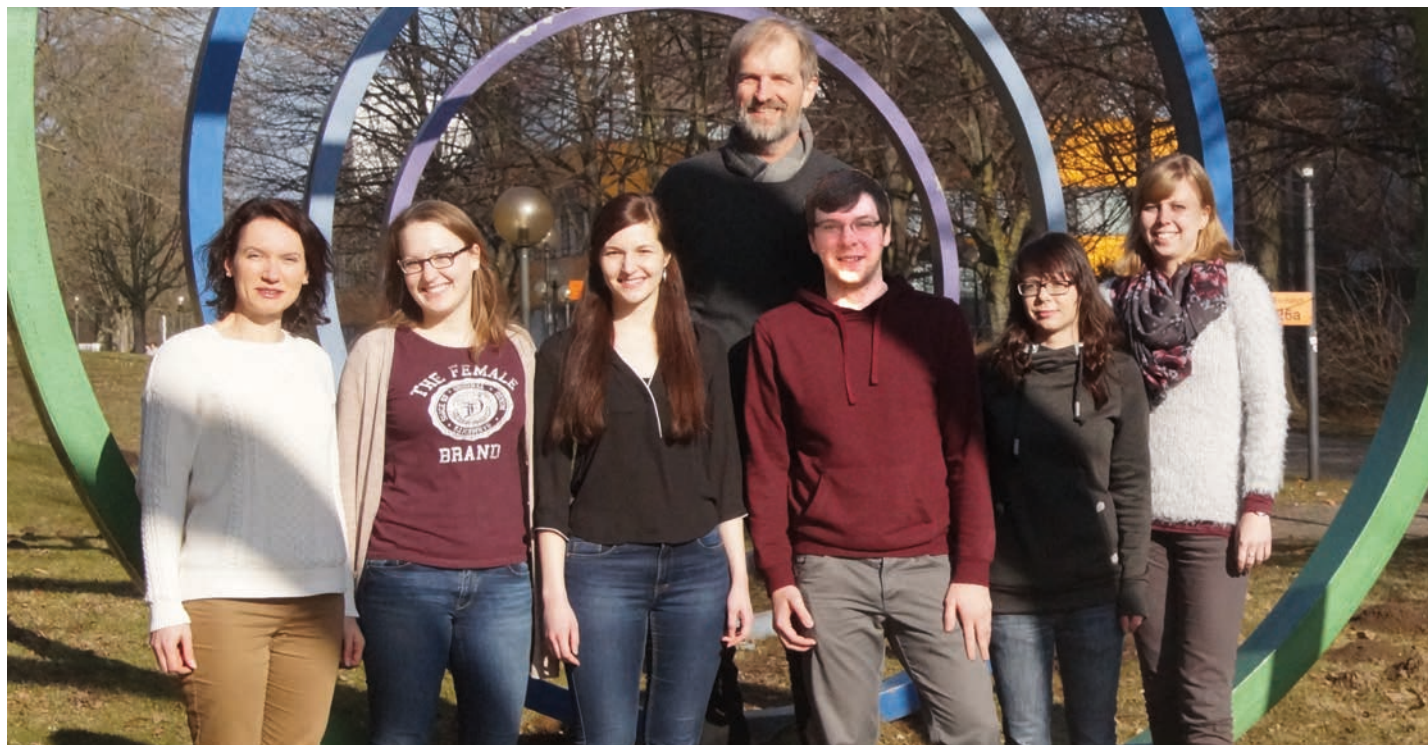
Proceedings & Book Chapters

2015

- M. Geier, T. Bachler, S. P. Hanlon, F. Eggimann, M. Kittelmann, H. Weber, S. Lütz, B. Wirz, M. Winkler
Human FMO2-based microbial whole-cell catalysts for drug metabolite synthesis
Microbial Cell Factories 14, 82 (2015)
- K. Rosenthal, F. Falke, O. Frick, C. Dusny, A. Schmid
An inert continuous microreactor for the isolation and analysis of a single microbial cell
Micromachines 6 (12), 1836-1855 (2015)
- J. Volmer, A. Schmid, B. Bühler
Guiding bioprocess design by microbial ecology
Current Opinion in Microbiology 25, 25-32 (2015)
- K. Lange, A. Schmid, M.K. Julsing
 Δ -9-Tetrahydrocannabinolic acid synthase production in *Pichia pastoris* enables chemical synthesis of cannabinoids
Journal of Biotechnology, 211, 68–76 (2015)
- K. Lange, A. Poetsch, A. Schmid, M.K. Julsing
Enrichment and identification of Δ -9-tetrahydrocannabinolic acid synthase from *Pichia pastoris* culture supernatants
Data in Brief, 4, 68–76 (2015)
- C. Willrodt, A. Hoschek, B. Bühler, A. Schmid, M.K. Julsing
Coupling limonene formation and oxyfunctionalization by mixed-culture resting cell fermentation
Biotechnology and Bioengineering, 112(9), 1738-1750 (2015)
- C. Looße, S. Galozzi, L. Debor, M.K. Julsing, B. Bühler, A. Schmid, K. Barkovits, T. Müller, K. Marcus
Direct infusion-SIM as fast and robust method for absolute protein quantification in complex samples
EuPA Open Proteomics, 7, 20-26 (2015)
- C. Willrodt, R. Karande, A. Schmid, M.K. Julsing
Guiding efficient microbial synthesis of non-natural chemicals by physicochemical properties of reactants
Current Opinion in Biotechnology, 35, 52-62 (2015)

2017

- L.M. Schmitz, K. Rosenthal, S. Lütz
Enzyme-Based Electrobiotechnological Synthesis
Advances in Biochemical Engineering/Biotechnolog. In: Advances in Biochemical Engineering/Biotechnology. Springer, Berlin, Heidelberg (2017)



Biochemical Engineering (BVT)

Process Improvement of fermentative Fusicocadiene Production

Lisa Halka, Rolf Wichmann

*Fusicocca-2.10(14)-diene (FCdiene), a fusicoccane, is a tricyclic diterpene which has use in the pharmaceutical industry as a precursor of the anti-cancer drug Fusicoccin A. Chemical synthesis of this diterpene is not economical as it requires 14 steps, partial stereospecific ones. FCdiene is naturally produced at low titers in phytopathogenic, filamentous fungi. However, production of FCdiene can also be achieved via expression of the fusicocadiene synthase in the yeast *Saccharomyces cerevisiae*.*

Batch and fed-batch cultivations of FCdiene producing *Saccharomyces cerevisiae* abfs were done in shaking flasks and in a 3.1 L KLF 2000 fermenter using a synthetic dropout medium and glucose as sole carbon source. In batch mode two main adjusting screws for the synthesis of FCdiene were identified, pH and DOT.



Figure 1: Lab-scale fermenter.

The results of several cultivations in shaking flask scale indicate that regulating pH while using glucose as sole carbon source decreases FCdiene productivity up to 70 % in comparison to unbuffered fermentations. Buffered cultivations using the KLF 2000 fermenter resulted in lower FCdiene concentrations as well. The results of this investigation indicate higher FCdiene yields with unregulated pH regardless of any buffering system. Additional uncontrolled pH shifts during cultivation may also be advantageous because of decreased risk of culture contamination at low pH (nearly 2.5).

In unbuffered cultivations with changed amino acid concentrations to avoid predicted limitations, FCdiene concentrations up to 270 mg/L were reached and more than 10X greater yields than previously achieved with this strain.

Contact:

lisa.halka@tu-dortmund.de

rolf.wichmann@tu-dortmund.de

No solubility limit for FCdiene is currently known. At the moment it is unclear if the concentration of FCdiene in culture media surpasses the solubility limit, or whether free fatty acids and other extracellular metabolites contribute to its solubility. No flocculent or second phase was apparent during fermentation and harvesting.

The influence of DOT on glucose cultivations was determined in stirred tank batch fermentations at different stirring frequencies. The highest FCdiene concentration was not found at the highest stirring rate but at values where microaerobic conditions slightly above 0 % DOT were maintained throughout the fermentation.

Microaerobic conditions seem to be the preferred condition for FCdiene production from *S. cerevisiae*, although the exact reason is not readily apparent. It is possible that the terpenoid metabolism in the yeast *S. cerevisiae* is influenced by the microaerobic conditions, or the conditions are favorable for the FCdiene secretion.

But as widely known the Crabtree effect occurs in these fermentations, thus a fed-batch fermentation mode with *S. cerevisiae* using glucose as a carbon source has been developed. The aim was an exponential feeding profile which avoids overfeeding of the used yeast culture and increases growth and production. Therefore, an iterative development of a feeding profile was carried out. The cell concentration was increased up to 246 % in comparison to the batch fermentations and the FCdiene concentration increased up to 2.8X within the first 28 h and increased further while extending the fermentation time of the fed-batch fermentation. The production of FCdiene in *S. cerevisiae* did not correlate with growth of the yeast.

The results of these studies indicate there is a potential for economical fed-batch fermentation processes for FCdiene production using this genetically modified *S. cerevisiae*. Yields presented here illustrate 3X improvement over former studies and concentrations show more stable values as batch fermentations. The new feed strategy of glucose would appear to present benefit of favorable terpene production from *S. cerevisiae*.

Foam Adsorption as a new Generation unit Operation for recovery of Amphiphilic Compounds

Intensification of fermentative production of rhamnolipids by integration of upstream and downstream process

Iva Anic, Arijit Nath, Pedro Franco, Ines Apolonia, Rolf Wichmann

In order to limit the formation of foam during fermentation processes antifoam agents are often added to the fermentation medium. Their separation from the product results in increase of downstream process costs. This issue in downstream processing can be solved with an innovative product capture method called "foam adsorption". The focus of our research is on the development and utilization of this new separation method which is based on the integration of the upstream and the downstream process.

Rhamnolipids (RLs) containing foam is created in the fermentor during aerated fermentation. Instead of suppressing the foam formation, foam is led by the air flow into the adsorption column attached to the gas exhaust line of the fermentor. Due to hydrophobic-hydrophobic interaction between the amphiphilic RLs and hydrophobic adsorbent, the RLs stay adsorbed in the column so that the resulting liquid phase can be recycled back into the fermenter, while the off gas is released out of the system.

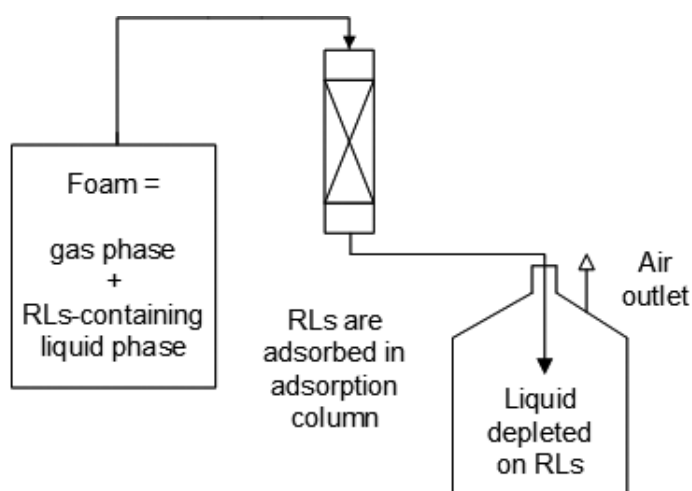


Figure 1: Schematic representation of the RLs separation principle using the foam adsorption method.

For this purpose five pre-selected, commercially available adsorbents were screened and rated regarding the adsorption capacity and product recovery. High concentration of the amphiphilic compound in the liquid lamella of the foam is favorable, so the adsorption capacity of the selected adsorbent was utilized extremely well with 0.38 g per g adsorbent.

An automated adsorption unit was designed to perform fed-batch experiments on lab-scale. It consists of two adsorption columns packed with C18 modified silica adsorbent operated in parallel during the fermentative production of RLs. Once the maximum capacity of the adsorbent is reached the adsorption column is washed with water and the product is eluted with ethanol.

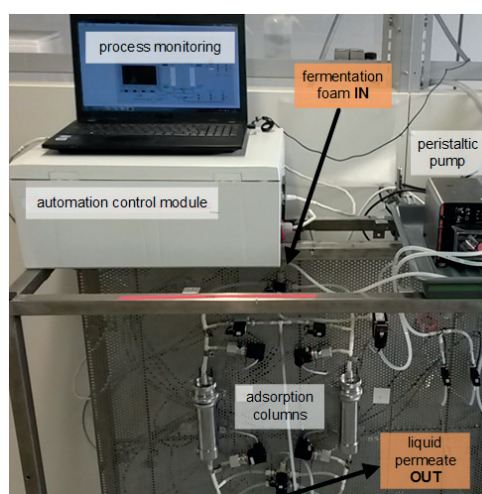


Figure 2: Experimental setup of automated adsorption unit: adsorption and desorption process was automatically operated during the fed-batch fermentation.

A fed-batch process for the production of rhamnolipids by *Pseudomonas putida* KT2440 was performed for 60 hours. 95 % of the product was captured in the adsorption columns. Product recovery of 85 % and a purity of 96 % were determined.

Foam adsorption can be integrated in fermentation processes where an amphiphilic product is produced continuously, which has inhibitory effects on the producing cells, or is unstable in the fermentation broth; whereby the product itself is stabilized and enriched in the foam phase.

Acknowledgement: We like to thank the Laboratory of Biomaterials and Polymer Science, TU Dortmund, for helpful discussion and the use of equipment.

Publications:

I. Anic, A. Nath, P. Franco, R. Wichmann, *Journal of Biotechnology* 258, 181–189 (2017).
DOI: 10.1016/j.jbiotec.2017.07.015.

Contact:

iva.anic@tu-dortmund.de
rolf.wichmann@tu-dortmund.de

Publications 2017 - 2015

2017

- I. Anic, J. Schwarz, R. Wichmann
Three liter scale process for fermentative production and separation of rhamnolipid biosurfactants produced by non-pathogenic *Pseudomonas putida* KT2440 strain
Journal of Biotechnology 256S, S20 (2017)
- I. Anic, A. Nath, P. Franco, R. Wichmann
Foam adsorption as an ex situ capture step for surfactants produced by fermentation
Journal of Biotechnology 258SI, 181-189 (2017)

Patent application

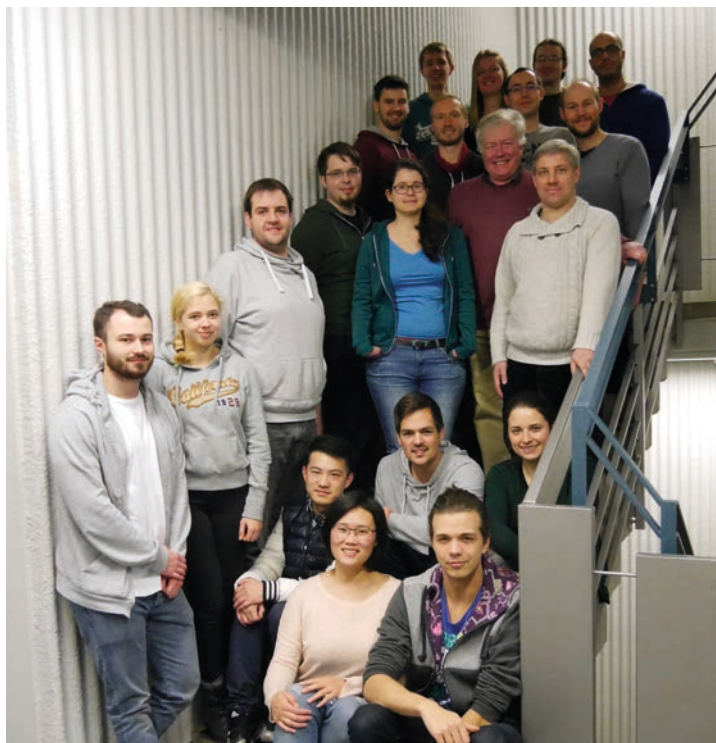
- LU No 93393, Priorität: 22.12.2016 (2016)
In Situ Separation of Amphipathic Compound by Foam Adsorption
I. Anic, R. Wichmann, A. Nath, P. Franco

2016

- D. von der Haar, G. Gofferjé, A. Stäbler, R. Wichmann, T. Herfellner
Kinetics of Lipase-catalyzed De-acidification of Degummed Rapeseed Oil Utilizing Monoacylglycerol as Acyl-group Acceptor
Journal of Molecular Catalysis B-Enzymatic 127, 40-46 (2016)
- M. Kampmann, N. Riedel, Y.L. Mo, L. Beckers, R. Wichmann
Tyrosinase Catalyzed Production of 3,4-Dihydroxyphenylacetic Acid Using Immobilized Mushroom (*Agaricus bisporus*) Cells and in Situ Adsorption
Journal of Molecular Catalysis B-Enzymatic 123, 113-121 (2016)
- L.M. Halka, S. Kockelke, R. Wichmann
In Situ Product Removal of Fermentatively Produced Fusicoccadiene Using a Two-phase System
Chemie-Ingenieur-Technik 9, 1328 (2016)
- T. Tiso, A. Germer, B. Küpper, R. Wichmann, L.M. Blank
Methods for Recombinant Rhamnolipid Production
In: T.L. McGenity, K.N. Timmis, B. Nogales Fernández (Hrsg.), Hydrocarbon and Lipid Microbiology Protocols: Synthetic and Systems Biology – Applications, Springer-Verlag, Berlin Heidelberg, 65-94 (2016)

2015

- M. Kampmann, A.C. Hoffrichter, D. Stalinski, R. Wichmann
Kinetic Characterization of Tyrosinase Containing Mushroom (*Agaricus bisporus*) Cells Immobilized in Silica Alginate
Journal of Molecular Catalysis B-Enzymatic 116, 124-133 (2015)
- D. von der Haar, A. Stäbler, R. Wichmann, U. Schweiggert-Weisz
Enzyme-assisted Process for DAG Synthesis in Edible Oils
Food Chemistry 176, 263-270 (2015)
- S. Tomic, L. Besnard, B. Fürst, R. Reithmeier, R. Wichmann, P. Schelling, C. Hakemeyer
Complete Clarification Solution for Processing High Density Cell Culture Harvests
Separation and Purification Technology 141, 269-275 (2015)
- D. von der Haar, A. Stäbler, R. Wichmann, U. Schweiggert-Weisz
Enzymatic Esterification of Free Fatty Acids in Vegetable Oils Utilizing Different Immobilized Lipases
Biotechnology Letters 37(1), 169-174 (2015)



Chemical Reaction Engineering (CVT)

Flexible Adjustment of liquid-liquid slug length in Micro-Channels

Linda Arsenjuk, Moritz Asshoff, David W. Agar

The slug length of liquid-liquid flow in micro-capillary reactors has a decisive influence on mass transfer and thus reactor performance. As it depends on material properties and fluid velocities, it used to be more of a system characteristic, than a controllable variable. A slug generator with variable mixing point geometry is presented which enables stable and reproducible adjustment of slug size, independent of material and system properties.

The implementation of multi-phase reactions in micro-fluidic devices offers a promising approach for process intensification. Short diffusion paths and large surface to volume ratios enhance heat and mass transfer, while low hold-up and system inertia make processes safer and easier to handle.

If two immiscible liquids are contacted in a micro-channel, a flow regime called slug flow occurs under certain conditions. It is characterized by periodically alternating segments of fluid, called slugs. Flow conditions in liquid-liquid slug flow further increase mass transfer through vortex structures in the fluid segments, while axial dispersion is reduced, providing a defined and narrow residence time distribution (Figure 1).

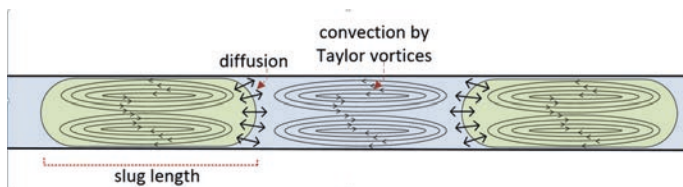


Figure 1: Schematic of liquid-liquid slug flow in a micro-channel.

The resulting slug length is dependent on flow rate, phase ratio and material properties, as well as the geometry of the mixing point of the phases. As it defines the phase interface and impacts the structures of the internal vortices, it has a decisive influence on mass transfer. It is thus desirable to decouple resulting slug lengths from material system and flow conditions, to allow independent adjustment, to a value optimal for the respective application.

For this purpose a slug generator with adjustable mixing point geometry has been designed (Figure 2). The disperse phase is supplied through a concentric metal capillary with a tapered head, while the continuous phase flows coaxially along the outer cylinder. The phases concur in a conical mixing point.

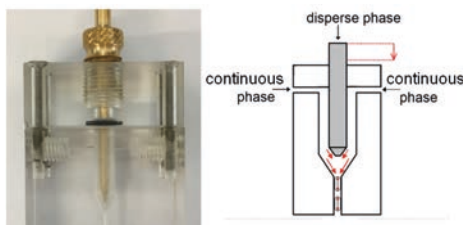


Figure 2: Slug generator with adjustable mixing point geometry and schematic thereof.

Contact:

linda.arsenjuk@tu-dortmund.de
david.agar@tu-dortmund.de

By increasing the insertion depth of the disperse inlet, the volume of the mixing chamber decreases. This reduces the available volume for slug generation and consequently slug size.

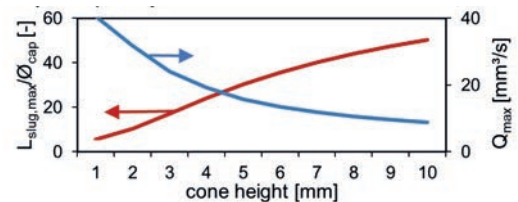


Figure 3: CFD simulated dependence of maximal flow rate Q_{max} and maximal achievable slug length $L_{slug,max}/D_{cap}$ on height of mixing cone.

With aid of CFD simulations, an operating region of the generator has been identified, where the droplet detachment process is governed by surface forces and thus predominantly dependent on size of the mixing chamber. Boundaries of the operation region, maximum flowrate and maximum achievable slug length, are dependent on the inclination of mixing chamber and thus height of the cone (Figure 3).

Simulated results were confirmed experimentally, for the material systems Kerosene/Water and Dodecan/Water. Stable, adjustable slug generation, with minor influence of material system or flow rate, but strong dependence on mixing point volume was achieved, with $\sigma_{max} < 0,17\text{mm}$ (Figure 4).

The developed slug generator successfully decouples slug length from other material and system influences and thus makes another important reactor parameter accessible for optimization.

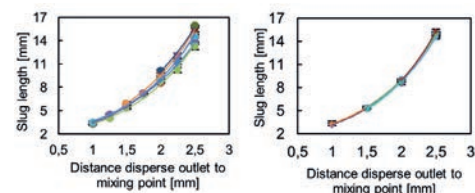


Figure 4: Experimental slug length resulting at different settings of slug generator, velocities ranging from 0.5-14mm/s, left: Kerosene/Water, right: Dodecan/Water.

Selective Partial Oxidation of Hydrogen Sulfide via BrOx Cycle

Maximilian Wieseahn, Mahsa Moghaddam, Thomas Kembügler, David W. Agar

The research on the bromination-oxidation (BrOx) cycle at the chair of chemical reaction engineering has been applied to hydrogen sulfide (H_2S) among other reactants. The utilization of bromine instead of oxygen to oxidize hydrogen sulfide is preferred in order to avoid the formation of corrosive and toxic sulfur dioxide (SO_2). Instead solid sulfur is formed, which is much easier to handle and the bromine is retrieved in a subsequent oxidation step. As long as the bromine recovery is complete and the formation of brominated side-products is avoided, the BrOx cycle has the potential to be applied for the desulfurization of sour gas.

Typically the neutralization of hydrogen sulfide from natural gas or oil is carried out within a Claus plant, where the highly toxic and corrosive gas is converted into sulfur. Because of the environmental problems, which H_2S would cause, the desulfurization is mandatory. However, multiple plant units are required to ensure complete H_2S conversion and sometimes additional tail gas treatment is necessary. Although the Claus process is well established in today's large scale industrial production, there is still a lot of research going on in this field and the investigation of alternative processes can prove beneficial.

The BrOx cycle is a novel way for removing hydrogen sulfide completely in two exothermic reaction steps. First H_2S is oxidized by bromine and the formed sulfur can be separated off. The second reaction, the oxidation of HBr serves for the regeneration of bromine, thus closing the cycle. Overall, the process generates energy with the products being sulfur and water.

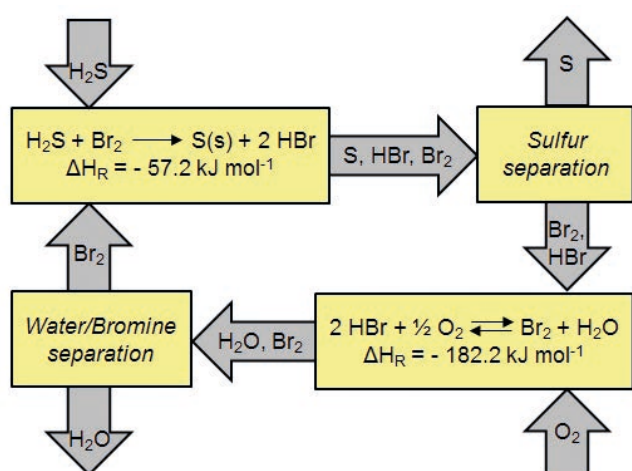


Figure 1: Schematic representation of the BrOx cycle.

The proof-of-principle for the H_2S bromination was provided in a testing plant by reaching HBr yields of up to 77 % at 450 °C. The prospective aim is to reach maximum H_2S conversions by using slight excesses of bromine.

During the H_2S bromination there is also the possibility of the formation of brominated sulfur by-products, like S_2Br_2 . Not only would this compound contaminate the sulfur but remove some bromine from the cycle as well, which would make an external feed of bromine a necessity. Because of this, the produced sulfur has been analyzed via EDX on its bromine content with a result of it containing 1 At.-% of bromine at maximum with none of that being chemically bound. Furthermore investigations regarding S_2Br_2 formation and decomposition indicated, that at temperatures above 150 °C - which is far below the reaction temperature - the presence of brominated sulfur species is negligible.

The second reaction, the oxidation of HBr, is strongly exothermic and has negative Gibbs free energy up to very high temperatures, which indicates that the equilibrium conversion will diminish with an increase in temperature (Figure 2). The oxidation can be carried out uncatalyzed at high temperatures or in presence of a catalyst. Experimentally, HBr conversions up to 90 % have been reached in the thermal stage at 830 °C and up to 93 % in a reactor with RuO_2 catalyst at 315 °C. Since thermal and catalytic oxidation are complementing each other, the proposal is to combine those methods and run the thermal process, followed by catalyzed oxidation to reach maximum conversion.

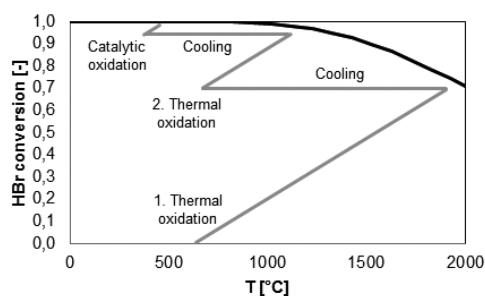


Figure 2: Proposal for a multistage oxidation of HBr.

Contact:
 maximilian.wieseahn@tu-dortmund.de
 david.agar@tu-dortmund.de

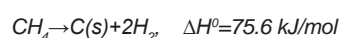
Theoretical and Experimental Studies on Reactors for the high Temperature Methane Pyrolysis

Finding new ways to produce hydrogen and energy from fossil fuels without CO₂ emissions

Alejandro A. Munera Parra, I. Schultz, David W. Agar

The question of how clean energy can be provided to an ever increasing population becomes more urgent every year. Last year, theoretical studies on an industrial reactor and experimental work on a novel reactor for the pyrolysis of methane were carried out. The theoretical work focused on the occurrence of multiplicities in moving bed reactors, while the experimental work further developed the concept of a molten metal capillary reactor.

The pyrolysis of methane:



can be carried out in an industrial scale in a moving bed reactor. In order to maximise the heat recovery, a heat integrated moving bed reactor is proposed as shown in Figure 1a with the corresponding simulated temperature and conversion profiles in Figure 1b. Although not extensively known, multiple steady states can occur in moving bed reactors, using continuation methods, these multiplicity regions can be mapped for different parameters in this case, the region for solid to gas flow ratio and inlet temperature is exemplified in Figure 1c.

In addition it can be proved that the multiplicity phenomenon pertains not only to exothermic reactions as most commonly found in the literature but that for endothermic reactions, depending on the way that heat is added to the reactor, multiple steady states can occur due to the interaction between the non-linear heat consumption, the non-linear heat input and the heat feedback due to the countercurrent flow.

This mapping of the regions helps to determine constraints where the reactor should not be operated and helping gain insight in the behaviour of the system.

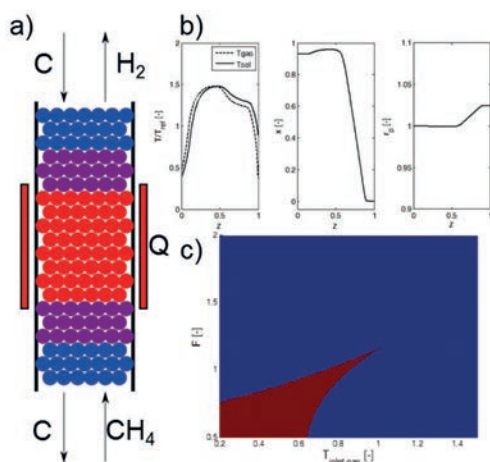


Figure 1: a) Heat integrated moving bed reactor. b) Concentration, particle size and temperature profiles alongside the reactor. c) Region of multiplicities for a standard moving bed reactor.

Contact:

alejandro.munera@tu-dortmund.de
david.agar@tu-dortmund.de

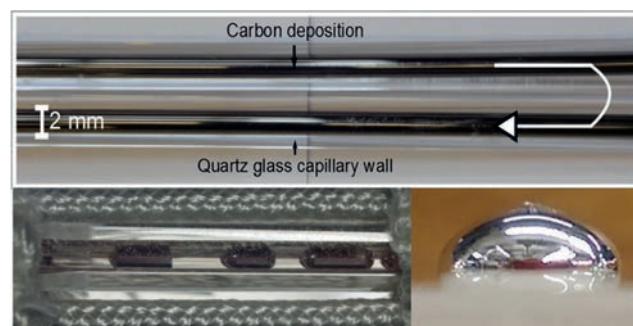


Figure 2: Top: Carbon deposition in the capillary reactor. Bottom left: slug-flow regime. Bottom right: Galinstan drop at room temperature

The two main hurdles found when carrying out the pyrolysis of methane, are the carbon formation and the need to introduce heat at higher temperatures. The use of liquid media such as molten metals has been used to circumvent both these problems in an elegant way, on the one hand, the liquid media acts as a barrier preventing the carbon deposition at the heat transfer area, as well as a heat transfer medium due to its excellent transport properties. A molten metal capillary reactor operated in slug flow regime (Figure 2b), offers besides the good transfer properties and the formation of a protective film with surface renewal, a sharper residence time distribution in comparison with other reactors found in the literature such as bubble columns. However, operation with pure Tin has shown that carbon deposition (Figure 1a) still occurs when the high temperatures (1200-1300 °C) needed to obtain full conversion are reached. The use of alloys with better wetting properties such as Galinstan (Gallium, Indium, and Tin eutectic) is being studied. In addition Galinstan remains liquid at room temperature as seen in Figure 2c, facilitating its use and allowing trying different pumpless scenarios to feed the reactor.

Publications:

A.A. Munera Parra, F. Platte, D.W. Agar, European Symposium on Chemical Reaction Engineering, ESCRE, Fürstenfeldbruck, Germany (2015)

I. Schultz, D.W. Agar, Int. J. Hydrogen Energy 40 (35), 11422-11427 (2015).

Publications 2017- 2015

2017

- A.A. Munera Parra, D.W. Agar
Molten metal capillary reactor for the high-temperature pyrolysis of methane
International Journal of Hydrogen Energy, 42 (19), 13641-13648. (2017)
- A.A. Munera Parra, C. Asmanoglo, D.W. Agar
Cyclic Steady-State Behavior of a Fixed-Bed Adsorptive Reactor for Reverse Water-Gas Shift Reaction
Chemical Engineering and Technology, 40 (5), 915-926. (2017)
- J. González Rebordinos, A.H.J. Salten, D.W. Agar
BrOx cycle: A novel process for CO₂-free energy production from natural gas
BrOx cycle: A novel process for CO₂-free energy production from natural gas
- J. González Rebordinos, J. Kampwerth, D.W. Agar
Flowsheeting and optimisation of the BrOx cycle for CO₂-free energy production from natural gas
Energy, 133, 327-337. (2017)
- M.G. Gelhausen, S. Yang, M. Cegla, D.W. Agar
Cyclic mass transport phenomena in a novel reactor for gas-liquid-solid contacting
AIChE Journal, 63 (1), 208-215. (2017)

2016

- N. Antweiler, S. Gatberg, G. Jestel, J. Franzke, D.W. Agar
Noninvasive Sensor for the Detection of Process Parameters for Multiphase Slug Flows in Microchannels
ACS Sensors, (2016)
- M.G. Gelhausen, S. Yang, M. Cegla, D.W. Agar
Cyclic mass transport phenomena in a novel reactor for gas-liquid-solid contacting
AIChE Journal 63(1), 208-215 (2016)
- N. Antweiler, Z. Wang, D.W. Agar
Evaluation of Ion Exchange Resins for the Esterification of Acrylic Acid with n-Butanol by Polytopic Kinetic Measurement
Chemie Ingenieur Technik 88 (8), 1095-1101 (2016)
- L. Arsenjuk, F. Kaske, J. Franzke, D.W. Agar
Experimental investigation of wall film renewal in liquid-liquid slug flow
International Journal of Multiphase Flow 85, 117-185 (2016)
- J.F. Horstmeier, A. Gomez Lopez, D.W. Agar
Performance improvement of vacuum swing adsorption processes for CO₂ removal with integrated phase change material
International Journal of Greenhouse Gas Control 47, 364-375 (2016)
- F. Kaske, S. Dick, S. Aref Pajoochi, D.W. Agar
The influence of operating conditions on the mass transfer performance of a micro capillary contactor with liquid-liquid slug flow
Chemical Engineering and Processing: Process Intensification 108, 10-16 (2016)

- A.A. Munera Parra, F. Platte, D.W. Agar
Multiplicity Regions in a Moving-Bed Reactor: Bifurcation Analysis, Model Extension, and Application for the High-Temperature Pyrolysis of Methane
Chemie Ingenieur Technik 88(11), 1703-17 (2016)

- A.A. Munera Parra, D.W. Agar
Molten Metal Capillary Reactor for the High Temperature Pyrolysis of Methane
International Journal of Hydrogen Energy, (2016)

2015

- N. Antweiler, S. Gatberg, J. Franzke, D.W. Agar
Neue kosteneffektive Mess- und Regeltechnik für das Numbering-up von reaktiven Pfropfenströmungen in Mikrokanälen
Chemie Ingenieur Technik 87(9), 1221-1229 (2015)
- A.K. Liedtke, F. Scheiff, F. Bornette, R. Philippe, D.W. Agar, C. de Bellefon
Liquid-solid mass transfer for microchannel suspension catalysis in gas-liquid and liquid-liquid segmented flow
Industrial & Engineering Chemistry Research 54(17), 4699-4708 (2015)
- I. Schulz, D.W. Agar
Decarbonisation of fossil energy via methane pyrolysis using two reactor concepts: Fluid wall flow reactor and molten metal capillary reactor
International Journal of Hydrogen Energy 40(35), 11422-11427 (2015)

Conference proceedings

2016

- M. Hussainy, D.W. Agar
Structural and Operational Optimality of Adsorptive Reactors
Chemical Engineering & Technology 39(11), 2135-2141 (2016)

Proceedings & Book Chapters

2016

- A. Behr, D.W. Agar, J. Jörissen, A.J. Vorholt
Einführung in die Technische Chemie
2. Aufl., Springer: Berlin. (2016)



Process Dynamics and Operations (DYN)

Application of Iterative Real-time Optimization in an Industrial Pilot Plant

The optimal operating point of a lithiation process in a containerized pilot plant is determined in real-time in the presence of process noise and significant plant-model mismatch

Anwesh Reddy Gottu Mukkula, Sebastian Engell

A lithiation process – a key organic synthesis step – which is performed in an intensified tubular reactor in a containerized pilot plant at INVITE in Leverkusen is optimized using modifier adaptation with quadratic approximation (MAWQA), a state-of-the-art real time optimization (RTO) algorithm developed at TU Dortmund. The iterative model and measurement based optimization scheme drives the process to the plant optimum which is different from the optimum which is obtained from the process model.

It is of great interest to identify the optimal point of a plant and to operate it at this point. Usually, the optimal operating point of a plant is identified by solving a model-based optimization problem. Developing an accurate mathematical model and estimating its parameters require a large amount of time and effort. Sometimes it may not be possible at all to develop an accurate model due to the complex phenomena that take place in the plant.

Modifier adaptation with quadratic approximation (MAWQA) is an iterative optimization scheme which uses the plant measurements to drive the plant to its true optimum in spite of having a plant-model mismatch. In MAWQA, the iterative gradient-modification optimization (IGMO) method is combined with a derivative free optimization (DFO) method to estimate the plant gradients along with an additional surrogate model.

The process under consideration is a lithiation reaction that takes place in a tubular reactor. The reaction mechanism and its kinetic parameters are not precisely known. The overall reaction is depicted in Figure 1.

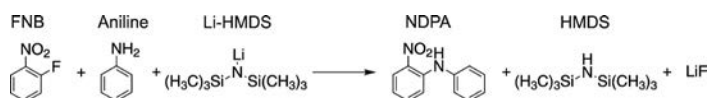


Figure 1: Overall lithiation reaction scheme.

Due to the unavailability of the complete reaction information, the mathematical model of the process is incomplete and does not represent the behavior of the plant accurately.

The aim of the controller is to operate the process at its economically optimal operating point using the concentration measurements from a novel online NMR device that was developed by BAM, Berlin. A challenge for the use of iterative optimization in this process and similar ones is the presence of long measurement delays due to the long piping and the low flow rates between the reactor and the measurement system. Two improved variants of the scheme were proposed to overcome the problems that are caused by the measurement delays by proactive probing of the plant [1, 2].

Contact:

anweshreddy.gottumukkula@tu-dortmund.de
sebastian.engell@tu-dortmund.de

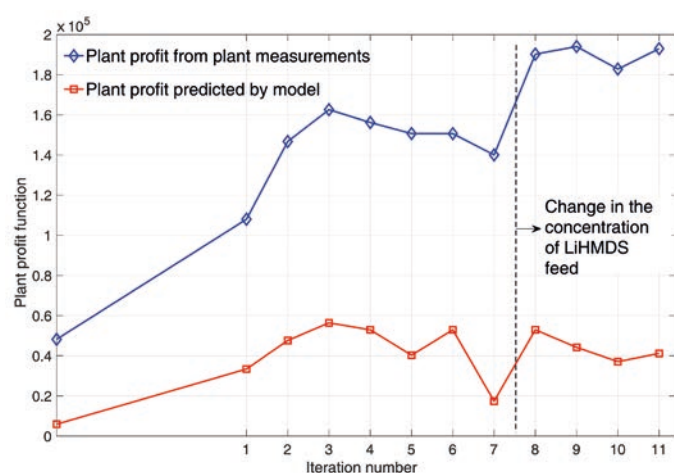


Figure 2: Plant cost over MAWQA iterations in the validation experiment performed at the pilot plant in INVITE, Leverkusen.

Results from experiments:

The evolution of the plant profit during the iterative optimization using the NMR measurements by the MAWQA iterations is shown in Figure 2. The blue line indicates the real plant profit as computed from the measurements whereas red line represents the plant profit as computed from the nominal model which has both structural and parametric plant-model mismatch. After an unknown change of the feed concentration of Li-HMDS, the algorithm improved the plant profit (blue line) significantly. In contrast the plant profit function that was predicted by the model drops as a fixed value for the feed concentration is assumed.

In summary, it was validated that the combination of the NMR measurement with the iterative optimization algorithm MAWQA could drive the plant to an optimal operation despite significant deviations between the plant model and the true plant behavior. MAWQA reacted quickly to changes in the process conditions and responded by making input moves to identify the true process optimum.

Publications:

A.R. Gottu Mukkula, S. Wenzel, and S. Engell, (2018). Active perturbation in modifier adaptation for real time optimization to cope with measurement delays. In Third IFAC International Conference on Advances in Control and Optimization of Dynamical Systems (Accepted).

A.R. Gottu Mukkula, S. Wenzel, and S. Engell, (2018). Active perturbation around estimated future inputs in modifier adaptation to cope with measurement delays. In Tenth IFAC International Conference on Advanced Control of Chemical Processes (Submitted).

Real-time Optimization of Chemical Processes under Uncertainty - Proof of Concept in a Miniplant

A reliable RTO scheme that can cope with plant-model mismatch has been developed and was applied to the hydroformylation of long-chain olefins in a continuously operated miniplant

Reinaldo Hernández, Sebastian Engell

Real-time Optimization (RTO) is a tool to improve the performance of chemical plants by a model-based optimization of the stationary operating point of the plant. A critical issue in RTO is the quality of the model. The DYN group has developed methods and algorithms to cope with model imperfections in RTO. Here, the application of a recently developed iterative RTO scheme to a homogeneously catalyzed process in a miniplant is described.

The goal of RTO is to optimize the performance of a production process while satisfying environmental, safety, quality and equipment-related constraints. A major challenge in RTO is plant-model mismatch. As a result of using an inaccurate model, suboptimal operation and constraint violations may occur. This is particularly relevant in the case of processes for the production of speciality chemicals where uncertainties related to thermodynamic parameters, reaction kinetics and catalyst activity limit the applicability of model-based optimization.

During the last years, the DYN group has tackled the problem of RTO under plant-model mismatch based on the iterative correction of the nominal optimization problem on the basis of plant measurements in the so-called modifier adaptation (MA) scheme. MA was improved by fitting local quadratic models to the measurements to estimate the plant gradient. Until now, the benefits of modifier adaptation were for the most part demonstrated in simulation studies. Only few published works deal with simple real processes.

In order to validate the potential of iterative real-time optimization based on modifier adaptation, we have applied it to the rhodium catalyzed hydroformylation of 1-dodecene in a thermomorphic solvent system in a miniplant. It makes use of transition metal complex catalysis which is considered as a key technology in green chemistry due to the high activity and selectivity at mild reaction conditions. The processing of this substrate poses similar challenges as the processing of oleochemicals. Hydroformylation is a model reaction due to its similarities to other transition metal catalyzed processes such as hydrocarbonylation, hydroesterification, amination, etc.

For the application, we have developed a reliable iterative Real-time Optimization scheme which is able to also handle measurement noise by integrating methods for automatic steady state identification and robust data reconciliation (see Figure 1). Simulations studies showed that the iterative

optimization is able to drive the plant to optimality despite the presence of model inaccuracies related to catalyst activity, mass transfer, and kinetic parameters. In collaboration with the Technical Chemistry Group, the scheme was implemented in the continuously operated miniplant for the hydroformylation of 1-dodecene.

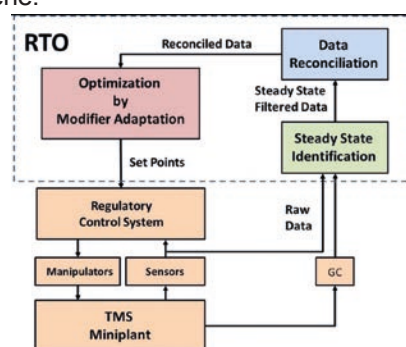


Figure 1: Implementation of the RTO scheme at the miniplant.

Figure 2 shows the yield of the target product (tridecanal) before and after the application of the proposed scheme. First, the optimal conditions that were computed based upon the process model were implemented and then the iterative Real-time Optimization algorithm was started. As it can be seen, a significant improvement of the performance of the process beyond the predictions of the nominal model could be realized. The modifier adaptation with quadratic approximation (MAWQA) scheme is a generally applicable tool to improve process performance even when no accurate process model is available.

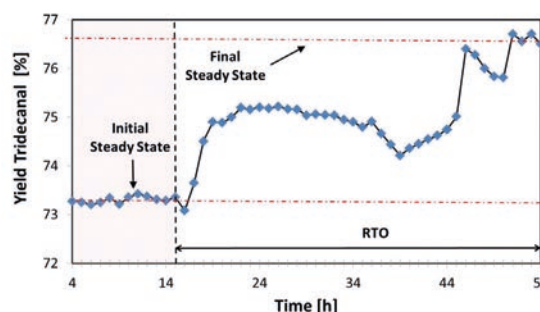


Figure 2: Yield of tridecanal in the continuously operated miniplant.

Publications:

R. Hernandez, J. Dreimann, A. Vorholt, A. Behr, S. Engell, An iterative Real-time Optimization Scheme for the optimal operation of chemical processes under uncertainty. Proof of concept in a miniplant. Ind. Eng. Chem. Res. Sub. (2018).

R. Hernández, S. Engell, Modelling and iterative Real-time Optimization of a homogeneously catalyzed hydroformylation process. Computer Aided Chemical Engineering. 38, 1-6 (2016).

W. Gao, R. Hernández, S. Engell, A study of exploratory moves during Modifier Adaptation with Quadratic Approximation. Processes, 4 (45), (2016).

Contact:

reinaldo.hernandez@tu-dortmund.de
sebastian.engell@tu-dortmund.de

Economics Optimizing Control of a Pilot-Scale Reactive Distillation Process

Improving the economic performance of a complex chemical process with several degrees of freedom by means of nonlinear model predictive control using economically motivated objectives

Daniel Haßkerl, Clemens Lindscheid, Steven Markert, Sebastian Engell

Dynamic Real-time Optimization (D-RTO) combines nonlinear model predictive control (NMPC) with economic objectives to improve the profitability of chemical processes. Such control strategies have been discussed intensely in the scientific literature, but their application to real processes so far has been limited. We have successfully applied this approach to a very complex real pilot-scale process that is described by a large DAE model. In the past, to use such complex models for online optimization was not feasible, but recently developed computational methods can overcome these limitations. In cooperation with the Chair of Fluid Separations, the successful application of economics optimizing control at a pilot-scale reactive distillation process that realizes the synthesis of ethyl methyl carbonate and of diethyl carbonate in a two-step transesterification reaction could be demonstrated.

Optimizing the plant economics in real-time (RTO) has become an established technique to improve the profitability of large chemical production plants. RTO performs a stationary optimization, the optimal set-points of the process are then implemented by conventional or MPC controllers. A new approach is to combine these two techniques into Dynamic Real-Time Optimization where an economically motivated cost function is optimized over a finite look-ahead horizon based on dynamic process models. To facilitate the development and application of D-RTO schemes, the software platform *do-mpc* [1] was developed in the *dyn* group. *do-mpc* employs efficient solvers and novel methods such as automatic differentiation and efficient line search algorithms. It can be used for simulation studies but also be coupled to real processes. The methods of *do-mpc* were developed further and transferred to a real-time environment that is based on multi-threading so that the state estimation and the optimization algorithm can run in parallel.

The transesterification process to which the D-RTO algorithm was applied can produce two products, ethyl methyl carbonate and diethyl carbonate, depending on the choice of the operating parameters. The process was modelled and studied experimentally in the dissertation of [2]. The so-called EQ-kin model developed in his work provided the basis for the online optimization and state estimation. The instrumentation and automation of the pilot-scale column was improved and online analytics using near-infrared spectroscopy were installed to provide information on the concentrations in the streams leaving the column.

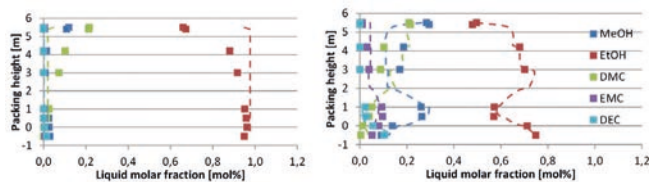


Figure 1: Real-time state estimation (dashed lines: estimated profile, dots: GC measurements); left: initial profile, right: profile after 1 h.

Contact:

daniel.hasskerl@tu-dortmund.de
sebastian.engell@tu-dortmund.de

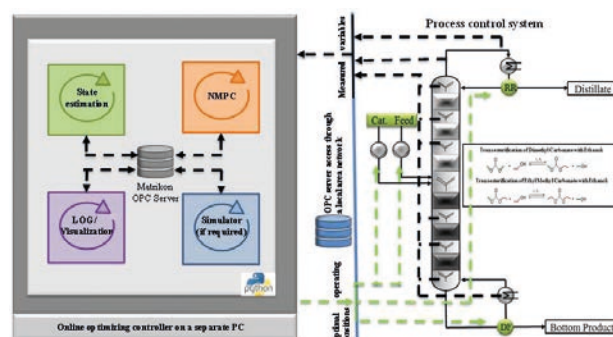


Figure 2: Schematic of the real-time environment and its connection to the pilot-scale plant; threads indicated by arcs.

The model that is used in the controller has approx. 500 dynamic and algebraic state variables that are estimated online from 19 measurements which are available at different sampling rates. The control task is to meet a certain purity of one of the valuable products while maximizing the profit and respecting further process constraints. The optimizing control algorithm steers the plant to its economic optimum and also the product changeover from the production of diethyl carbonate to ethyl methyl carbonate is performed in the most profitable way.

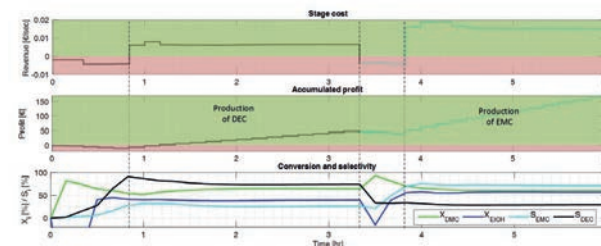


Figure 3: Process variables during the transient changeover from the production of DEC to the production of EMC.

Publications:

D. Haßkerl, S. Subramanian, S. Markert, S. Kaiser, S. Engell, Chemical Engineering Science, (submitted 2017).

References:

S. Lucia, A. Tatulea-Codrean, C. Schoppmeyer, S. Engell. Control Engineering Practice, 60, 51-62, (2017).

Keller, T. Reactive distillation for multiple-reaction systems: experimental investigation, modelling and optimisation. Dissertation, Dortmund, (2013).

Publications 2017 - 2015

Proceedings & Book Chapters

2017

- R. Hernández, S. Engell
Stochastic Approximation in Online Steady State Optimization under noisy measurements
Comput. Aided Chem. Eng. 40, 1747-1752 (2017)
- A.R. Gottu Mikkula, R. Paulen
Model-based design of optimal experiments for nonlinear systems in the context of guaranteed parameter estimation
Computers & Chemical Engineering 99, 198 - 213 (2017), ISBN 0098-1354
- T. Janus, C. Foussette, M. Urselmann, S. Tlatlik, A. Gottschalk, M. Emmerich, T. Bäck, S. Engell
Optimierungsbasierte Prozesssynthese auf Basis eines kommerziellen Flowsheet Simulators
Chemie Ingenieur Technik 13 (2017), ISBN DOI: 10.1002/cite.201600179
- S. Lucia, A. Tatulea-Codrean, C Schoppmeyer, S. Engell
Rapid Development of Modular and Sustainable Nonlinear Model Predictive Control Solutions
Control Engineering Practice, 51-62 (2017) - ISBN 0967-0661
- S. Wenzel, R. Paulen, B. Beisheim, S. Krämer, S. Engell
Market-Based Coordination of Shared Resources in Cyberphysical Production Sites
Chemie Ingenieur Technik 89, 636-644 (2017)
- M. Kalliski, S. Engell
Real-time resource efficiency indicators for monitoring and optimization of batch-processing plants
Canadian Journal of Chemical Engineering, 95 (2) 265-280 (2017) ISSN: 00084034
- A. Sharma, M. Jelemský, R. Paulen, M. Fikar
Modeling and optimal operation of batch closed-loop diafiltration processes
Chem Eng Res Des 122 198-210 (2017) ISSN: 02638762
- F. Lamnabhi-Lagarrigue, A. Annaswamy, S. Engell, A. Isaksson, P. Khargonekar, RM. Murray, et al.
Systems & Control for the future of humanity, research agenda: Current and future roles, impact and grand challenges
Annual Reviews in Control 43 1-64 (2017)

2017

- D. Haßkerl, S. Subramanian, R Hashemi, M. Arshad, S. Engell
State estimation using a multi-rate particle filter for a reactive distillation column de-scribed by a DAE model
Proc. IEEE The 25th Mediterranean Conference on Control and Automation (MED), Valet-ta/Malta, 2017, - ISBN DOI: 10.1109/MED.2017.7984230, 876-881
- T. Siwczyk, S. Engell
Solving Two-Stage Stochastic MILP Chemical Batch Scheduling Problems by Evolutionary Algorithms and Ordinal Optimization
Proc. FOCAPO, Foundations of Computer Aided Process Operations / Chemical Process Control, Tuscan, Arizona USA, 2017
- S. Subramanian, S. Lucia, S. Engell
A novel tube-based output feedback MPC for constrained linear systems
Proc. American Control Conference (ACC) IEEE, Seattle, WA, 2017, 3060-3065
- S. Subramanian, S. Lucia, S. Engell
An Improved Output Feedback MPC scheme for Constrained Linear Systems
Proc. IFAC International Federation of Automatic Control World Congress, Toulouse, France, 2017 In IFAC-PapersOnLine Bd. 50, 2017, 15506-15511
- S. Wenzel, R. Paulen, S. Engell
Quadratic approximation in price-based coordination of constrained systems-of-systems
Proc. Foundations of Computer Aided Process Operations / Chemical Process Control, Tuc-son, Arizona, 2017, 1-6
- W. Gao, R. Hernandez, S. Engell
Real-time optimization of a novel hydroformylation process by using transient measurements in modifier adaptation
Proc. IFAC International Federation of Automatic Control World Congress, Toulouse, France, 2017. In IFAC-PapersOnLine 50,1 (2017) 5731-5736. ISSN: 2405-8963
- W. Gao, S. Engell
Dynamic MAWQA: Towards Efficient Real-time Optimization of Slow Dynamic Processes
Proc. 36th Chinese Control Conference, Dalian, China 2017. IEEE (2017) ISSN 19341768
- A.R. Gottu Mikkula, R. Paulen
Model-Based Optimal Experiment Design for Nonlinear Parameter Estimation Using Exact Confidence Regions
Proc. IFAC International Federation of Automatic Control World Congress, Toulouse, France, 2017, In IFAC-PapersOnLine,50,1 (2017). 13760 - 13765 ISSN 2405-8963
- S. Nazari, S. Wenzel, L. Maxeiner, C. Sonntag, S. Engell
A Framework for the Simulation and Validation of Distributed Control Architectures for Technical Systems of Systems
Proc. IFAC International Federation of Automatic Control World Congress, Toulouse, France, 2017, In IFAC-PapersOnLine,50,1 (2017) 12458-12463. ISSN 2405-8963

- S. Thangavel, S. Lucia, R. Paulen, S. Engell
Robust Nonlinear Model Predictive Control with Reduction of Uncertainty via Dual Control
Proc. 21st International Conference on Process Control (PC) IEEE, June 2017 - ISBN 978-1-5386-4011-1
- S. Thangavel, S. Subramanian, S. Engell
Offset-free NMPC with robust constraint satisfaction using model-error modeling
Proc. Foundations of Computer Aided Process Operations / Chemical Process Control, January 2017
- A. Ahmad, W. Gao, S. Engell
Effective Model Adaptation in Iterative RTO
Proc. ESCAPE-27, European Symposium on Computer Aided Process Engineering, Barcelona Spain, 2017. In: España, Antonio; Graells, Moisès; Puigjaner, Luis (Hrsg.): Computer-Aided Chemical Engineering 40, 2017 - ISSN 1570-7946, 1717-1722
- F. Benski, C. Nentwich, S. Engell
Optimization-based early phase design of a homogeneously catalysed process in a thermomorphic solvent system
Proc. ESCAPE-27, European Symposium on Computer Aided Process Engineering, Barcelona Spain, 2017. In: España, Antonio; Graells, Moisès; Puigjaner, Luis (Hrsg.): Computer-Aided Chemical Engineering 40, 2017 - ISBN 1570-7946, 715-720
- T. Keßler, N. Mertens, S. Kunde, C. Nentwich, D. Michaels, S. Engell, A. Kienle
Efficient global optimization of a novel hydroformylation process
Proc. ESCAPE-27, European Symposium on Computer Aided Process Engineering, Barcelona Spain, 2017. In: España, Antonio; Graells, Moisès; Puigjaner, Luis (Hrsg.): Computer-Aided Chemical Engineering 40. 2017 - ISBN 1570-7946, 2113-2118
- S. Wenzel, V. Yfantis, W. Gao
Comparison of regression data selection strategies for quadratic approximation in RTO. *Proc. ESCAPE-27, European Symposium on Computer Aided Process Engineering, Barcelona Spain, 2017. In: España, Antonio; Graells, Moisès; Puigjaner, Luis (Hrsg.): Computer-Aided Chemical Engineering 40. 2017*
- A.R. Gottu Mukkula, R. Paulen
Robust model-based design of experiments for guaranteed parameter estimation
Proc. ESCAPE-27, European Symposium on Computer Aided Process Engineering, Barcelona Spain, 2017. In: España, Antonio; Graells, Moisès; Puigjaner, Luis (Hrsg.): Computer-Aided Chemical Engineering 40. 2017, Barcelona, Spain. - ISBN 9780444639707
- S. Wenzel, R. Paulen, B. Beisheim, S. Krämer, S. Engell
Adaptive pricing for optimal resource allocation in industrial production sites
Proc. IFAC International Federation of Automatic Control World Congress, Toulouse, France, 2017 In IFAC-PapersOnLine 50 (2017), 12446 - 12451. - ISSN 2405-8963
- R. Hernandez, M. Buckova, S. Engell
An efficient RTO scheme for the optimal operation of chemical processes under uncertainty
Proc. 21st International Conference on Process Control (PC). IEEE (2017). 364-369 ISBN 978-153864011-1
- J. Cadavid, R. Hernández, S. Engell
Speed-up of Iterative Real-Time Optimization by Estimating the Steady States in the Transient Phase using Nonlinear System Identification
Proc. IFAC International Federation of Automatic Control World Congress, Toulouse, France, 2017. In IFAC-PapersOnLine 2017;50(1):11269-11274. ISSN: 24058963
- A. Sharma, M. Jelemensky, M. Fikar, R. Paulen
Optimal operation of nanofilter based diafiltration processes using experimental per-meation models
Proc. 2017 21st International Conference on Process Control, PC 2017; 2017. IEEE, 7976211, 185-190. ISBN: 978-153864011-1
- M. Jelemenský, M. Fikar, R. Paulen
Time-Optimal Operation of Membrane Processes in the Presence of Fouling with Set-membership Parameter Estimation
Proc. IFAC International Federation of Automatic Control World Congress, Toulouse, France, 2017. In IFAC-PapersOnLine 2017;50(1):4690-4695. ISSN: 24058963

Presentations/ Posters

2017

- T. Goerke, S. Engell
Batch-to-Conti Transfer of the Production of a Highly Viscous Copolymer System
Proc. International Process Intensification Conference IPIC1, Barcelona, October 2017
- T. Goerke, S. Engell
Übertragung einer Copolymerisation vom Batch Prozess in eine kontinuierliche Produktion: Von der Modellierung über Prozessentwicklung zur Prozessführung
ProcessNet Fachgemeinschaft Jahrestreffen "Prozess-, Apparate- und Anlagentechnik" 2017, Würzburg, November 2017
- D. Haßkerl, C. Lindscheid, S. Markert, S. Engell
Dynamische Echtzeitoptimierung einer Umesterung in einer Pilotanlage für Reaktivrektifikation
ProcessNet Fachgemeinschaft Jahrestreffen "Prozess-, Apparate- und Anlagentechnik" 2017, Würzburg, November 2017

- T. Siwczyk, S. Engell
A Fast Hybrid Evolutionary Algorithm with Inexact Fitness Evaluation for Solving Two-Stage Stochastic Scheduling Problems
ProcessNet Fachgemeinschaft Jahrestreffen "Prozess-, Apparate- und GECCO '17 Companion, 2017

2016

- D. Ackerschott, B. Beisheim, S. Engell
Decision support for optimised cooling tower operation using weather forecasts
Chemical Engineering Transactions 52, AIDIC, 1009-1014 (2016)
- C. Dowidat, M. Kalliski, G. Schembecker, C. Bramsiepe
Synthesis of batch heat exchanger networks utilizing a match ranking matrix
Applied Thermal Engineering 100, 78-83 (2016)
- W. Gao, S. Engell
Using Transient Measurements in Iterative Steady-State Optimizing Control
Computer Aided Chemical Engineering 38:511-516 (2016)
- T. Goerke, D. Kohlmann, S. Engell
Transfer of Semibatch Processes to Continuous Processes with Side Injections - Opportunities and Limitations, Macromolecular Reaction Engineering
Special Issue: Batch to Conti Transfer of Polymer Production Processes 10 (4), 364-388 (2016)
- A. Gottu Mukkula, R. Paulen
Optimal dynamic experiment design for guaranteed parameter estimation
Computer Aided Chemical Engineering 38, 757-762 (2016)
- W. Gao, S. Wenzel, S. Engell
A reliable modifier-adaptation strategy for real-time optimization
Computers & Chemical Engineering 91, 318-328(2016)
- R. Hashemi, D. Kohlmann, S. Engell
Optimizing Control and State Estimation of a Continuous Polymerization Process in a Tubular Reactor with Multiple Side-streams
Macromolecular Reaction Engineering 10 (4), Special Issue: Batch to Conti Transfer of Polymer Production Processes, 415-434 (2016)
- H. Hadera, R. Labrik, S. Engell, I. Harjunkoski
An Improved Energy-awareness Formulation for General Precedence Continuous-time Scheduling Models
Industrial and Engineering Chemistry Research 55, 1336-1346 (2016)
- M. Kalliski, S. Engell
Real-Time Resource Efficiency Indicators for Monitoring and Optimization of Batch-Processing Plants
Canadian Journal of Chemical Engineering 95 (2), 265-280 (2016)
- M. Kalliski, B. Beisheim, D. Krahé, U. Enste, S. Krämer, S. Engell
Real-time Resource Efficiency Indicators
atp edition - Automatisierungstechnische Praxis 1-2, 64-71 (2016)
- D. Kohlmann, M.C. Chevrel, S. Hoppe, D. Meimaroglou, D. Chapron, P. Bourson, C. Schwede, W. Loth, S. Engell, F. Durand
Modular, Flexible, and Continuous Plant for Radical Polymerization in Aqueous Solution
Macromolecular Reaction Engineering, Special Issue: Batch to Conti

Transfer of Polymer Production Processes 10 (4), 339-353 (2016)

- R. Paulen, M. Fikar
Optimal Operation of Batch Membrane Processes
Springer, ISBN 978-3-319-20475-8, (2016)
- C. Schoppmeyer, H. Vermue, S. Subbiah, D. Kohlmann, P. Ferlin, S. Engell
Operation of Flexible Multiproduct Modular Continuous Polymerization Plants
Macromolecular Reaction Engineering 10 (4), Special Issue: Batch to Conti Transfer of Polymer Production Processes, 435-457 (2016)
- S. Wenzel, R. Paulen, G. Stojanovski, S. Krämer, B. Beisheim, S. Engell
Optimal resource allocation in industrial complexes by distributed optimization and dynamic pricing
at – Automatisierungstechnik 64, 428-442 (2016)
- R. Hernández, S. Engell
Modelling and iterative Real-time Optimization of a homogeneously catalyzed hydroformylation process
Computer Aided Chemical Engineering 38, Elsevier, 1-6 (2016)
- H. Hadera, R. Labrik, J. Mäntysaari, G. Sand, I. Harjunkoski, S. Engell
Integration of Energy-cost Optimization and Production Scheduling Using Multiparametric Programming
Computer Aided Chemical Engineering 38, Elsevier, 559-564 (2016)
- F. Shamim, R. Hernández, R. Paulen, S. Engell
A hierarchical coordination approach to the optimal operation of a sugar crystallization process
Computer Aided Chemical Engineering 38, Elsevier, 703-708 (2016)
- L. Maxeiner, S. Engell
Distributed minimum batch time optimization for batch reactors with shared resources
Computer Aided Chemical Engineering 38, Elsevier, 1593-1598 (2016)
- J. Steimel, S. Engell
Optimization-based support for process design under uncertainty: A case study
AIChE Journal 62(9), 3404-3419 (2016)
- M. Urselmann, T. Janus, C. Foussette, S. Tlatlik, A. Gottschalk, M. Emmerich, T. Bäck, S. Engell
Derivative-Free Chemical Process Synthesis by Memetic Algorithms Coupled to Aspen Plus Process Models
Computer-Aided Chemical Engineering 38, Elsevier, 187-192 (2016)

Proceedings & Book Chapters

2016

- R. Hernández, S. Engell
Modelling and iterative Real-time Optimization of a homogeneously catalyzed hydroformylation process
Computer Aided Chemical Engineering. 38, 1-6 (2016)
- A. Gottu Mukkula, R. Paulen
Optimal design of dynamic experiments for guaranteed parameter estimation
Proc. American Control Conference 1826-1831 (2016)

- D. Haßkerl, M. Arshad, R. Hashemi, S. Subramanian, S. Engell
Simulation Study of the Particle Filter and the EKF for State Estimation of a Large-scale DAE-system with Multi-rate Sampling
11th IFAC Symposium on Dynamics and Control of Process Systems, including Biosystems, IFAC PapersOnline 49 (7), Elsevier, 490-496 (2016)
 - D. Haßkerl, S. Markert, S. Engell
Application of Model-based Experimental Design for the Calibration of Online Composition Measurement by Near-infrared Spectroscopy
Proc. IEEE Mediterranean Conference on Control and Automation, 967-972 (2016)
 - L. Hebing, T. Neymann, T. Thüte, A. Jockwer, S. Engell
Efficient Generation of Models of Fed-Batch Fermentations for Process Design and Control
11th IFAC Symposium on Dynamics and Control of Process Systems, including Biosystems, IFAC PapersOnline 49 (7), Elsevier, 621-626 (2016)
 - C. Nentwich, S. Engell
Application of surrogate models for the optimization and design of chemical processes, Proc. IEEE World Congress of Computational Intelligence
International Joint Conference on Neural Networks (IJCNN), 1291-1296 (2016)
 - S. Subramanian, A. Ahmad, S. Engell
Robust control of a supermarket refrigeration system using multi-stage NMPC
11th IFAC Symposium on Dynamics and Control of Process Systems, including Biosystems, IFAC-PapersOnLine Bd. 49 (7), Elsevier, 2016, 901-906 (2016)
 - T. Siwczyk, S. Engell
Solving two-stage stochastic mixed-integer linear problems by ordinal optimization and evolutionary algorithms
Proc. IEEE Congress on Evolutionary Computation, CEC 2016, 2836-2843 (2016)
 - A. Tatuela-Codrean, D. Haßkerl, M. Urselmann, S. Engell
Steady-state Optimization and Nonlinear Model-predictive Control of a Reactive Distillation Process using the Software Platform do-mpc1
Proc. IEEE Conference on Control Applications (CCA), 1513-1518 (2016)
 - T. Goerke, S. Engell
Application of evolutionary algorithms in guaranteed parameter estimation
Proc. IEEE Congress on Evolutionary Computation (CEC), 5100-5105 (2016)
 - C. Lindscheid, D. Haßkerl, A. Meyer, A. Potschka, H.-G. Bock, S. Engell
Parallelization of modes of the Multi-Level Iteration Scheme for Nonlinear Model-Predictive Control of an Industrial Process
Proc. IEEE Conference on Control Applications (CCA), 1506-1512 (2016)
 - R. Paulen, S. Nazari, S.A. Shahidi, C. Sonntag, S. Engell
Primal and Dual Decomposition for Distributed MPC – Theory, Implementation, and Comparison in a Tailored Validation Framework
Proc. 24th Mediterranean Conference on Control and Automation, Institute of Electrical and Electronics Engineers Inc., 286-291 (2016)
 - M. Urselmann, C. Foussette, T. Janus, S. Tlatlik, A. Gottschalk, M.T.M. Emmerich, S. Engell, T. Bäck
Selection of a DFO Method for the Efficient Solution of Continuous Constrained Sub-Problems within a Memetic Algorithm for Chemical Process Synthesis
Proc. Genetic and Evolutionary Computation Conference (GECCO), 1029-1036 (2016)
 - R. Hashemi, S. Engell
Effect of Sampling Rate on the Divergence of the Extended Kalman Filter for a Continuous Polymerization Reactor in Comparison with Particle Filtering
11th IFAC Symposium on Dynamics and Control of Process Systems, including Biosystems, IFAC PapersOnLine 49 (7), Elsevier, 365-370 (2016)
 - T. Ebrahim, R. Hernandez, S. Subramanian, M. Kalliski, S. Krämer, S. Engell
NCO-Tracking with Changing Set of Active Constraints using Multiple Solution Models
11th IFAC Symposium on Dynamics and Control of Process Systems, including Biosystems IFAC PapersOnLine 49 (7), Elsevier, 79-84 (2016)
 - S. Wegerhoff, S. Engell
Control of the production of *Saccharomyces cerevisiae* on the basis of a reduced metabolic model
6th IFAC Conference on Foundations of Systems Biology in Engineering, 49(26), Elsevier 201-206 (2016)
- ## 2015
- M. Urselmann, S. Engell
A Memetic Algorithm for the Efficient Optimization of Chemical Process Synthesis Problems with Structural Restrictions
Computers & Chemical Engineering 72 - Special Issue: Mixed Integer Nonlinear Optimization – A Tribute to Ignacio E. Grossmann's Contributions to the Field of Process Systems Engineering, 87–108 (2015)
 - M. Behrens, H.G. Bock, S. Engell, P. Khobkhu, A. Potschka
Real-Time PDE Constrained Optimal Control of a Periodic Multicomponent Separation Process
In: Leugering, G., Benner, P., Engell, S., Griewank, A., Harbrecht, H., Hinze, M., Rannacher, R., Ulbrich, S., (Hrsg.): Trends in PDE Constrained Optimization, Heidelberg, Springer, 521-537 (2015)
 - T. Goerke, S. Engell
Analysis of the transfer of radical co-polymerization systems from semi-batch to continuous plants
Computer Aided Chemical Engineering 37, 227-232 (2015)
 - H. Hadera, I. Harjunkski, G. Sand, I.E. Grossmann, S. Engell
Optimization of steel production scheduling with complex time-sensitive electricity cost
Computers and Chemical Engineering 76, 117-136 (2015)
 - H. Hadera, R. Labrik, S. Engell, I. Harjunkski
An Improved Energy-awareness Formulation for General Precedence Continuous-time Scheduling Models
Industrial and Engineering Chemistry Research 55, 1336-1346 (2016)
 - H. Hadera, P. Wide, I. Harjunkski, J. Mäntysaari, J. Ekström, S. Engell
A Mean Value Cross Decomposition Strategy for Demand-side Management of a Pulping Process
Computer Aided Chemical Engineering 37, 1931-1936 (2016)
 - M. Jelemenský, R. Paulen, M. Fikar, Z. Kovacs
Time-Optimal Operation of Multi-Component Batch Diafiltration
Computers & Chemical Engineering 85, 131 – 138 (2015)
 - M. Jelemenský, A. Sharma, R. Paulen, M. Fikar
Time-optimal Operation of Diafiltration Processes in the Presence of Fouling
Computer Aided Chemical Engineering 37, 1577-1582 (2015)

- M. Kalliski, D. Krahé, B. Beisheim, S. Krämer, S. Engell
Resource efficiency indicators for real-time monitoring and optimization of integrated chemical production plants
Computer Aided Chemical Engineering 37, 1949-1954 (2015)
- M. Kalliski, D. Krahé, N. Melchert, S. Engell
Real-time Resource Efficiency Indicators for Monitoring and Optimization of Batch-Processing Plants
The Canadian Journal of Chemical Engineering 95 (2), ECCE10 Special Issue, 265-280 (2015)
- R. Marti, S. Lucia, D. Sarabia, R. Paulen, S. Engell, C. de Prada
Improving scenario decomposition algorithms for robust nonlinear model predictive control
Computers & Chemical Engineering 79, 30-45 (2015)
- S. Nazari, C. Sonntag, G. Stojanovski, S. Engell
A Modelling, Simulation, and Validation Framework for the Distributed Management of Large-scale Processing Systems
Computer Aided Chemical Engineering 37, 269-274 (2015)
- R. Paulen, M. Jelemenský, Z. Kovacs, M. Fikar
Economically optimal batch diafiltration via analytical multi-objective optimal control
Journal of Process Control 28, 73-82 (2015)
- C. Schoppmeyer, C. Sonntag, S. Gajjal
Optimal Management of Shuttle Robots in a Laboratory Automation System of a Cement Plant
Computer Aided Chemical Engineering 37, 1895-1900 (2015)
- J. Steimel, S. Engell
Conceptual design and optimization of chemical processes under uncertainty by two-stage programming
Computers and Chemical Engineering 81, 200-217 (2015)
- P.H. Taskinen, J. Steimel, L. Gräfe, S. Engell, A. Frey
A Competency Model for Process Dynamics and Control and Its Use for Test Construction at University Level
Peabody Journal of Education 90, 477-490 (2015)
- M. Urselmann, S. Engell
Design of memetic algorithms for the efficient optimization of chemical process synthesis problems with structural restrictions
Computers and Chemical Engineering 72, 87-108 (2015)
- T. Goldschmidt, M. Murugaiah, C. Sonntag, B. Schlich, S. Biallas, P. Weber
Cloud-Based Control: A Multi-Tenant, Horizontally Scalable Soft-PLC
Proc. 8th IEEE International Conference on Cloud Computing, New York, USA, 909 – 916 (2015)
- W. Gao, S. Wenzel, S. Engell
Integration of gradient adaptation and quadratic approximation in real-time optimization
Proc. 34th Chinese Control Conference, Hangzhou, China, 2780 – 2785 (2015)
- W. Gao, S. Wenzel, S. Engell
Comparison of modifier adaptation schemes in real-time optimization
Proc. 9th IFAC Symposium on Advanced Control of Chemical Processes ADCHEM 2015, IFAC Papers OnLine 48 (8), 182-187 (2015)
- W. Gao, S. Wenzel, S. Engell
Modifier Adaptation with Quadratic Approximation in Iterative Optimizing Control
Proc. 2015 European Control Conference, 15-17 (2015)
- R. Hashemi, R. Schilling, S. Engell
Optimizing Control of a Tubular Polymerization Reactor: Comparison of Single Shooting and Full Discretization
Proc. 9th IFAC Symposium on Advanced Control of Chemical Processes ADCHEM 2015, IFAC Papers OnLine 48 (8), 557 – 562 (2015)
- M. Jelemenský, A. Sharma, R. Paulen, M. Fikar
Multi-Objective Optimization of Batch Dialfiltration Processes in the Presence of Membrane Fouling,
M. Fikar, M. Kvasnica (Hrsg.): Proceedings of the 20th International Conference on Process Control Slovak Chemical Library, Štrbské Pleso, Slovakia, 84-89 (2015)
- R. Marti, S. Lucia, D. Sarabia, R. Paulen, S. Engell, C. de Prada
An Efficient Distributed Algorithm for Multi-Stage Robust Nonlinear Predictive Control
Proc. European Control Conference 2015, Linz, Austria, 2669-2674 (2015)
- S. Nazari, C. Sonntag, S. Engell
A Modelica-based Modeling and Simulation Framework for Large-scale Cyber-physical Systems of Systems
Proc. MATHMOD 2015, IFAC PapersOnLine 48 (1), 920-921. (2015)

Proceedings & Book Chapters

2015

- B. Chachuat, B. Houska, R. Paulen, N. Peric, J. Rajyaguru, M. Villanueva
Set-Theoretic Approaches in Analysis, Estimation and Control of Nonlinear Systems
Proc. 9th IFAC Symposium on Advanced Control of Chemical Processes ADCHEM 2015, IFAC Papers OnLine 48 (8), Elsevier, 981-995 (2015)
- S. Engell, R. Paulen, M.A. Reniers, H. Thompson, C. Sonntag
Core Research and Innovation Areas in Cyber-Physical Systems of Systems: Initial Findings of the CPSoS project
Lecture Notes in Computer Science Bd. 9361, Springer Amsterdam, 11-13 (2015)
- R. Paulen
On the Design of a Guaranteed Extended Kalman Filter using Set Inversion Techniques
Proc. 54th IEEE Conference on Decision and Control Osaka, Japan, 5014-5019 (2015)
- A. Sharma, M. Jelemenský, R. Paulen, M. Fikar
Modelling and Optimal Control of Membrane Process with Partial Recirculation
in: M. Fikar, M. Kvasnica (Hrsg.): In Proceedings of the 20th International Conference on Process Control Slovak Chemical Library, Štrbské Pleso, Slovakia, 90-95 (2015)
- S. Subramanian, S. Lucia, S. Engell
Economic Multi-stage Output Feedback NMPC using the Unscented Kalman Filter
Proc. 9th IFAC Symposium on Advanced Control of Chemical Processes ADCHEM 2015, IFAC-PapersOnLine, 48 (8), 38-43 (2015)

- S. Subramanian, S. Lucia, S. Engell
Handling Structural Plant-model Mismatch via Multi-stage Nonlinear Model Predictive Control
Proc. European Control Conference (ECC) 2015, 1596-1601 (2015)
- S. Subramanian, S. Lucia, S. Engell
Adaptive Multi-stage Output Feedback NMPC using the Extended Kalman Filter for time varying uncertainties applied to a CSTR
Proc. 5th IFAC Conference on Nonlinear Model Predictive Control NMPC 2015, IFAC-PapersOnLine 48 (23), Elsevier, 242-247 (2015)
- S. Subramanian, S. Lucia, R. Paulen, S. Engell
Robust Output Feedback NMPC with Guaranteed Constraint Satisfaction
Proc. 8th IFAC Symposium on Robust Control Design, IFAC-PapersOnLine 48 (14), Elsevier, 325-330 (2015)
- S.A. Shahidi, R. Paulen, S. Engell
Two-layer Hierarchical Predictive Control via Negotiation of Active Constraints
Proc. 5th IFAC Conference on Nonlinear Model Predictive Control, IFAC PapersOnLine 48 (23), Elsevier, 404-409 (2015)
- S. Thangavel, S. Lucia, R. Paulen, S. Engell
Towards Dual Robust Nonlinear Model Predictive Control: A Multi-stage Approach
Proc. 2015 American Control Conference, Chicago, IL, USA, 428-433 (2015)
- S. Wenzel, W. Gao, S. Engell
Handling Disturbances in Modifier Adaptation with Quadratic Approximation
Proc. 6th IFAC Workshop on Control Applications of Optimization CAO'2015, IFAC-PapersOnLine 48 (25), Elsevier, 132-137 (2015)
- G. Stojanovski, L.S. Maxeiner, S. Krämer, S. Engell
Real-time Shared Resource Allocation by Price Coordination in an Integrated Petrochemical Site
Proc. 14th European Control Conference, Linz, Austria, 1498-1503 (2015)
- S. Lucia, S. Engell
Potential and Limitations of Multi-stage Nonlinear Model Predictive Control
Proc. 9th IFAC Symposium on Advanced Control of Chemical Processes ADCHEM, Canada, IFAC Papers OnLine 48 (8), Elsevier, 1015-1020 (2015)
- D. Kampert, S. Nazari, C. Sonntag, U. Epple, S. Engell
A Framework for Simulation, Optimization and Information Management of Physically-Coupled Systems of Systems
Proc. 15th IFAC Symposium on Information Control Problems in Manufacturing, Ottawa, Canada, IFAC Papers OnLine 28 (3), Elsevier, 1553-1558 (2015)



Solids Process Engineering (FSV)

Scaling Strategies for Twin Screw Extrusion

Preserving the Residence Time Distribution as Crucial Process Parameter

J. Wesholowski¹, K. Hoppe¹, K. Nickel², C. Muehlenfeld³, M. Thommes¹

¹ Lehrstuhl für Feststoffverfahrenstechnik, TU Dortmund, Dortmund, Deutschland, ² Leistritz AG, Nürnberg, Deutschland, ³ Ashland Specialty Ingredients (ASI), Pharmaceutical R&D, Düsseldorf, Germany

Hot Melt Extrusion (HME) in a co-rotating Twin Screw Extruder is an established pharmaceutical application. Main advantage next to a continuous processing is the combination of different unit operations within one apparatus. A parameter reflecting all appearing mechanisms is the Residence Time Distribution (RTD). The aim of this study was therefore to identify suitable approaches to maintain the RTD during scaling of HME processes.

Usually a scaling of an extrusion process is performed for geometrically similar machines in order to isolate the process parameters as crucial variables. The typically applied scale-up concepts for HME focus on a constant specific feed load SFL or total specific mechanical energy input SME_{total} . The volumetric approach assumes a constant fill level expressed by the specific feed load SFL as beneficial, which depends on the mass flow \dot{m} , material density ρ and the barrel diameter D , while the screw speed n is kept constant for different scales of machine 1 and machine 2.

$$SFL = \frac{\dot{m}}{\rho n D^3} \xrightarrow{n_1 = n_2} \frac{\dot{m}_1}{\rho_1 D_1^3} = \frac{\dot{m}_2}{\rho_2 D_2^3} \quad (1)$$

The SME_{total} is the main objective for the energy input approach and is expressed by the torque τ , screw speed n and mass flow \dot{m} of the material. The torque cannot be adjusted independently from the screw speed and mass flow. Typically the screw speed is kept constant.

$$SME_{total} = \frac{\tau n}{\dot{m}} \Rightarrow \frac{\tau_1 n_1}{\dot{m}_1} = \frac{\tau_2 n_2}{\dot{m}_2} \quad (2)$$

However, the applied energy can be differentiated in consumed energy for material transport ($SME_{pumping}$), shearing (SME_{shear}) and for the base load (SME_{empty}).

The recently developed balanced energy input approach within this study focuses on the ratio between applied energy for shearing respectively mixing to transport.

$$SME_{balance} = \frac{SME_{shear}}{SME_{total} - SME_{empty}} \quad (3)$$

Experiments were carried out on co-rotating twin screw extruders (reference: 27 GL; scale down: ZSE 18 HPe) from Leistritz (Nuremberg, Germany) with a L/D of 20 for the processing section. The RTD was measured in-line with an UV/Vis spectroscope (InSpectro X, ColVisTec AG, Berlin, Germany) in transmission and analyzed at a wavelength of 330 nm. A model system containing 95 w% polyvinylpyrrolidone vinylacetate (Plasdone S-630, Ashland, Germany) as polymer and 5 w% theophylline-anhydrot (Fagron, Netherlands) as active pharmaceutical ingredient (API) was used. quinine-dihydrochlorid (Caesar & Loretz, Germany) served as marker for the RTD determination. A

reference point for the evaluation of the scaling concepts was determined by an independent optimization scheme (IOS). The approaches were applied based on the reference point as well as the IOS for the scale down and the RTD measured (Figure 1).

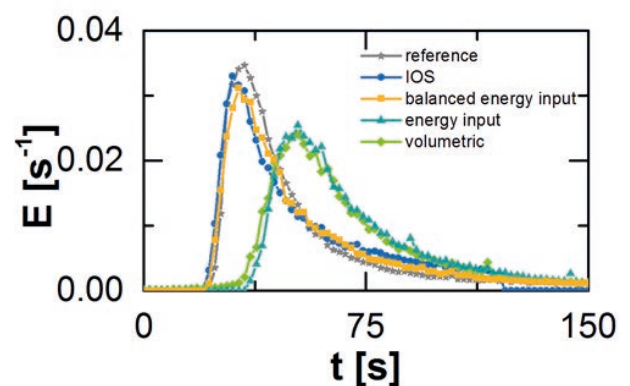


Figure 1: Determined RTDs of scaled and optimized extrusion processes in comparison to the reference for one repetition.

The RTDs are presented by the residence time density function E . This type of function can be compared directly since the overall integral is one by definition. The reference process (circular symbols) is linked to a typical RTD for an extrusion process. The applied approaches can be classified according to the obtained results in two groups. The IOS as well as the balanced energy input approach are suitable to preserve the RTD of the pre-defined reference, while volumetric and energy input approach are not. For these the location of the on-set, peak and off-set of the curve are all shifted to higher values. Basically a second operating point regarding the RTD is observed. Here the overall exposure time to thermal and mechanical stress is enlarged. This might lead to enhanced degradation.

In conclusion, the developed balanced energy approach as well as an independent optimization scheme for extrusion processes have been found suitable to preserve the RTD of HME during scale up. These concepts and the reference have in common a comparable ratio of shear to transport energy input in the same dimension.

Contact:

jens.wesholowski@tu-dortmund.de
markus.thommes@tu-dortmund.de

Influence of Slicing Parameters on Properties of 3D Printed Products

Tim Feuerbach, Stefanie Kock, Markus Thommes

Fused Deposition Modeling (FDM) 3D printing is emerging as a pharmaceutical manufacturing process for drug dosage forms and implants. The main incentives are the personalization of drug dosage, the customization of implant geometry and an economic single-unit production. Slicing software generates machine instructions for the printer, based on a digital 3D model to print an object layer-by-layer. The aim of this study was to investigate the influence of individual slicing parameters on specific properties of printed objects. For this purpose, custom slicing software was written in Python due to inaccessible slicing parameters and missing transparency in commercial slicing software.

In the following results, the influence of the slicing parameters *parallel strand distance* and *over-extrusion ratio* on the object properties *dimension* and *porosity* are presented. The printed objects were cuboids. The cuboid dimensions are represented by cuboid ratios, which are the ratios between the measured dimensions and the set dimensions. The porosity was calculated by determination of the cuboid volume, the cuboid weight and the material density. The parallel strand distance is the distance between two extrudates, which are parallel deposited by the printer nozzle (Figure 1). The over-extrusion ratio describes the applied volumetric flow rate relative to the volumetric flow rate necessary for the intended layer height.

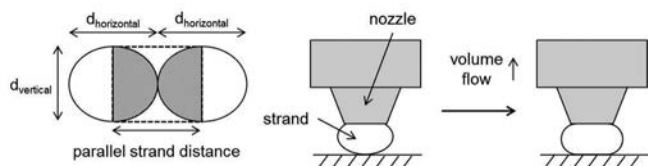


Figure 1: Qualitative depiction of the parallel strand distance (left) and the over-extrusion ratio (right).

Three different deposition strategies have been investigated (Figure 2). In the cross strategy, the strand orientation is altered by 90° in each consecutive layer. In the contour strategy, the strand orientation is similar to the layer contour, while the gap strategy has one strand orientation, but the deposition location is shifted by half a strand width in each consecutive layer.

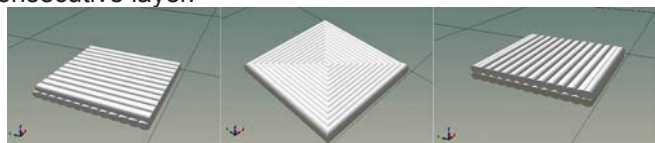


Figure 2: Deposition strategies (from left to right): cross, contour, gap

The cuboids were printed in a custom-built FDM printer with a poly-lactid acid (PLA) filament (RepRap-Austria, Austria), a printing temperature of 200 °C and a layer height of 400 µm. Figure 3 shows decreasing object porosity with decreasing strand distance. The cuboid ratios are showing only small variations for parallel strand distance / nozzle diameter > 1.05. For parallel strand distance / nozzle diameter < 1.05,

the cuboid ratios are increasing due to excess material suppressed to the object surfaces. The horizontal cuboid ratios were > 1 while the vertical cuboid ratios were < 1 due to a flattening of the deposited extrudate strands to an elliptic shape.

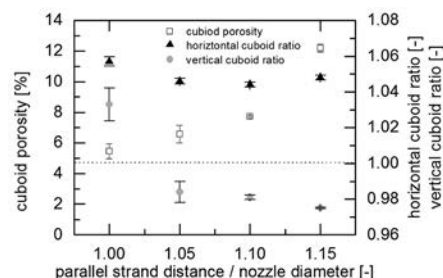


Figure 3: Cuboid porosity and cuboid ratios, dependent on the parallel strand distance for an over-extrusion ratio = 1 (n = 3).

In Figure 4, the cuboid porosities for the three different deposition strategies are compared. The strategies yield different porosity levels for the same slicing parameters. The over-extrusion ratio can be increased to further decrease the cuboid porosity without an increase in cuboid ratios for over-extrusion ratios < 1.26.

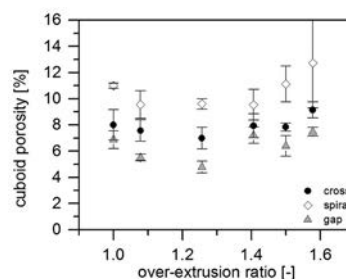


Figure 4: Cuboid porosity, dependent on over-extrusion ratio for a parallel strand distance / nozzle diameter = 1.05 (n = 3).

The strand deposition strategy can be selected to have an optimal strand orientation in the pharmaceutical product, which has a major impact on the mechanical properties of the product. The product porosity can be further adjusted to a desired value by slicing parameters like the parallel strand distance and the over-extrusion ratio, while the object dimensions remain in specification.

Preparation of Submicron Particles by Spray Drying

Pharmaceutical submicron sized particles by spray drying - production, precipitation and characterization

Adrian Dobrowolski, Ramona Strob, Gerhard Schaldach, Helmut Wiggers, Peter Walzel, Markus Thommes

The preparation of particles in the submicron sized range (0.1-1 μ m) is of common interest for many different application fields, like chemistry, food and pharmaceutical application. Due to the low water solubility of newly identified drugs, the nanomization of particles is one possibility to increase their bioavailability.

One of the major obstacles for the preparation of new pharmaceuticals is the low water solubility of newly identified active pharmaceutical ingredients (APIs). More than 40 % have a low water solubility. The preparation of particles down to the submicron range (0.1-1 μ m) and the corresponding increase in the specific surface area directly increases the dissolution rate, thus leads to a higher bioavailability. This is described by the Nernst-Brunner equation. Despite the increased dissolution rate, according to the Ostwald-Freundlich equation, a decrease in particle size down to 1 μ m increases the saturation concentration.

So far, different preparation methods for submicron sized particles, like bottom-up and top-down methods exist. Spray drying is a bottom-up technique, where particles are generated from a pure solution. Spray drying has a high potential for the generation of submicron sized particles. It is a simple step process where particle size, shape and morphology can be adjusted by controlled process parameters. In addition, heat sensitive substances can be used due to the moderate drying temperature. Nevertheless, conventional spray drying devices show certain limitations, for the production of submicron sized particles, regarding small droplet sizes and the precipitation of submicron particles.

In this work, a newly designed spray drying device is presented. The spray dryer was designed to ensure a compact structure without redirections (see Figure 1).

Firstly, an aerosol, produced with a pneumatic atomizer, is sprayed into a cyclone droplet separator with a cut-off size of about 2 μ m. Thus, only the amount of fine droplets, smaller than the cut-off size is introduced into the drying chamber.

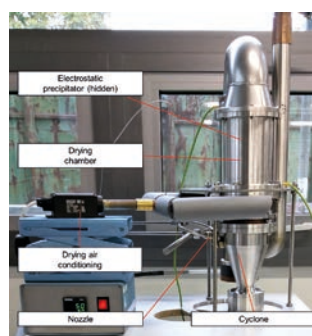


Figure 1: Picture of the designed spray dryer for the production of submicron particles.

Contact:

adrian.dobrowolski@tu-dortmund.de
markus.thommes@tu-dortmund.de

A resulting challenge is the collection of these dispersed particles from a gas flow. The separation in electrostatic precipitators (ESP) is a common technique for air purification purposes where powder particles can be collected rather independently from the particle size. An adapted ESP design is necessary to achieve high separation efficiencies and a robust process.

The ESP design in this work uses the precipitation method of Penney filters which separates charging and collection into two zones. Submicron particles tend to follow the gas flow in appearing turbulences. The setting of a laminar flow in the second zone prevents the appearance of eddies, provides the necessary time for the particles to move to the collection electrode and enhances the efficiency compared to single stage ESPs. Several experiments are conducted with the model substance povidone (Kollidon® K30, BASF, Ludwigshafen, Germany) to examine the ESP and characterize its behaviour in long term tests (see Figure 2). This ESP shows a separation efficiency in a continuous experiment of higher than 99% for 10 hours for 500 nm particles. These high efficiencies compared to single stage ESPs result in a production rate of 1 g/h.

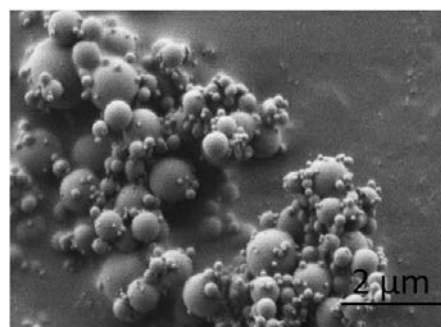


Figure 2: SEM picture of spray dried submicron povidone particles.

Publications:

R. Strob, Preparation of Spray Dried Submicron particles: Part A: Spray Drying of Submicron particles using Aerosol Conditioning, submitted.

A. Dobrowolski, Preparation of Spray Dried Submicron Particles: Part B: Particle Recovery by Electrostatic Precipitation, submitted.

Publications 2017 - 2015

2017

- D. Weis, M. Niesing, M. Thommes, S. Antonyuk
Particle Kinematics in Spheronization of Pharmaceutical Pellets
Chemie Ingenieur Technik 89 (8), 1083-1091 (2017)
- D. Weis, M. Niesing, M. Thommes, S. Antonyuk
Effect of the particle shape on the particle dynamics in a spheronization process
EPJ Web of Conferences 140, 15005 (2017)
- D. Hegyesi, M. Thommes, P. Kleinebudde, P. Jr. Kása, A. Kelemen, K. Pintye-Hódi, G. Jr. Regon
Preparation and physicochemical characterization of matrix pellets containing APIs with different solubility via extrusion process
Drug Development and Industrial Pharmacy 43 (3), 458-464 (2017)

Proceedings & Book Chapters

- M. Thommes, P. Kleinebudde
The Science and Practice of Extrusion-Spheronization in: A. R. Rajabi-Siahboomi (Editor), Multiparticulate Drug Delivery Formulation, Processing and Manufacturing
New York: Springer Science+Business Media LLC, 37-63 (2017)

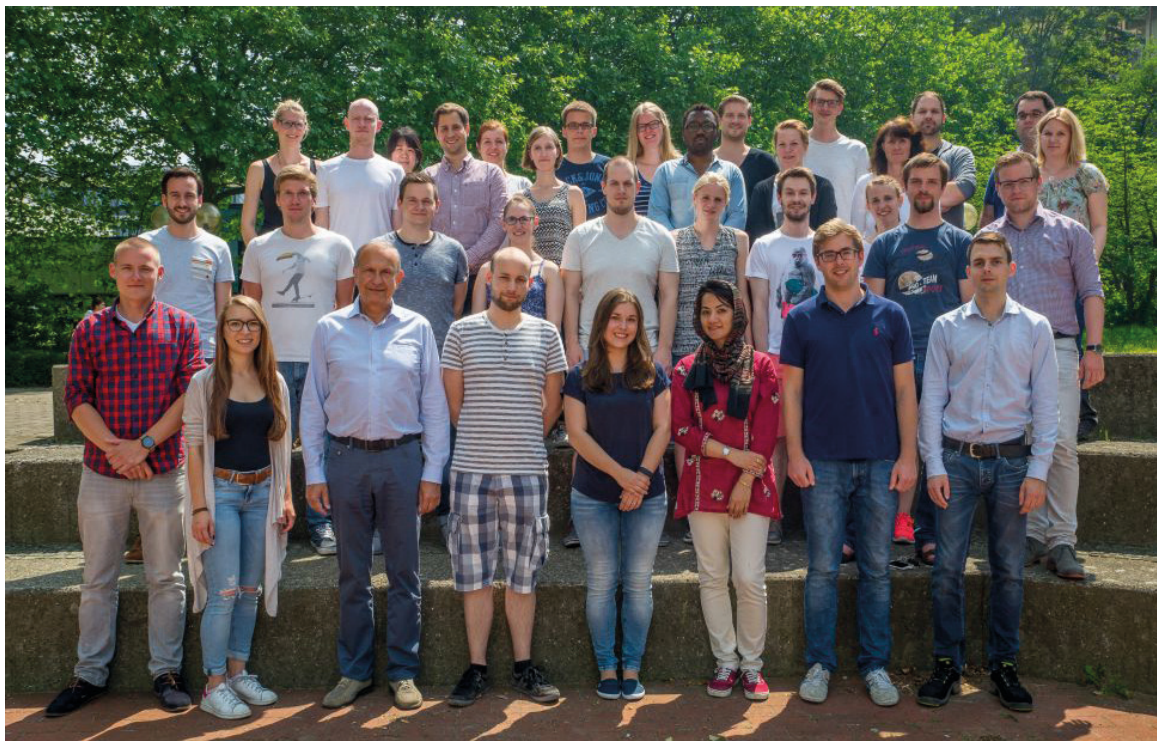
2016

- D. T. Hegyesi, M. Thommes, P. Kleinebudde, T. Sovány, P. Jr Kása, A. Kelemen, K. Pintye-Hódi, G. Jr Regdon
Preparation and Physicochemical Characterization of Matrix Pellets Containing APIs with Different Solubility via Extrusion Process
Drug Development and Industrial Pharmacy dx.doi.org/10.1080/03639045.2016.1261150 (2016)
- E. J. Laukamp, K. Knop, M. Thommes, J. Breitzkreutz
Micropellet-Loaded Rods with Dose-Independent Sustained Release Properties for Individual Dosing via the Solid Dosage Pen
International Journal of Pharmaceutics 499, 271-279 (2016)
- R. Meier, M. Thommes, N. Rasenack, K.P. Moll, M. Krumme, P. Kleinebudde
Granule Size Distributions after Twin-Screw Granulation - Do Not Forget the Feeding Systems
European Journal of Pharmaceutics and Biopharmaceutics 106, 59-69 (2016)

2015

- F.E. Kiene, M. Pein, M. Thommes
Orientation to Determine Quality Attributes of Flavoring Excipients Containing Volatile Molecules
Journal of Pharmaceutical and Biomedical Analysis 110, 20-26 (2015)
- E.J. Laukamp, A.K. Vynckier, J. Voorspoels, M. Thommes, J. Breitzkreutz
Development of Sustained and Dual Drug Release Co-Extrusion Formulations for Individual Dosing
European Journal of Pharmaceutics and Biopharmaceutics 89, 357-364 (2015)

- G.F. Petrovick, M. Pein, M. Thommes, J. Breitzkreutz
Spheronization of Solid Lipid Extrudates: A Novel Approach on Controlling Critical Process Parameters
European Journal of Pharmaceutics and Biopharmaceutics 92, 15-21 (2015)
- J. Ronowicz, M. Thommes, P. Kleinebudde, J. Krysinski
A Data Mining Approach to Optimize Pellets Manufacturing Process Based on a Decision Tree Algorithm
European Journal of Pharmaceutical Science 73, 44-48 (2015)
- M. W. Tackenberg, C. Geisthovel, A. Marmann, H.P. Schuchmann, P. Kleinebudde, M. Thommes
Mechanistic Study of Carvacrol Processing and Stabilization as Glassy Solid Solution and Microcapsule
International Journal of Pharmaceutics 478, 597-605 (2015)
- M. W. Tackenberg, R. Krauss, A. Marmann, M. Thommes, H.P. Schuchmann, P. Kleinebudde
Encapsulation of Liquids Using a Counter Rotating Twin Screw Extruder
European Journal of Pharmaceutics and Biopharmaceutics 89, 9-17 (2015)



Fluid Separations (FVT)

Additive Manufacturing of Packings for Rotating Packed Bed

Konrad Gładyszewski, Andrzej Górak, Mirko Skiborowski

During the last 30 years HIGEE technology and specifically rotating packed beds (RPBs) have gained considerable interest as compact contacting equipment for process intensification. Through a considerable improvement of mass transfer efficiency, they have the potential for significant volume reductions compared to classical contacting equipment, such as packed columns. The acceleration of the liquid by centrifugal force furthermore enables the use of internals with high packing density and the processing of highly viscous liquids. However, while a wide variety of internals is available for classical columns, including diverse random and structured packing, the range of available packing materials for RPBs is yet very narrow.

While classical manufacturing technologies seem rather of limited suitability in developing tailored packings for use in RPBs (Neumann et al. 2017), the given constraints make them specifically interesting for modern Additive Manufacturing (AM) techniques. Being developed in the 1980s, AM, which is also known as Rapid Prototyping, originated around the same time as RPBs were first introduced at ICI in the UK (Reay et al. 2013). According to the American Society of Testing and Materials (ASTM) AM is "the process of joining materials to make objects from 3D model data, usually layer upon layer, as opposed to subtractive manufacturing methodologies" (F2792-12a). Today, AM has evolved to a mature technology which provides a pathway for inexpensive and flexible manufacturing of specialized components and one-off parts (Engstrom et al. 2014). It allows for computer-assisted design and manufacturing of advanced functional materials, which have been used in all kinds of diverse applications, ranging from medical applications, such as prosthetics and tissue engineering, over drug delivery systems, food and optical applications, applications in art and architecture to the energy and chemical industry (Femmer et al. 2016). Despite the complexity of selecting a specific AM process, the possibility of varying the structure with almost unlimited degrees of freedom makes AM predestined for the design of tailored packing materials. The comparable small packing volume, coming from a range of cubic meters for packed columns to liters in RPBs, as well as the unique geometrical shape of the required packing, further increase the suitability of a combination of RPBs and AM. Yet, there is no indication of such a combination in open literature. The current investigations demonstrate the possibility of the manufacturing of packing material by means of 3D printing, directly taking into account a pilot scale RPB. In order to illustrate the competitiveness of the approach, first an available metal foam packing

was investigated experimentally, providing basic results concerning hydrodynamics and mass transfer. Afterwards a model of the foam packing was generated and a replica was produced by means of AM using a polymer resin (Figure 1). The generated results indicate the comparability of the different packing materials and demonstrate the suitability of AM as an approach for rapid prototyping in order to generate and test innovative packing materials for RPBs. Future research is dedicated to the development of improved packing structures using the AM approach.

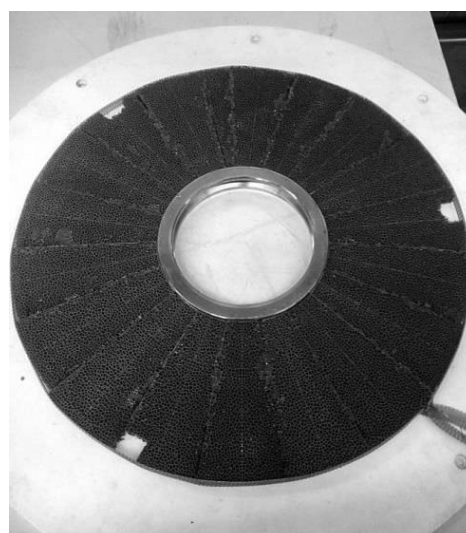


Figure 1: Fully 3D printed packing at Fluid Separations Chair for rotating packed bed. D.S.

Contact:

konrad.gladyszewski@tu-dortmund.de
mirko.skiborowski@tu-dortmund.de
andrzej.gorak@tu-dortmund.de

Publications:

D.S. Engstrom, B. Porter, M. Pacios, H. Bhaskaran, (2014): Additive nanomanufacturing – A review. In *Journal of Materials Research* 29 (17), pp. 1792–1816. DOI: 10.1557/jmr.2014.159.

T. Femmer, I. Flack, M. Wessling, (2016): Additive Manufacturing in Fluid Process Engineering. In *Chemie Ingenieur Technik* 88 (5), pp. 535–552. DOI: 10.1002/cite.201500086.

K. Neumann, S. Hunold, K. Groß, A. Górak, (2017): Experimental investigations on the upper operating limit in rotating packed beds. In *Chemical Engineering and Processing: Process Intensification* 121 (Supplement C), pp. 240–247. DOI: 10.1016/j.cep.2017.09.003.

D. Reay, C. Ramshaw, A. Harvey, (2013): Chapter 6 - Intensification of Separation Processes. In: *Process Intensification (Second edition) : Isotopes in Organic Chemistry*. Oxford: Butterworth-Heinemann, pp. 205–249.

A Systematic Approach towards Synthesis and Design of Pervaporation-Assisted Separation Processes

Bettina Scharzec, Thomas Waltermann, Mirko Skiborowski

Although membrane-assisted processes, such as pervaporation-assisted distillation, are considered as sustainable alternatives to thermal separation processes, they are rarely considered in early stages of conceptual design. In order to enable an identification of promising applications, a systematic approach was developed that includes the synthesis of pervaporation-assisted process variants and applies optimization-based methods for process analysis. It allows for a limitation of the experimental investigations to a necessary minimum and considers competitive reference processes as well as further means for process intensification in the evaluation.

Membrane-assisted hybrid processes, such as the combination of pervaporation (PV) and distillation, provide a tremendous potential for an energy efficient separation of complex and particularly azeotropic multicomponent mixtures. However, the benefits of membrane processes, as e.g. the capability to overcome limitations of other separation techniques are often exploited best when integrated in hybrid processes. Nevertheless, industrial applications are still limited due to a lack of suitable design methods that allow for the consideration of PV-assisted processes in an early stage of conceptual design. Current design methods often require the knowledge of suitable membranes as well as a respective membrane model that, in turn, require an intensive membrane screening. It is of crucial importance to evaluate the potential of a membrane-assisted process prior to any cost- and time-consuming experiments. Further, an appropriate analysis should consider methods for process intensification, such as options for energy integration, for both, membrane-assisted processes and alternative process variants. That allows for a meaningful comparison of the generated configurations regarding the overall potential of each process.

In order to overcome these current limitations, a systematic five-step design approach was developed for the evaluation of the potential of energy intensified PV-assisted processes [1]. An illustration of the proposed methodology is given in Figure 1. Within the first step, the potential feasibility of PV-assisted separation processes is examined by means of thermodynamic insight on different levels of detail. Based on that analysis, suitable process configurations are generated and a proper benchmark process is to be determined. The second step focuses on the evaluation of the PV-assisted process variants under the assumption of a perfect membrane separation by minimizing the total energy demand. That provides an estimate of the maximum benefit obtained by the PV-assisted process prior to any cost- and time-consuming experiment.

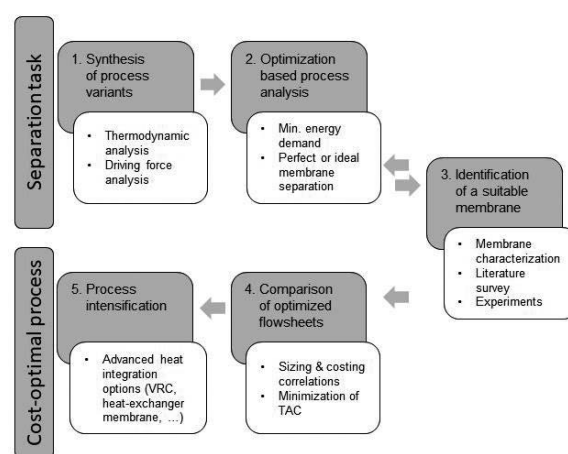


Figure 1: Flowchart for the synthesis and design approach for PV-assisted hybrid processes.

In case of a promising PV-assisted variant, a suitable membrane, as well as a membrane model, has to be determined in the third step. That is achieved either by a literature survey or experiments based on the previous model-based analysis in step two that defines the requirements for the membrane and restricts the experimental design space. In the fourth step, optimized designs of the PV-assisted process variants are determined and compared to the considered reference process in terms of total annualized costs. In the last step, additional means for process intensification are taken into account. For the PV-assisted processes, advanced heat-integrated membrane modules are considered allowing for a nearly isotherm operation resulting in a reduced membrane area as well as costs. In case of a single distillation column, vapor recompression is considered for a direct heat-integration of reboiler and condenser. That final step is essential for a meaningful comparison of the generated process variants.

Publications:

[1] B. Scharzec, T. Waltermann, M. Skiborowski, *Chemie Ingenieur Technik* 89, 1534-1549 (2017).

Contact:

bettina.scharzec@tu-dortmund.de
mirko.skiborowski@tu-dortmund.de
andrzej.gorak@tu-dortmund.de

Publications 2017 - 2015

2017

- I. Aspras, M. Jaworska, A. Górak
Kinetics of chitin deacetylase activation by the ionic liquid [Bmim] [Br]
Journal of biotechnology 251, 94–98 (2017)
 - A. Górak, C. Gourdon, F. Spits, A. Stankiewicz
Importance of Knowledge and Technology Transfer in PI
NPT Procestecnologie 4, 18–19 (2017)
 - M. Leimbrink, S. Sandkämper, L. Wardhaugh, D. Maher, P. Green, G. Puxty, W. Conway, R. Bennett, H. Botma, P. Feron, A. Górak, M. Skiborowski
Energy-efficient solvent regeneration in enzymatic reactive absorption for carbon dioxide capture
Applied Energy 208, 263–276 (2017)
 - T. Waltermann, M. Skiborowski
Conceptual Design of Highly Integrated Processes – Optimization of Dividing Wall Columns
Chemie Ingenieur Technik 89 (5), 562–581 (2017)
 - K. Neumann, S. Hunold, M. Skiborowski, A. Górak
Dry pressure drop in rotating packed beds – systematic experimental studies
Industrial & Engineering Chemistry Research 56 (43), 12395–12405 (2017)
 - J. Dreimann, F. Hoffmann, M. Skiborowski, A. Behr, A. Vorholt
Merging Thermomorphic Solvent Systems and Organic Solvent Nanofiltration for Hybrid Catalyst Recovery in a Hydroformylation Process
Industrial & Engineering Chemistry Research 56 (5), 1354–1359 (2017)
 - H. Kuhlmann, M. Skiborowski
Optimization-Based Approach To Process Synthesis for Process Intensification: General Approach and Application to Ethanol Dehydration
Industrial & Engineering Chemistry Research 56 (45), 13461–13481 (2017)
 - B. Scharzec, T. Waltermann, M. Skiborowski
A Systematic Approach towards Synthesis and Design of Pervaporation-Assisted Separation Processes
Chemie Ingenieur Technik 89 (11), 1534–1549 (2017)
 - K. Neumann, S. Hunold, K. Groß, A. Górak
Experimental investigations on the upper operating limit in rotating packed beds
Chemical Engineering and Processing: Process Intensification 121, 240–247 (2017)
 - M. Wierschem, M. Skiborowski, A. Górak, R. Schmuhl, A. Kiss
Techno-economic evaluation of an ultrasound-assisted Enzymatic Reactive Distillation process
Computers & Chemical Engineering 105, 123–131 (2017)
 - M. Barecka, M. Skiborowski, A. Górak
A novel approach for process retrofitting through process intensification
Chemical Engineering Research and Design 123, 295–316 (2017)
 - M. Jaworska, A. Górak, J. Zdunek
Modification of Chitin Particles with Ionic Liquids Containing Ethyl Substituent in a Cation
Advances in Materials Science and Engineering 2017, 1–9 (2017)
 - M. Leimbrink, S. Tlatlik, S. Salmon, A.-K. Kunze, T. Limberg, R. Spitzer, A. Gottschalk, A. Górak, M. Skiborowski
Pilot scale testing and modeling of enzymatic reactive absorption in packed columns for CO₂ capture
International Journal of Greenhouse Gas Control 62 (3), 100–112 (2017)
 - K. Werth, P. Kaupenjohann, M. Skiborowski
The potential of organic solvent nanofiltration processes for oleochemical industry
Separation and Purification Technology 182 (3), 185–196 (2017)
 - K. Werth, P. Kaupenjohann, M. Knierbein, M. Skiborowski
Solvent recovery and deacidification by organic solvent nanofiltration
Journal of Membrane Science 528 (3), 369–380 (2017)
 - K. Kruber, M. Krapoth, T. Zeiner
Interfacial mass transfer in ternary liquid-liquid systems
Fluid Phase Equilibria 440, 54–63 (2017)
 - J.-C. de Hemptinne, J.-H. Ferrasse, A. Górak, S. Kjelstrup, F. Maréchal, O. Baudouin, R. Gani
Energy efficiency as an example of cross-discipline collaboration in chemical engineering
Chemical Engineering Research and Design 119, 183–187 (2017)
 - M. Wierschem, S. Schlimper, R. Heils, I. Smirnova, A.A. Kiss, M. Skiborowski, P. Lutze
Pilot-Scale Validation of Enzymatic Reactive Distillation for Butyl Butyrate Production
Chemical Engineering Journal 312, 106–117 (2017)
 - M. Wierschem, O. Walz, A. Mitsos, M. Termuehlen, A.L. Specht, K. Kissing, M. Skiborowski
Enzyme kinetics for the transesterification of ethyl butyrate with enzyme beads, coated packing and ultrasound assistance
Chemical Engineering and Processing: Process Intensification 111, 25–34 (2017)
- Peer-reviewed conference papers
- T. Waltermann, D. Muenchrath, M. Skiborowski
Efficient optimization-based design of energy-intensified azeotropic distillation processes
Computer Aided Chemical Engineering 40 (5), 1045–1050 (2017)
 - M. Leimbrink, K. Neumann, K. Kupitz, A. Górak, M. Skiborowski
Enzyme accelerated carbon capture in different contacting equipment - a comparative study
Energy Procedia 114C, 795–812 (2017)
 - M. Leimbrink, T.-L. Limberg, A.-K. Kunze, M. Skiborowski
Different strategies for accelerated CO₂ absorption in packed columns by application of the biocatalyst carbonic anhydrase
Energy Procedia 114C, 781–794 (2017)

- T.-J. Kim, A. Lang, A. Chikukwa, E. Sheridan, P. Dahl, M. Leimbrink, M. Skiborowski, J. Roubroeks
Enzyme Carbonic Anhydrase Accelerated CO₂ Absorption in Membrane Contactor
Energy Procedia 114C, 17–24 (2017)

Book chapters

- M.H. Barecka, M. Skiborowski, A. Górak
Process Intensification in Practice: Ethylene Glycol Case Study
In: Lecture Notes on Multidisciplinary Industrial Engineering (Eds. M. Ochowiak, S. Woźniowski, M. Doligalski, P. Mitkowski) Springer (2017)

2016

- J. Dreimann, P. Lutze, M. Zagajewski, A. Behr, A. Górak, A. J. Vorholt
Highly integrated reactor–separator systems for the recycling of homogeneous catalysts
Chemical Engineering and Processing: Process Intensification. 99, 124–131 (2016)
- T. Goetsch, P. Zimmermann, S. Enders, T. Zeiner
Tunable extraction systems based on hyperbranched polymers
Chemical Engineering and Processing: Process Intensification. 99 (3), 175–182 (2016)
- T. Goetsch, P. Zimmermann, R. van den Bongard, S. Enders, T. Zeiner
Superposition of Liquid–Liquid and Solid–Liquid Equilibria of Linear and Branched Molecules: Binary Systems
Industrial & Engineering Chemistry Research. 55 (42), 11167–11174 (2016)
- M. M. Jaworska, A. Górak
Modification of chitin particles with chloride ionic liquids
Materials Letters. 164, 341–343 (2016)
- A. Kubiczek, W. Kamiński, A. Górak
Modeling of single- and multi-stage extraction in the system of water, acetone, butanol, ethanol and ionic liquid
Fluid Phase Equilibria. 425, 365–373 (2016)
- H. Kuhlmann, M. Skiborowski
Synthesis of Intensified Processes from a Superstructure of Phenomena Building Blocks
Computer Aided Chemical Engineering. 38, 697–702 (2016)
- K. Neumann, K. Werth, A. Martín, A. Górak
Biodiesel production from waste cooking oils through esterification: Catalyst screening, chemical equilibrium and reaction kinetics
Chemical Engineering Research and Design. 107, 52–62 (2016)
- R. Schulz, R. van den Bongard, J. Islam, T. Zeiner
Purification of Terpenyl Amine by Reactive Extraction
Industrial & Engineering Chemistry Research. 55 (19), 5763–5769 (2016)
- T. Waltermann, M. Skiborowski
Efficient optimization-based design of energetically intensified distillation processes
Computer Aided Chemical Engineering. 38, 571–576 (2016)
- M. Wierschem, S. Boll, P. Lutze, A. Górak
Evaluation of the Enzymatic Reactive Distillation for the Production of Chiral Compounds
Chem. Ing. Tech. 88 (1–2), 147–157 (2016)

- K. Groß, K. Neumann, K. Kupitz, M. Skiborowski, A. Górak
HiGee-Technologie – Untersuchung von Hydrodynamik und Stofftransport
Chemie-Ingenieur-Technik, 88 (9), p. 1283 (2016)
- J. Dreimann, P. Lutze, M. Zagajewski, A. Behr, A. Górak, A.J. Vorholt
Highly integrated reactor–separator systems for the recycling of homogeneous catalysts
Chemical Engineering and Processing: Process Intensification, 99, pp. 124–131 (2016)
- C. Kunde, D. Michaels, J. Micovic, P. Lutze, A. Górak, A. Kienle
Deterministic global optimization in process design of distillation and melt crystallization
Chemical Engineering and Processing: Process Intensification, 99, pp. 132–142 (2016)

2015

- T. Färber, R. Schulz, O. Riechert, T. Zeiner, A. Górak, G. Sadowski, A. Behr
Different recycling concepts in the homogeneously catalysed synthesis of terpenyl amines
Chemical Engineering and Processing: Process Intensification (98), 22–31 (2015)
- A. Kulaguin Chicaroux, A. Górak, T. Zeiner
Demixing behavior of binary polymer mixtures
Journal of Molecular Liquids. 209 (3), 42–49 (2015)
- A. Kulaguin Chicaroux, M. Plath, T. Zeiner
Hyperbranched polymers as phase forming components in aqueous two-phase extraction
Chemical Engineering and Processing: Process Intensification. 149 (3), 66–73 (2015)
- A. Kulaguin Chicaroux, T. Zeiner
Investigation of interfacial properties of aqueous two-phase systems by density gradient theory
Fluid Phase Equilibria. 149 (2015)
- A.-K. Kunze, P. Lutze, M. Kopatschek, J. F. Maćkowiak, J. Maćkowiak, M. Grünwald, A. Górak
Mass transfer measurements in absorption and desorption: Determination of mass transfer parameters
Chemical Engineering Research and Design. 104, 440–452 (2015)
- A.-K. Kunze, G. Dojchinov, V. S. Haritos, P. Lutze
Reactive absorption of CO₂ into enzyme accelerated solvents: From laboratory to pilot scale
Appl. Energy (156), 676–685 (2015)
- M. Leimbrink, A.-K. Kunze, D. Hellmann, A. Górak, M. Skiborowski
Conceptual Design of Post-Combustion CO₂ Capture Processes - Packed Columns and Membrane Technologies
Computer Aided Chemical Engineering. 37, 1223–1228 (2015)
- J. Muendges, A. Zalesko, A. Górak, T. Zeiner
Multistage aqueous two-phase extraction of a monoclonal antibody from cell supernatant
Biotechnology Progress. 31 (4), 925–936 (2015)
- J. Muendges, I. Stark, S. Mohammad, A. Górak, T. Zeiner
Single stage aqueous two-phase extraction for monoclonal antibody purification from cell supernatant
Fluid Phase Equilibria. 385 (0), 227–236 (2015)

- A. Niesbach, N. Fink, P. Lutze, A. Górak
Design of reactive distillation processes for the production of butyl acrylate: Impact of bio-based raw materials
Chinese Journal of Chemical Engineering. 23 (11), 1840-1850 (2015)
- P. Rdzaneek, S. Heitmann, A. Górak, W. Kamiński
Application of supported ionic liquid membranes (SILMs) for biobutanol pervaporation
Separation and Purification Technology. 155, 83-88 (2015)
- D. Sudhoff, M. Leimbrink, M. Schleinitz, A. Górak, P. Lutze
Modelling, design and flexibility analysis of rotating packed beds for distillation
Chemical Engineering Research and Design. 94, 72-89 (2015)
- K. Werth, K. Neumann, M. Skiborowski
Computer-aided process analysis of an integrated biodiesel process incorporating reactive distillation and organic solvent nanofiltration
Computer Aided Chemical Engineering. 37, 1277-1282 (2015)
- M. Wierschem, R. Heils, S. Schlimper, I. Smirnova, A. Górak, P. Lutze
Enzymatic Reactive Distillation for the Transesterification of Ethyl Butyrate: Model Validation and Process Analysis
Computer Aided Chemical Engineering 37, 2135-2140 (2015)
- K. Werth, P. Lutz, A.A. Kiss, A.I. Stankiewicz, G.D. Stefanidis, A. Górak
A systematic investigation of microwave-assisted reactive distillation: Influence of microwaves on separation and reaction
Chemical Engineering and Processing: Process Intensification, 93, pp. 87-97 (2015)
- M. Wierschem, M. Skiborowski, A. Górak
Continuous enzymatic reactive distillation with immobilized enzyme beads
Separations Division 2015 – Core Programming Area at the 2015 AIChE Annual Meeting, 2, pp. 648-655 (2015)
- D.K. Babi, J. Holtbruegge, P. Lutze, A. Górak, J.M. Woodley, R. Gani
Sustainable process synthesis–intensification
Computers and Chemical Engineering, 81, pp. 218-244 (2015)



Fluid Mechanics (SM)

Filling Flow into Thin Porous Media

Modeling of one-phase and a displacement flow through thin porous media

Konrad Boettcher, Tim Neumann, Peter Ehrhard

If the pores of a porous medium are much smaller than its macroscopic dimensions, the fluid flow through the porous medium can usually be considered to be homogeneous. But if the pores are not that small, the influence of the containment onto the flow as well as onto the structure of a porous medium has to be taken into account. The distortion of the pore arrangement near a wall is the so-called wall effect. This effect plays a major role in the filling process of Li-Ion batteries, where an electrolyte has to flow in the porous media of the electrodes and the separator, confined by impermeable collector foils.

As the propagation speed of the wetting front tends to zero at the end of the process, the Reynolds number is small with $Re \approx 10^{-5}$. Also in recent literature there are several authors proclaiming a low Reynolds number flow regime where the Darcy law, mainly used for describing flows through porous media, is not valid. This so-called Pre-Darcy flow regime starts from Reynolds numbers smaller than $Re \approx 10^{-2} - 10^{-4}$ and has some importance e.g. to the enhanced oil recovery. Finicky experiments are performed to investigate the validity of the Darcy law. Glycerin is used as it is a Newtonian liquid with a high viscosity and easy to handle. It can be shown, that the linear Darcy law holds for all experiments down to a Reynolds number of $Re \approx 10^{-9}$ (see Figure 1). Here, the mean velocity is about 40 nm/s and three days needed to get the last data point. Therefore, it seems as if the Pre-Darcy flow region does not exist and that deviations to the theory are due to other influences like temperature gradients or impurities in the one-phase flow. As the Darcy law holds, the porosity depending on the wall distance in straight reservoirs is examined, showing some differences to the oscillation in cylindrical reservoirs.

To choose a suitable method which correlates the permeability with the porosity ϵ in the wall-effect domain, the similarity with a characteristic pore diameter is exploited. Several porous media are fixed with epoxy resin, and the porosity and pore diameter is determined in wall-parallel layers.

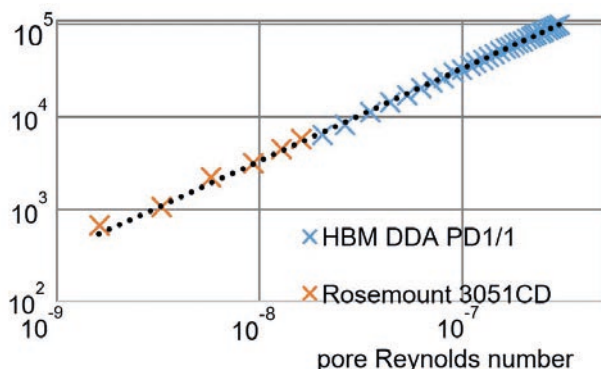


Figure 1: Pressure drop vs. pore Reynolds number for two different pressure sensors.

Contact:

konrad.boettcher@tu-dortmund.de
tim.neumann@tu-dortmund.de
peter.ehrhard@tu-dortmund.de

It is found, that the well-known law by Carman-Kozeny holds in the bulk region of porous media but not in the oscillating region (see Figure 2).

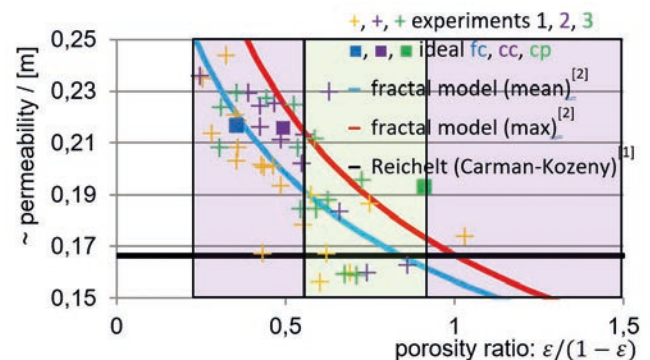


Figure 2: Permeability over porosity ratio: experimental results, mean (blue) and max (red) fractal methods and Carman-Kozeny (black). The latter model is valid only in the bulk (green area) of the porous media but not in the oscillating region (purple).

Here, a fractional law by Cai^[2] is applicable. The models are implemented into ANSYS CFX and numerical simulations are performed and shown in Figure 3. They are compared to the experimental velocity profile in a porous medium in a cylindrical domain^[3]. The amplitude and position of the minima and maxima are computed quite well.

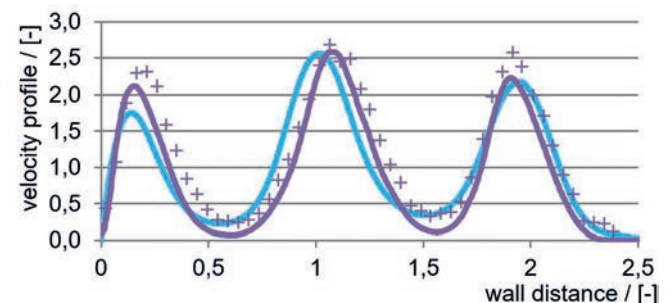


Figure 3: Circumferential averaged velocity in a porous domain: Experimental results^[3] and own numerical results (lines).

[1] Reichelt, Chem. Ing J., 44 (1972), 1068-1071

[2] Cai et Yu, Fractals, 18 (2010), 417-423

[3] Zeiser, Dissertation TU Erlangen-Nürnberg (2008)

Publications:

T. Neumann, K. Boettcher, P. Ehrhard: Numerical investigation into a liquid displacing a gas in thin porous layers, Proc. Appl. Math. Mech. 16 (2014).

Pressure Drop in Fibrous Filters

Jayotpaul Chaudhuri, Peter Ehrhard

Coalescing filtration is a mechanical process which is employed to remove dispersed aerosol particles from a gas stream. This kind of filtration is a depth filtration process and is widely used in process industries to remove particulate matter from exhaust gases or in compressed air applications to filter oil particles introduced during the compression process. Fibrous filters are often used due to low cost, high capture efficiency and low pressure drop. There, droplets are first captured on fibres, then coalesce, and eventually drain out. The performance of a filter medium is judged based on its capture efficiency and pressure drop characteristics. In the present study, numerical simulations using ANSYS CFX are used to predict the pressure drop caused due to air flow through the randomly oriented fibrous filter medium. A fictitious domain approach is used to simulate solid fibres without the need to create a case-specific mesh for different fibre alignment.

Theoretical investigations to predict flows around fibres have started as early as 1930 with 2D flow analysis around a single isolated fibre. The most widely used pressure drop correlation was developed in 1959 using the cell model which also accounts for fibre-fibre interaction. The theoretical approach is only valid for 2D cases and negligible inertial effects. To investigate the influence of inertial effects and the effects of randomly oriented 3D fibres a CFD simulation was setup to measure the Δp . A special fictitious domain approach was used where the fibres are replaced with a region of low permeability. This is advantageous because there is no need to create case-specific meshes as is the case with traditional body-fitted meshes.

The model is extended to a 3D case with multiple fibres, the fibre regions described by a function with five degrees of freedom, namely the gradient angle α , the rotational angle β , and the displacement of the center point coordinates x_m , y_m and z_m ; all varied randomly.

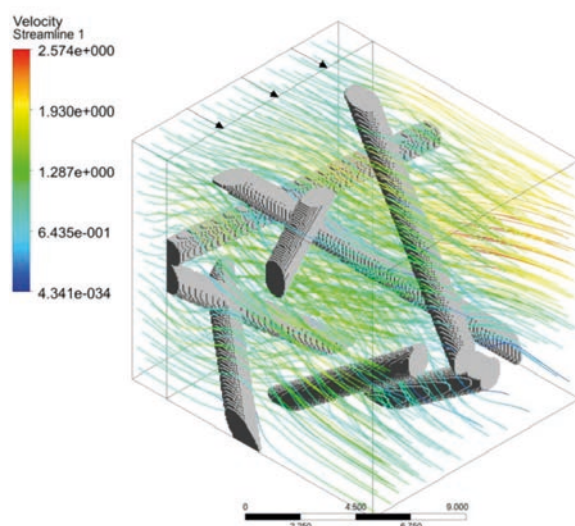


Figure 1: Numerical results showing randomly oriented fibres and air streamlines.

The resulting flow field is visualized in Figure 1, where the grey zones signify solid fibres and the colored lines are streamlines of the air. The results of the simulations, both 2D and randomized 3D case can be directly compared with the theoretical cell model, only in the region of low Reynolds number ($Re = 0.001$). As expected the 2D model gives similar results as the cell model but both are much bigger than the results with 3D randomized fibres.

A possible explanation may be that randomly generated fibre structures yield regions of low solidity, which have a low resistivity to fluid flow; the bulk of the fluid flows through these regions and results in a lower pressure drop. The non-dimensional pressure drop gradient is shown in Figure 2.

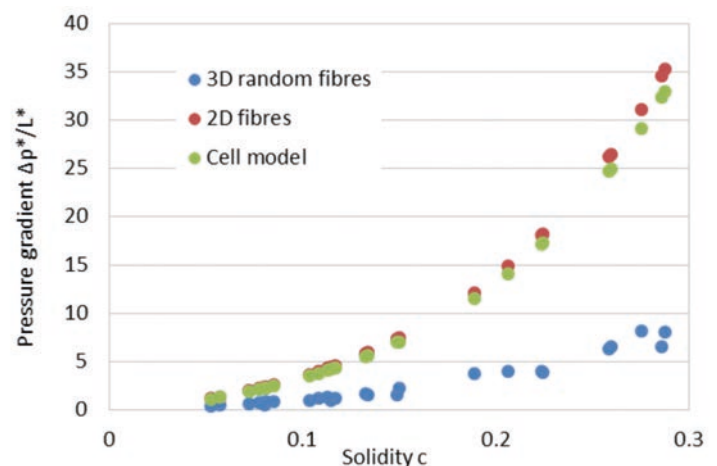


Figure 2: Comparison between Happel-Kuwabara, 2D and 3D randomized simulations for $Re=0,001$.

Experimental Analysis of Bubble-Entrapment during Droplet Impact on solid Walls

Sabrina Grünendahl, Lutz Gödeke, Peter Ehrhard

Droplet impact on solid walls often leads to the entrapment of thin films of gas underneath the droplet during the spreading process. These films rapidly form small substrate-pinned bubbles by formation of multiple contact lines. These substrate-pinned bubbles are stationary and lead to problems, e.g. spray painting. The resulting film is distorted and optical and mechanical properties do not meet the requirements (see Fig. 2). The process is dependent on both, fluid and solid properties (surface tension, viscosity) as well as application parameters (droplet diameter, impact velocity).

Droplets ($d_{drop} = 1.8 - 2.2$ mm) are generated by a continuous flow through a thin capillary ($d_{cap} = 0.15 - 0.3$ mm) and dripping on NBK-7 borosilicate glass substrate wafers. The process is filmed from an axis perpendicular to the droplet trajectory, i.e. side-view, and for transparent substrates from below along the trajectory axis (Figure 1). Due to the rapid formation of the entrapped bubbles, the frame-rates have to be in the range of 20.000 - 35.000 fps.

The obtained pictures allow for diameter and velocity measurements shortly before impact and capture the spreading dynamics after impact. At the same time, we do obtain a series of 10 - 30 pictures that capture the dynamic process of bubble formation. The observed time scale for this rapid process is $t_{bubble} = 10^{-1} - 10^1$ ms.

Dimensional analysis leads to a set of dimension-less groups that are used to create a map-of-occurrence (see Figure 3) for substrate-pinned bubbles.

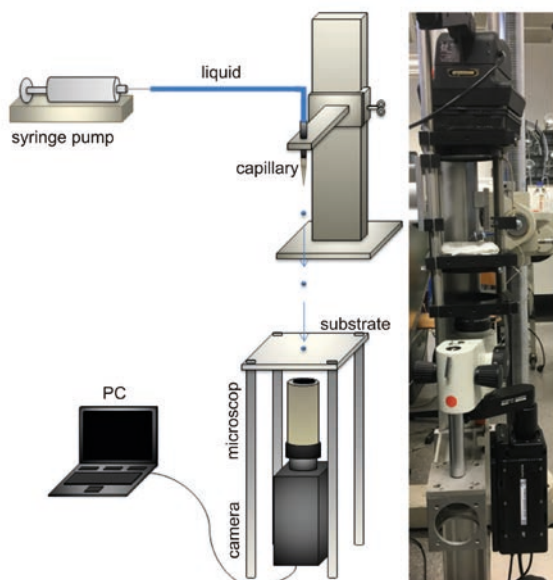


Figure 1: Experimental setup, left: schematic, right: laboratory setup with high-speed camera, microscope, light-source and dripping needle.

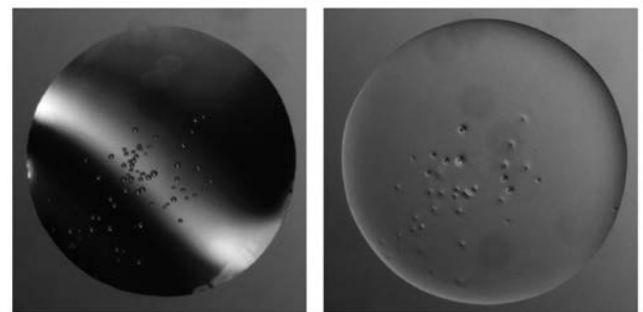


Figure 2: Left side: fluid droplet shortly after impact with substrate-pinned bubbles. Right side: dry film with pinholes and encased bubbles in solidified material. Sterocoll SHT 1.7 % / SXT 0.3 %, Oh = 0.06, Re = 800.

These groups are varied by using mixtures of water and glycerol, thus changing the liquid properties and by changing the capillary-to-substrate distance, thus changing the impact velocity.

Further experiments show, that the diameters of the resulting bubbles and the velocities of corresponding contact lines are dependent on Weber and Reynolds number. The size of entrapped bubbles can be reduced by increasing impact velocity, the characteristic entrapment time t_{bubble} increases with viscosity.

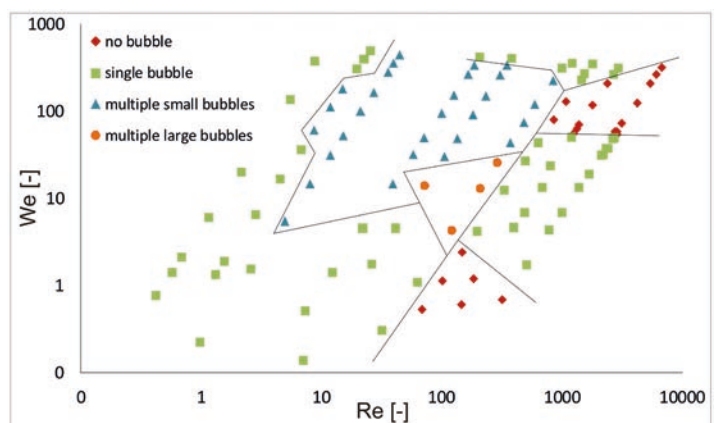


Figure 3: Map-of-occurrence for bubble entrapment displayed as We-over-Re-nomogram. Four major types of bubble formation can be identified (see legend). Lines proportional to Re^1 correspond to same fluid. Left side: Glycerol, right side: Water, in between mixtures.

Publications 2017 - 2015

2017

- C. Heckmann, S.K. Kurt, P. Ehrhard, N. Kockmann
Mass Transport in a Liquid-Liquid Plug Flow in a Micro-Capillary Reactor
Chemie Ingenieur Technik 89 (12), 1642-1649 (2017)

- P. Lakshmanan, P. Ehrhard
Gas bubbles in micro capillaries – hydrodynamics and mass transfer
Proc. Angewandte Mathematik und Mechanik 15, 513 (2015)

2016

- P. Ehrhard
Mikroströmungen
in: Prandtl-Führer durch die Strömungslehre, ed. H.H. Oertel, 14. Auflage, 663-714, Springer Vieweg, Wiesbaden (2016)
- M. Meier
Modellierung und Simulation von Strömungen und biologischen Reaktionen innerhalb eines Belebtschlammbeckens
Chemie Ingenieur Technik 88, 1128-1137 (2016)
- P. Lakshmanan, P. Ehrhard
Enhanced mass transfer in micro-capillary two-phase flow
Proc. Angewandte Mathematik und Mechanik 16, 603 (2016)
- A.K. Höffmann, P. Lakshmanan, P. Ehrhard, Th. Ostermann
The Jungebad apparatus for the production of oil-dispersion baths
Proc. Angewandte Mathematik und Mechanik 16, 599 (2016)
- T. Neumann, K. Boettcher, P. Ehrhard
Numerical investigation into a liquid displacing a gas in thin porous layers
Proc. Angewandte Mathematik und Mechanik 16, 605 (2016)
- Ch. Heckmann, P. Ehrhard
Simulation of mass transfer in liquid/liquid slug flow
Proc. Angewandte Mathematik und Mechanik 16, 597 (2016)

2015

- W. Tillmann, J. Pfeiffer, N. Sievers, K. Boettcher
Analysis of the spreading kinetics of AgCuTi melts on silicon carbide below 900 °C, using a large-chamber SEM
Colloids and Surfaces A: Physicochemical Engineering Aspects 468, 167-173 (2015)
- T. Neumann, K. Boettcher, P. Ehrhard
Numerical investigation of a liquid displacing a gas in thin porous layers
Proc. Angewandte Mathematik und Mechanik 15, 517 (2015)
- K. Boettcher, T. Externbrink
Linear stability of a thin non-isothermal droplet spreading on a rotating disk
Proc. Angewandte Mathematik und Mechanik 15, 503 (2015)
- Ch. Heckmann, P. Lakshmanan, P. Ehrhard
Simulation of mass transfer at free liquid/liquid interfaces
Proc. Angewandte Mathematik und Mechanik 15, 509 (2015)



Technical Biochemistry (TB)

Engineering Yeasts as Platform Organisms for Cannabinoid Biosynthesis

First Reconstitution of the Final Cannabinoid Biosynthesis Pathway in Yeast

Bastian Zirpel, Friederike Degenhardt, Chantale Martin, Oliver Kayser, Felix Stehle

Δ^9 -tetrahydrocannabinolic acid (THCA) is a plant derived secondary natural product from the plant *Cannabis sativa* L. The discovery of the human endocannabinoid system in the late 1980s resulted in a growing number of known physiological functions of both synthetic and plant derived cannabinoids. Thus, manifold therapeutic indications of cannabinoids currently comprise a significant area of research. Here we reconstituted the final biosynthetic cannabinoid pathway in yeasts. This study is an important step toward total biosynthesis of valuable cannabinoids and derivatives and demonstrates the potential for developing a sustainable and secure yeast bio-manufacturing platform.

Δ^9 -tetrahydrocannabinolic acid (THCA) is a plant derived secondary natural product from the plant *Cannabis sativa* L. with therapeutic indications like analgesics for cancer pain, decreasing intraocular pressure in glaucoma or reducing spasticity associated with multiple sclerosis. Here we reconstituted the late biosynthetic pathway for THCA production from *C. sativa* in yeasts.

In a first approach, the heterologous expression of the native CBGA forming enzyme CBGAS from *C. sativa* was investigated in *S. cerevisiae*, but no functionally active protein was obtained.

Alternatively, the use of the soluble prenyltransferase NphB from *Streptomyces* sp. strain CL190 was tested to replace the native transmembrane prenyltransferase CBGAS. Beside the desired product cannabigerolic acid, NphB catalyzes an *O*-prenylation leading to 2-*O*-geranyl olivetolic acid.

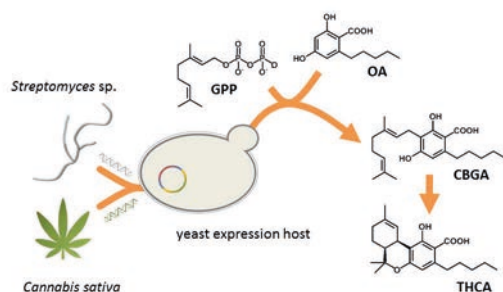


Figure 1: Reconstitution of the final biosynthetic cannabinoid pathway in yeasts.

Based on these results we tried to express both coding sequences *nphB* and *thcas* simultaneously in *S. cerevisiae* to produce THCA. Neither expression of *thcas* and *nphB* driven by the same promoter nor the expression of both enzymes using a bidirectional Gal10/Gal1 promoter system led to formation of sufficient amounts of CBGA which could serve as substrate for THCAS.

Contact:
oliver.kayser@tu-dortmund.de
felix.stehle@tu-dortmund.de

In order to improve *nphB* expression we tried to make use of *K. phaffii*'s ability to express proteins at high levels upon multi-copy integration of the coding sequences into its genome. Finally, the performed screening for strains with higher NphB activities, in a strain containing a high copy insertion of the *thcas* coding sequence, yielded a *K. phaffii* strain that can produce 82 ± 4.6 pmol L⁻¹ OD⁻¹ h⁻¹ THCA.

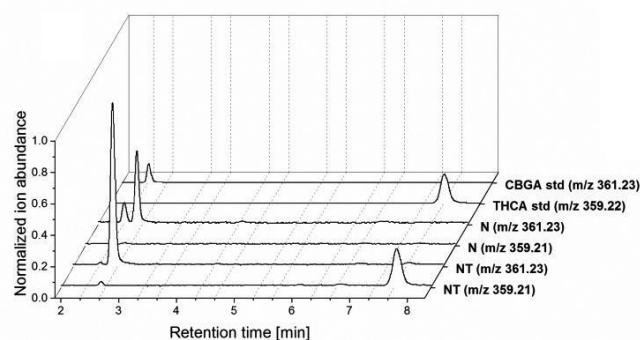


Figure 2: LC-MS analysis of cannabinoids produced with extracts of *K. phaffii* expressing both *nphB* and/or *thcas*. The yeast extracts were incubated with 1mM GPP and OA, respectively. N – assay of lysed yeast expressing only NphB; T – assay of lysed yeast expressing only THCAS; NT – assay of lysed yeast expressing both NphB and THCAS.

We show for the first time that the bacterial prenyltransferase and the final enzyme of the cannabinoid pathway tetrahydrocannabinolic acid synthase can both be actively expressed in the yeasts *S. cerevisiae* and *K. phaffii* simultaneously. While enzyme activities in *S. cerevisiae* were insufficient to produce THCA from olivetolic acid and geranyl diphosphate, genomic multi-copy integrations of the enzyme's coding sequences in *K. phaffii* resulted in successful synthesis of THCA from olivetolic acid and geranyl diphosphate.

Publications:
B. Zirpel, F. Degenhardt, C. Martin, O. Kayser, F. Stehle,
Journal of Biotechnology 259, 204–212 (2017).

Publications 2017 - 2015

2017

- B. Zirpel, F. Degenhardt, C. Martin, O. Kayser, F. Stehle
Engineering yeasts as platform organisms for cannabinoid biosynthesis
J Biotechnol 259, 204–212 (2017)
- F. Stehle, F. Degenhardt, B. Zirpel, O. Kayser
Biotechnological synthesis of tetrahydrocannabinolic acid
PHARMAKON 5, 142–147 (2017)
- Â. Carvalho, E.H. Hansen, O. Kayser, S. Carlsen, F. Stehle
Designing microorganisms for heterologous biosynthesis of cannabinoids
FEMS Yeast 17 (4), fox037 (2017)
- K.L. Kohnen, S. Sezgin, M. Spiteller, H. Hagels, O. Kayser
Localization and Organization of Scopolamine Biosynthesis in *Duboisia myoporoides*
Plant Cell Physiol. 59 (1), 107-118 (2017)
- F. Daoud, D. Pelzer, S. Zuehlke, M. Spiteller, O. Kayser
Ozone pretreatment of process waste water generated in course of fluoroquinolone production
Chemosphere 185, 953-963 (2017)
- S.F. Ullrich, A. Rothauer, H. Hagels, O. Kayser
Influence of Light, Temperature, and Macronutrients on Growth and Scopolamine Biosynthesis in *Duboisia* species
Planta Med 83, 937-945 (2017)

2016

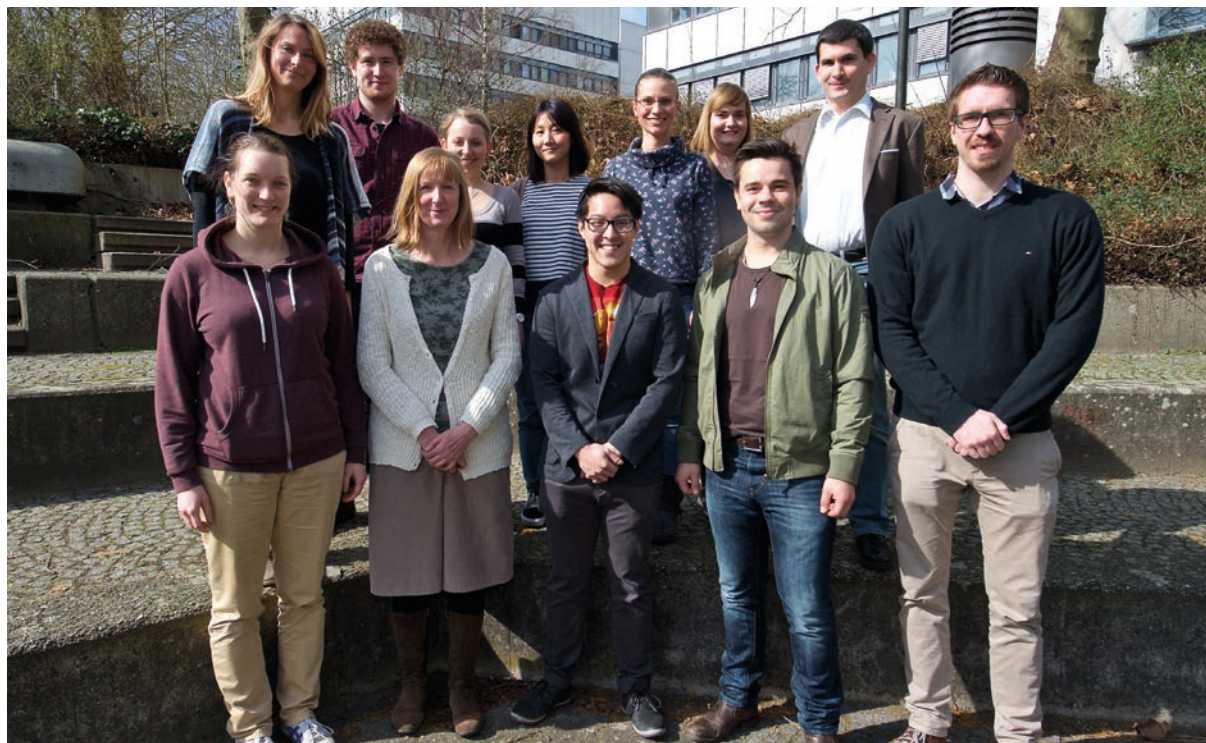
- S.F. Ullrich, H. Hagels, O. Kayser
Scopolamine: a journey from the field to clinics
Phytochem Rev 2016, DOI: 10.1007/211101-016-9477-x
- J. Sasse, M. Schlegel, L. Borghi, S.F. Ullrich, M. Lee, G.-W. Liu, J.-L. Giner, O. Kayser, L. Bigler, E. Martinoia, Kretzschmar
T. *Petunia hybrida* PDR2 is involved in herbivore defense by controlling steroidal contents in trichomes
Plant, Cell & Environment 2016, DOI: 10.1111/pce. 12828
- S.F. Ullrich, N.J.H. Aversch, L. Castellanos, Y.H. Choi
A. Rothauer, O. Kayser
Discrimination of wild types and hybrids of *Duboisia myoporoides* and *Duboisia leichhardtii* at different growth stages using ¹H NMR-based metabolite profiling and tropane alkaloid targeted HPLC-MS analysis
Phytochemistry 2016, 131: 44-56
- N. Happyana, O. Kayser
Monitoring metabolite profiles of *Cannabis sativa* L. trichomes during flowering period using ¹H NMR-based metabolomics and Real-Time PCR
Planta Med 2016, DOI: 10.1055/s-0042-108058
- W.-X. Wang, S. Kusari, H. Laatsch, C. Golz, P. Kusari, C. Strohmam, O. Kayser, M. Spiteller
Antibacterial azaphilones from an endophytic fungus, *Colletotrichum* sp. BS4
J Nat Prod 2016, 79: 704-710

Proceedings & Book Chapters

- S. Farag, O. Kayser
The Cannabis Plant: Botanical Aspects
In: Preedy V (Hrsg.). Handbook of cannabis and related pathologies: biology, pharmacology, diagnosis, and treatment. Elsevier B.V., 3–12 (2017)
- F. Degenhardt, F. Stehle, O. Kayser
The biosynthesis of cannabinoids
In: Preedy V (Hrsg.). Handbook of cannabis and related pathologies: biology, pharmacology, diagnosis, and treatment. Elsevier B.V., 13–23 (2017)

2015

- E. Gruchattka, O. Kayser
In vivo validation of *in silico* predicted metabolic engineering strategies in yeast: disruption of alpha-ketoglutarate dehydrogenase and expression of ATP-citrate lyase for terpenoid production
PLoS One. 2015, 10(12): e0144981
- S. Farag, O. Kayser
Cultivation and breeding of *Cannabis sativa* L.
In: Medicinal and aromatic plants of the world. Vol. 1, Springer Netherlands, Dordrecht, ISBN 978-94-017-9810-5, 2015, 165-186
- S. Farag, O. Kayser
Cannabinoids production by hairy root cultures of *Cannabis sativa* L.
Am. J. Plant Sciences 2015, 6: 1874-1884
- G. Li, S. Kusari, P. Kusari, O. Kayser, M. Spiteller,
Endophytic *Diaporthe* sp. LG23 produces a potent antibacterial tetracyclic triterpenoid
J. Nat. Prod. 2015, 78: 2128-2132
- B. Zirpel, F. Stehle, O. Kayser
Production of Delta-9-tetrahydrocannabinolic acid from cannabigerolic acid by whole cells of *Pichia (Komagataella) pastoris* expressing Delta-9-tetrahydrocannabinolic acid synthase from *Cannabis sativa* L.
Biotechn. Lett. 2015. doi: 10.1007/s10529-015-1853-x
- P. Kusari, S. Kusari, M. Spiteller, O. Kayser
Implications of endophyte-plant crosstalk in light of quorum responses for plant biotechnology
Appl. Microbiol. Biotechnol. 2015, 99: 5383-5390
- W.-X. Wang, S. Kusari, S. Sezgin, M. Lamshöft, P. Kusari, O. Kayser, M. Spiteller
Hexacyclopeptides secreted by an endophytic fungus *Fusarium solani* N06 act as crosstalk molecules in *Narcissus tazetta*
Appl. Microbiol. Biotechnol. 2015, 99: 7651-7662



Technical Biology (TBL)

Rewiring Natural Product Biosynthesis

Improving the production of a bacterial lipopeptide by genetic engineering

Florian Baldeweg, Hirokazu Kage, Markus Nett

In biotechnological processes precise expression of metabolic pathway genes is essential for high production of desired products. Here, we developed an orthogonal regulatory circuit for the biosynthesis of the fungicide ralsolamycin and introduced this system into the native producer organism. By combining this genetic engineering approach with procedural improvement, the production of ralsolamycin could be increased by a factor of 70. The facilitated production of this compound set the stage for the determination of its chemical structure.

The natural product ralsolamycin, an inducer of chlamydospore formation in fungi, was previously reported from the soil bacterium *Ralstonia solanacearum*. Although tandem mass data and bioinformatics were used for a preliminary chemical characterization, the full structure of this natural product could not be resolved owing to an extremely low production level ($\sim 0.1 \text{ mg L}^{-1}$) under standard laboratory cultivation conditions.

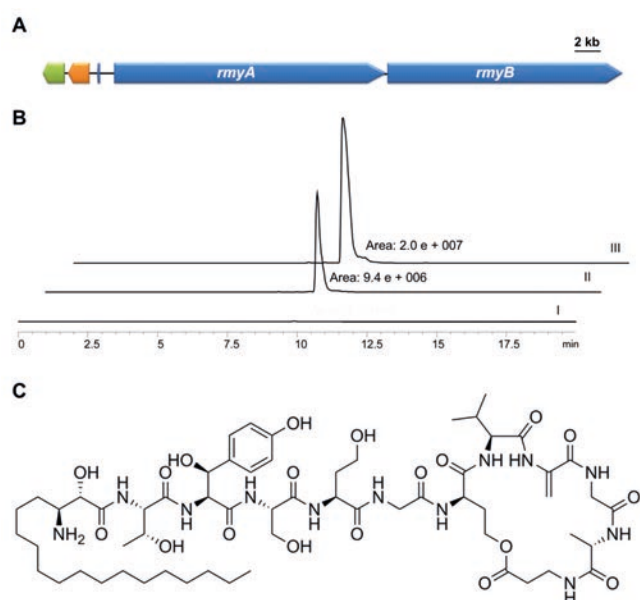


Figure 1: (A) Organization of the ralsolamycin gene locus; core and accessory biosynthesis genes (blue), transporter gene (green), gene of unknown function (orange). (B) Extracted ion chromatograms of ralsolamycin from a negative control (profile I), the wildtype strain (profile II), and the overproduction strain (profile III). (C) Structure of ralsolamycin.

In order to secure sufficient quantities of this compound for further testing, we constructed an overproduction strain by refactoring the regulation of ralsolamycin biosynthesis in the original producer. For this, native promoters and ribosomal binding sites were replaced by synthetic ones, enabling a stringent control of gene expression by defined chemical stimuli. Surprisingly, this approach led only to a modest increase of ralsolamycin production (Figure 1).

Subsequent analyses indicated that the gene overexpression had created bottlenecks in precursor supply, which limited the productivity in batch fermentations. To circumvent this problem, a new optimized production medium was devised. Using this medium, a maximum product concentration of 4.3 mg L^{-1} was achieved with the recombinant *R. solanacearum* strain. This value could be further increased up to 7.0 mg L^{-1} when the production strain was grown in the presence of an adsorber resin. These findings illustrate the importance of integral process development, taking equal account of biotechnological and procedural factors.

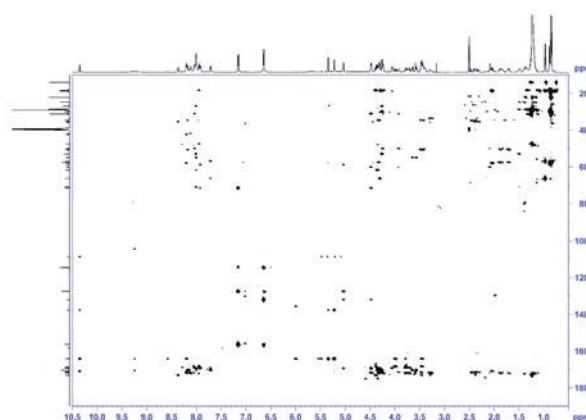


Figure 2: ^1H , ^{13}C HMBC spectrum of ralsolamycin in DMSO-d_6 .

Overall, we generated 200 mg of ralsolamycin in 30-L batch fermentation over 72 h. The obtained material was purified by open column chromatography and reversed-phase HPLC. The structure of ralsolamycin was eventually elucidated following extensive spectroscopic analyses (Figure 2) as well as chemical derivatization.

Exploration of Novel Biological Resources

Identification of novel bacterial species and evaluation of their biosynthetic potential

Xinli Pan, Hirokazu Kage, Markus Nett

*With the advent of genomics, it has become evident that far more microbes than previously anticipated are capable to produce bioactive natural products and other compounds of commercial interest. The genus *Herpetosiphon* is an illustrative example of a bacterial taxon with notable, yet unexploited biosynthetic potential. Recent analyses of this underexplored microbe led to the discovery of a novel diterpene. Moreover, we obtained new data regarding the taxonomic diversity in this genus.*

Bacteria of the genus *Herpetosiphon* occur in a number of soil and freshwater habitats. Furthermore, they are commonly found in the activated sludge of sewage treatment plants. Despite their widespread distribution, information about these filamentous microorganisms (Figure 1) is rather scarce. Some *Herpetosiphon* strains were reported to feed on other soil bacteria. However, it is still unclear whether predation is a common trait in this genus. For the killing of other microbes, *Herpetosiphon* spp. are assumed to resort to a wolf pack strategy, in which a large number of predatory cells congregate in order to lyse the prey by the combined secretion of hydrolytic enzymes. Genomic analyses suggest further that *Herpetosiphon* strains are competent producers of bioactive secondary metabolites. It has even been speculated that a correlation between predation and antibiotic biosynthesis might exist. This would make the genus *Herpetosiphon* a promising resource for antimicrobial compounds.

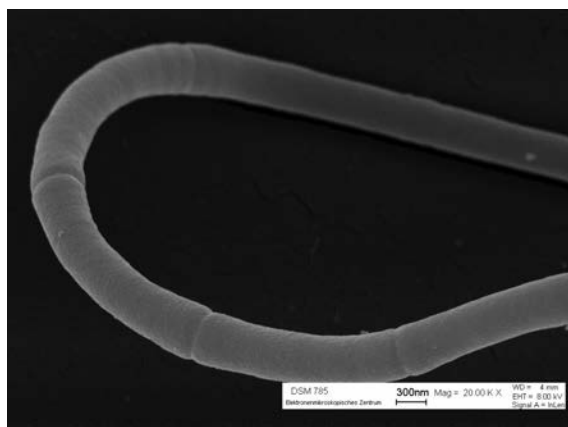


Figure 1: Scanning electron micrograph of a multicellular filament from *Herpetosiphon aurantiacus* DSM 785.

To assess the biotechnological potential of the genus *Herpetosiphon*, several strains were investigated. During our screening, we noted significant differences between the *Herpetosiphon* strains in substrate utilization as well as phenotype, which ultimately led to the recognition of two novel species, *H. gulosus* and *H. giganteus*. Representative strains of both species were fully characterized regarding

their phylogenetic position, fatty acid profiles, menaquinone composition and enzymatic activities.

These analyses supported the proposed taxonomic classification as distinct species. Furthermore, we confirmed the predatory behavior of all *Herpetosiphon* strains tested.

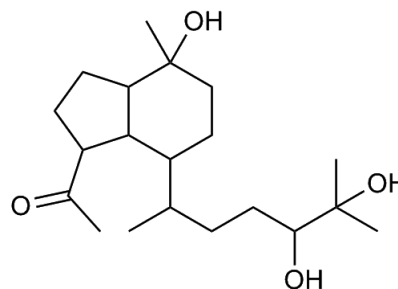


Figure 2: Structure of herpetopanone, which was identified from *H. aurantiacus* DSM 785 using an isotope labeling strategy.

A specific objective of this project was the analysis of isoprenoid biosynthesis in the genus *Herpetosiphon*. Isoprenoids are widely used as pharmaceuticals, flavors and colorants in food, fragrances in perfumes, and biofuels. To identify these compounds in the complex metabolome of a natural product-producing bacterium, we developed a new method, which is based on the feeding of isotopically labeled glucose. The linear oligoprenyl units, which constitute the carbon backbones of isoprenoids, arise from the condensation of activated isoprene units, namely isopentenyl diphosphate (IPP) and dimethylallyl diphosphate (DMAPP). The metabolism of singly ^{13}C -labeled glucose gives rise to a characteristic carbon labeling pattern in IPP and DMAPP. This feature has proven extremely useful to unravel cyclization cascades and carbon-carbon rearrangements in the biosynthesis of some isoprenoids. We anticipated that the resulting mass shifts could also be valuable in the field of natural product discovery. To validate the feasibility of this strategy, we compared the ion chromatograms of *Herpetosiphon* cultures that were grown in the presence or absence of singly labeled glucose. This approach resulted in the discovery of a novel diterpene with a rare octahydro-1*H*-indenyl skeleton (Figure 2). The properties of this compound are currently under investigation.

Publications:

X. Pan, H. Kage, K. Martin, M. Nett, *International Journal of Systematic and Evolutionary Microbiology* 67, 2476-2481 (2017).

X. Pan, N. Domin, S. Schieferdecker, H. Kage, M. Roth, M. Nett, *Beilstein Journal of Organic Chemistry* 13, 2458-2465 (2017).

Contact:

markus.nett@tu-dortmund.de

Publications 2017 - 2015

2017

- F. Baldeweg, H. Kage, S. Schieferdecker, C. Allen, D. Hoffmeister, M. Nett
Structure of ralsolamycin, the interkingdom morphogen from the crop plant pathogen *Ralstonia solanacearum*
Organic Letters 19, 4868-4871 (2017)
- P. Brandt, M. Garcia-Altare, M. Nett, C. Hertweck, D. Hoffmeister
Induced chemical defense of a mushroom by a double-bond-shifting polyene synthase
Angewandte Chemie International Edition 56, 5937-5941 (2017)
- X. Pan, N. Domin, S. Schieferdecker, H. Kage, M. Roth, M. Nett
Herpetopanone, a diterpene from *Herpetosiphon aurantiacus* discovered by isotope labeling
Beilstein Journal of Organic Chemistry 13, 2458-2465 (2017)
- X. Pan, H. Kage, K. Martin, M. Nett
***Herpetosiphon gulosus* sp. nov., a filamentous predatory bacterium isolated from sandy soil and *Herpetosiphon giganteus* sp. nov., nom. rev.**
International Journal of Systematic and Evolutionary Microbiology 67, 2476-2481 (2017)
- S. Schieferdecker, S. König, S. Pace, O. Werz, M. Nett
Myxochelin-inspired 5-lipoxygenase inhibitors: synthesis and biological evaluation
ChemMedChem 12, 23-27 (2017)
- V. Valiante, D. J. Mattern, A. Schöffler, F. Horn, G. Walther, K. Scherlach, L. Petzke, J. Dickhaut, R. Guthke, C. Hertweck, M. Nett, E. Thines, A. A. Brakhage
Discovery of an extended austinoid biosynthetic pathway in *Aspergillus calidoustus*
ACS Chemical Biology 12, 1227-1234 (2017)

2016

- D. Braga, D. Hoffmeister, M. Nett
A non-canonical peptide synthetase adenylates 3-methyl-2-oxovaleric acid for auriculamide biosynthesis
Beilstein Journal of Organic Chemistry 12, 2766-2770 (2016)
- E. Walther, S. Boldt, H. Kage, T. Lauterbach, K. Martin, M. Roth, C. Hertweck, A. Sauerbrei, M. Schmidtke, M. Nett
Zincophorin – biosynthesis in *Streptomyces griseus* and antibiotic properties
GMS Infectious Diseases 4, 08.20161128 (2016)
- I. Seccareccia, A. T. Kovacs, R. Gallegos-Monterrosa, M. Nett
Unraveling the predator-prey relationship of *Cupriavidus necator* and *Bacillus subtilis*
Microbiological Research 192, 231-238 (2016)
- C. Kurth, H. Kage, M. Nett
Siderophores as molecular tools in medical and environmental applications
Organic & Biomolecular Chemistry 14 (35), 8212-8227 (2016)
- D. Kalb, T. Heinekamp, S. Schieferdecker, M. Nett, A. A. Brakhage, D. Hoffmeister
An iterative O-methyltransferase catalyzes 1,11-dimethylation of *Aspergillus fumigatus* fumaric acid amides
ChemBioChem 17 (19), 1813-1817 (2016)
- J. Korp, M. S. Vela-Gurovic, M. Nett
Antibiotics from predatory bacteria
Beilstein Journal of Organic Chemistry 12, 594-607 (2016)

- A. M. Schaible, R. Filosa, V. Krauth, V. Temml, S. Pace, U. Garscha, S. Liening, C. Weinigel, S. Rummler, S. Schieferdecker, M. Nett, A. Peduto, S. Collarile, M. Scuto, F. Roviezzo, G. Spaziano, M. de Rosa, H. Stuppner, D. Schuster, B. D'Agostino, O. Werz
The 5-lipoxygenase inhibitor RF-22c potently suppresses leukotriene biosynthesis in cellulose and blocks bronchoconstriction and inflammation *in vivo*
Biochemical Pharmacology 112, 60-71 (2016)
- D. Schwenk, P. Brandt, R. A. Blanchette, M. Nett, D. Hoffmeister
Unexpected metabolic versatility in a combined fungal fomannoxin/vibrallactone biosynthesis
Journal of Natural Products 79 (5), 1407-1414 (2016)
- C. Kurth, S. Schieferdecker, K. Athanasopoulou, I. Seccareccia, M. Nett
Variochelins, lipopeptide siderophores from *Variovorax boronicumulans* discovered by genome mining
Journal of Natural Products 79 (4), 865-872 (2016)
- S. Schieferdecker, M. Nett
A fast and efficient method for the preparation of the 5-lipoxygenase inhibitor myxochelin A
Tetrahedron Letters 57 (12), 1359-1360 (2016)

2015

- H. Kage, E. Riva, J. S. Parascandolo, M. F. Kreutzer, M. Tosin, M. Nett
Chemical chain termination resolves the timing of ketoreduction in a partially reducing iterative type I polyketide synthase
Organic & Biomolecular Chemistry 13 (47), 11414-11417 (2015)
- J. S. Bauer, M. G. K. Ghequire, M. Nett, M. Josten, H.-G. Sahl, R. De Mot, H. Gross
Biosynthetic origin of the antibiotic pseudopyronines A and B in *Pseudomonas putida* BW11M1
ChemBioChem 16 (17), 2491-2497 (2015)
- J. Korp, S. König, S. Schieferdecker, H.-M. Dahse, G. M. König, O. Werz, M. Nett
Harnessing enzymatic promiscuity in myxochelin biosynthesis for the production of 5-lipoxygenase inhibitors
ChemBioChem 16 (17), 2445-2450 (2015)
- M. H. Medema, R. Kottmann, P. Yilmaz, ..., M. Nett, ..., R. Breitling, E. Takano, F. O. Glöckner
Minimum information about a biosynthetic gene cluster
Nature Chemical Biology 11 (9), 625-631 (2015)
- I. Seccareccia, C. Kost, M. Nett
Quantitative analysis of *Lyso bacter* predation
Applied and Environmental Microbiology 81 (20), 7098-7105 (2015)
- S. Schieferdecker, N. Domin, C. Hoffmeister, D. A. Bryant, M. Roth, M. Nett
Structure and absolute configuration of auriculamide, a natural product from the predatory bacterium *Herpetosiphon aurantiacus*
European Journal of Organic Chemistry (14), 3057-3062 (2015)
- E. C. Barnes, P. Bezerra-Gomes, M. Nett, C. Hertweck
Dandamycin and chandranamycin E, benzoxazines from *Streptomyces griseus*
Journal of Antibiotics 68 (7), 463-468 (2015)
- S. Schieferdecker, S. König, A. Koeberle, H.-M. Dahse, O. Werz, M. Nett
Myxochelins target human 5-lipoxygenase
Journal of Natural Products 78 (2), 335-338 (2015)

Patents

- F. Surup, H. Steinmetz, K. Mohr, K. Viehriig, R. Müller, M. Nett, S. Schieferdecker, H.-M. Dahse, M. Wolling, A. Kirschning
Novel macrolide antibiotics *Pub. No.:* WO/2016/005049 (2016)



Technical Chemistry (TC)

Isomerizing Hydroformylation of Unsaturated Ester Compounds

Development of a new bimetallic tandem catalytic system

Jonas Bianga, Tom Gaide, Kim E. Schlipkoeter, Thomas Seidensticker, Dieter Vogt

The substitution of common polymer precursors from fossil raw materials through some out of renewables is one major issue for the chemical research and industry. Suitable molecules which could be used for such an approach are fatty acid methyl esters because of their long hydrocarbon chains and their relatively low number of functional groups. A wide variety of reactions exist for the implementation of FAMEs as substrate for polymer precursors.

Through the isomerizing hydroformylation it is possible to synthesize α,ω -functionalized molecules out of fatty acid methyl esters (FAMEs). In comparison to reactions like the isomerizing methoxycarbonylation in which diesters are synthesized, a formation of bifunctional and asymmetric aldehyde esters is possible in case of using the isomerizing hydroformylation. This facilitates the synthesis of many different polymer precursors through e.g. an oxidation, a hydrogenation or a reductive amination of this compound. The isomerizing hydroformylation of methyl oleate (Figure 1) is a very challenging reaction. In literature the highest reported yields were limited to 26 % of the linear product. Especially the hydrogenation of the substrate limited the reaction performance. Most approaches focused on the development of a single, auto-tandem catalyst for both reaction steps. In our research we developed a new orthogonal catalytic system, which consists of two different catalysts. One is responsible for the isomerization of the double bond and the other facilitates the linear hydroformylation of the terminal double bond.

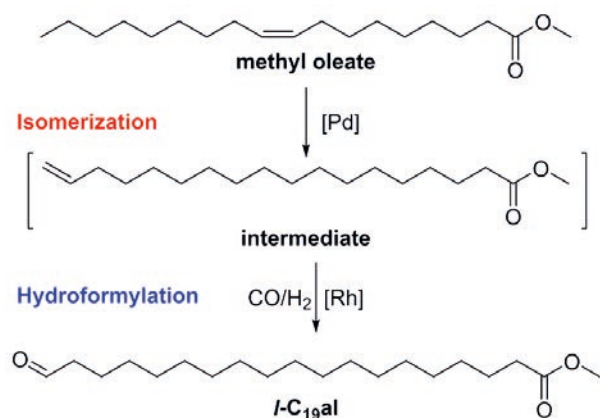


Figure 1: Isomerizing hydroformylation of methyl oleate (1).

For the isomerizing hydroformylation of methyl oleate (1), which is shown in Figure 1, the used catalysts need to fulfill the following requirements under hydroformylation conditions:

- High isomerization activity
- Low hydrogenation activity
- High hydroformylation activity
- High hydroformylation selectivity

Contact:

thomas.seidensticker@tu-dortmund.de

Former research in our workgroup showed, that the catalyst system consisting of Rh(acac)(CO)₂ and the ligand Biphephos is a very effective system for the hydroformylation part of the reaction.

Very high activities and selectivities can be obtained by the use of this catalyst system in hydroformylation reactions. For the isomerization step another catalyst is necessary. Different metals like Pd, Rh, Ru, Ir, Pt, Co or Ni were investigated. Only a Pd dimer as precursor which was presented before by Gooßen et al. showed a very promising isomerization activity in combination with the hydroformylation catalyst. Because of the instability and the relatively high costs of this catalyst complex, an in situ formation of the catalyst was investigated. The active isomerization species was formed through an addition of Pd₂ and Pd(^tBuP)₂ to the reaction mixture. Finally, the new orthogonal catalytic system (Figure 2) led to the highest ever reported yields for the linear selective isomerization hydroformylation of methyl oleate. However, total suppression of the hydrogenation was not achieved in this system.

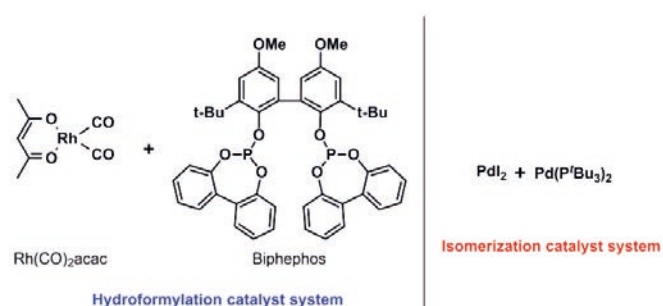


Figure 2: The new developed tandem catalytic system for high linear and high active isomerization / hydroformylation reactions.

In our work, we successfully developed an orthogonal tandem catalytic system for the linear selective isomerizing hydroformylation of methyl oleate in a 100 g scale. Through the new reaction system the highest yields (74 %) and *l/b*-selectivities (91 : 9) to the linear aldehyde ester yet reported were achieved.

Publications:

T. Gaide, K.E. Schlipkoeter, J. Bianga, A. Behr, A.J. Vorholt, ACS Catal., 7, 4163 – 4171 (2017).

Recycling of Homogeneous Catalysts in Reactive Ionic Liquids – Solvent-Free Aminofunctionalizations of Alkenes

First example of a recycling of homogeneous transition metal catalysts in reactive ionic liquids

Michael Terhorst, Thiemo A. Faßbach, Andreas J. Vorholt, Arno Behr, Thomas Seidensticker, Jens M. Dreimann

The recycling of homogeneous transition metal catalysts in amination reactions is a challenging task. Especially on industrial scale, the reuse of the precious metals is economically and ecologically important. The use of a reactive ionic liquid, e.g. dimethyl ammonium dimethyl carbamate, is an elegant solution to combine reactivity and recycling of the catalyst, due to immobilization of the catalyst in the polar carbamate phase.

Methylamines are one of the most important building blocks in the fine chemical industry. Especially the worldwide demand of dimethylamine is high, due to the usage of synthetic unsymmetric tertiary amines as solvents, agrochemicals, or surfactant precursors.

To obtain precursors for surfactants in a straight forward way, we applied β -farnesene in the hydroamination and butadiene in the telomerisation, both in combination with dimethyl amine, which led to the corresponding long chained asymmetric tertiary amines.

As dimethyl amine source, the ionic liquid dimethyl ammonium dimethyl carbamate (dimcarb) consisting of the two gases dimethyl amine and carbon dioxide was used (Figure 1).

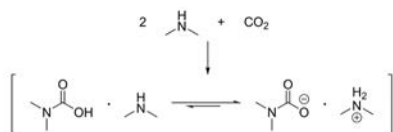


Figure 1: Formation of dimethyl ammonium dimethyl carbamate and equilibrium of ionic and non-ionic form of dimcarb.

Fortunately, this compound is liquid at room temperature and distillable, so that polar by-products will not accumulate in the polar catalyst phase, like in conventional ionic liquids. During the study of the synthesis of surfactant precursors it soon became apparent, that solvent free reaction is possible, which results in high space-time-yields, higher economic impact and the possibility to recycle the catalyst in the reactive ionic liquid. Therefore, the active catalyst species needs to be highly polar, which was achieved by using sulfonated analogues of the used phosphine ligands, to be dissolved in the dimcarb phase.

In case of the hydroamination of β -farnesene, tetrasulfonated 1,4-bis(diphenylphosphino)butane (DPPBTS) was used and a catalyst recycling over 8 runs could be achieved without any loss of activity (Figure 2). Subsequently, an oxidation of the ligand was observed and the reaction performance decreased. Nevertheless, a total turn over number (TON) of 8724 was accomplished. The catalytic system was also applied to other 1,3-dienes, like β -myrcene and isoprene, whereby these two showed slightly lower overall yields.

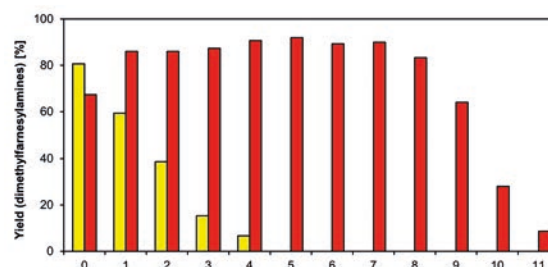


Figure 2: Isolated product yields of the palladium catalyzed hydroamination β -farnesene using the DPPB-ligand (yellow bars) and the tetrasulfonated analog DPPBTS (red bars). Reaction conditions: $\text{Pd}(\text{tfa})_2$, 0.1 mol%, metal/ligand = 1/4, $n_{\text{dimcarb}} = 45$ mmol, $n_{\beta\text{-farnesene}} = 15$ mmol, $T = 100$ °C, $t = 3$ h, 500 rpm. Recycling conditions: dimcarb was refilled to 45 mmol (addition of 7.5 mmol), phase separation at room temperature under schlenk technique, addition of 15 mmol β -farnesene, restart of the reaction.

In case of the telomerisation, an even higher performance of the recycling of the catalyst was achieved. With TPPTS (triphenyl phosphine trisulfonate) as ligand no loss of activity over 30 recycling runs (Figure 3) was accomplished. The TTON was at 90712.

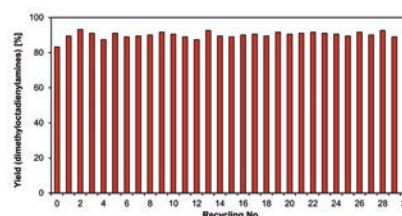


Figure 3: Isolated product yields of the palladium catalyzed telomerization of 1,3-butadiene with dimcarb to N,N-dimethyl octadienylamines. Reaction conditions: Precursor = $\text{Pd}(\text{acac})_2$, 0.03 mol% based on 1,3 butadiene, ligand = TPPTS (= triphenylphosphine-trisulfonate), metal/ligand = 1/4, $n_{\text{dimcarb}} = 30$ mmol, $n_{1,3\text{-butadiene}} = 38$ mmol, $T = 80$ °C, $t = 2$ h, 500 rpm. Recycling conditions: Extraction of the product with cyclohexane (2×2 mL), dimcarb was refilled to 30 mmol (addition of 11 mmol), addition of 38 mmol 1,3-butadiene, restart of the reaction. TTON defined as converted moles of 1,3-butadiene to the desired products per molecule palladium.

Furthermore, we were able to show, that a recycling of the rhodium catalyst for the hydroaminomethylation of 1-dodecene with dimcarb is promising, although a slight loss of activity was observed due to little leaching of the catalyst.

In conclusion, we were able to show that dimcarb is a very good compound for an application in the recycling of homogeneous transition metal catalysts in amination reactions. We were able to establish three different reactions with very good recycling results.

Contact:

michael.terhorst@tu-dortmund.de
jens.dreimann@tu-dortmund.de

Publications:

T. A. Faßbach, R. Kirchmann, A. Behr, A. J. Vorholt
Green Chemistry 19, 5243-5249 (2017).

Process Development of the Continuously Operated Synthesis of *N,N*-Dimethylformamide Based on Carbon Dioxide

An evaluation of stability, selectivity and recyclability of a RuCl_3 – BISBI catalyst complex

Kai Künnemann, Rene Kuhlmann, A. Prüllage, Arno Behr, Andreas J. Vorholt

The utilization of carbon dioxide, CO_2 , is currently a hot topic for the sustainable production of chemicals and storage of renewable energy. *N,N*-Dimethylformamide (DMF) is an important solvent in the fine chemicals industry and for extractions. The direct synthesis of DMF from CO_2 and Dimethylamine with hydrogen was performed in this work with a ruthenium catalyst in a miniplant. Stable operation was demonstrated over a period of 160 hours, demonstrating the feasibility of this approach.

Due to rising environmental constraints and limitations of fossil resources the chemical industry focuses more and more on the substitution of the usually applied C1-carbon sources like carbon monoxide, methanol, formaldehydes etc. by CO_2 . In order to compete economically and ecologically against existing processes, carbon dioxide based processes need well-developed reaction systems. In this work, the process development for the homogenously catalyzed hydrogenation of carbon dioxide in presence of dimethylamine to *N,N*-dimethylformamide (Figure 1) will be demonstrated.

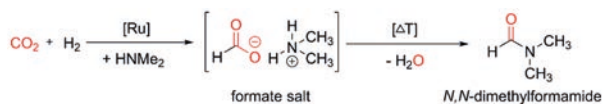


Figure 1: Formation of *N,N*-dimethylformamide.

Since questions about the substrate and catalyst recycling cannot fully be answered just by batch experiments in laboratory scale, this reaction system was transferred into a continuously operated miniplant (Figure 2) in order to investigate the recycling concept of the catalyst and the reaction behavior regarding both the selectivity and the long-term stability of the catalyst.

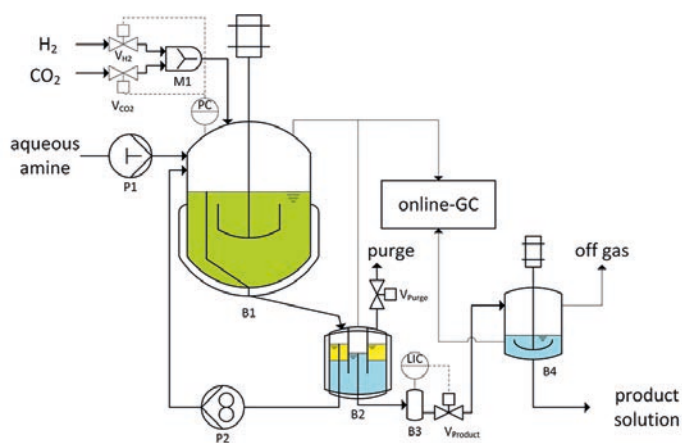


Figure 2: Simplified flow sheet of the continuously operated miniplant for the DMF synthesis.

Various experiments have shown promising results for the reaction systems towards long term stability and selectivity by achieving a stable run-time of 95 h with yields of DMF >40 % (Figure 3). Further investigations of all process streams revealed also that only carbon monoxide is formed as byproduct in very low concentrations (<50ppm).

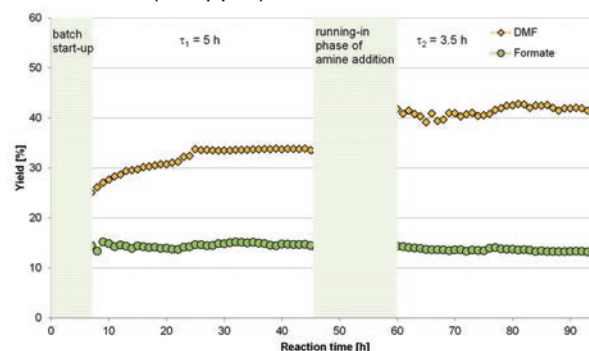


Figure 3: Miniplant results with purge flow regulation. Reaction conditions: Precursor: $\text{RuCl}_3 \cdot \text{H}_2\text{O}$, Ligand: BISBI, $C_{\text{Ru}} = 2 \text{ mmol/l}$, $C_{\text{BISBI}} = 1.6 \text{ mmol/l}$, $C_{\text{DMA}} = 3.8 \text{ mol/l}$, $m_{\text{DMA-solution}} : m_{\text{2-ethylhexan-1-ol}} = 1:1$, $V_{\text{reactor}} = 2000 \text{ ml}$, $V_{\text{liquid}} = 330 \text{ ml}$, $t_{\text{batch}} = 6 \text{ h}$, $U_{\text{stirrer}} = 700 \text{ 1/min}$, $\tau_{\text{reactor}} = 3.4 \text{ h}$, $T_{\text{reactor}} = 140 \text{ }^\circ\text{C}$, $T_{\text{separator(B2)}} = 30 \text{ }^\circ\text{C}$, $p_{\text{total}} = 40 \text{ bar}$, $V_{\text{CO}_2/\text{H}_2} = 0.5 : 1$, $V_{\text{dimethylamine-solution}} = V_{\text{recycle}} = 33 \text{ ml/h}$, $V_{\text{dimethylethanolamine}} = 24 \text{ ml/h}$.

Especially the gas composition had a major impact on the activity of the catalyst. A defined ratio of CO_2 to amine increased the yield from 14 % to 34 % at an even lower residence time. Furthermore, the catalyst leaching was low with 0.3 wt.%/h in average and had no measurable influence on the activity during the investigated time frame, even at temperatures up to 160 °C. A subsequent product isolation via distillation was successfully realized and showed moreover no product decomposition.

Selective Product Crystallization for Sustainable Recycling of Homogeneous Catalyst

Norman Herrmann, Andreas J. Vorholt, Thomas Seidensticker

Conversion of renewable raw materials by homogeneous transition metal catalysis can play a great role in the chemical industry of the future, both from a sustainability and economic point of view. The crux lies in the recovery of the homogeneously dissolved catalyst. In this context, a simple process for selective product crystallization was developed that enables the catalyst used in the product to be recycled for high-purity products. The renewable methyl-10-undecenoate obtained from castor oil used here supplies economic diesters with methoxycarbonylation and linear alcohols in reductive hydroformylation for ester alcohol synthesis.

Environmental awareness and sustainability are becoming increasingly important in the chemical industry. One important aspect in this context is the implementation of renewable resources in chemical processes. The homogeneously catalyzed hydro-formylation of unsaturated long-chained oleo compounds is a promising strategy for adding value to renewable resources. Unfortunately in this context, the recycling of the homogeneous catalyst is a great challenge. This is particularly true in carbonylation reactions of oleobased compounds, since these often suffer from high boiling points and/or high degrees of functionalization. Often distillation cannot be used because at the elevated temperatures that are required. Extraction is also not of interest because a large amount of extractant must be used to separate the catalyst. One approach for catalyst recovery at mild conditions is the crystallization of the product and subsequent separation of the catalyst and the solid product. The principle is to cool down the reaction solution slowly in certain temperature intervals. After precipitation of the product, the catalyst solution is separated via filtration. This technique is gentle in terms of thermal stress to the product, the catalyst and the applied ligands (Figure 2 and 3).

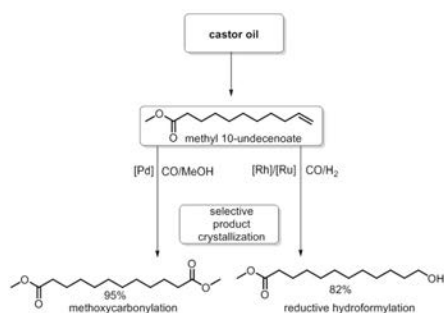


Figure 1: Homogeneously catalysed synthesis of polymer precursors from the renewable methyl 10-undecenoate and catalyst recycling by selective product crystallization.

To show the feasibility of this approach, the above-mentioned methoxycarbonylation of methyl-10-undecenoate was investigated, as well as the tandem hydroformylation/hydrogenation reaction applying the same substrate (Figure 1).

A palladium/ DTBPMB complex was used as catalyst for the methoxycarbonylation. This reaction system gave a high *n*-selectivity (95 %). The yield of the isolated linear diester after crystallization is 95 %.

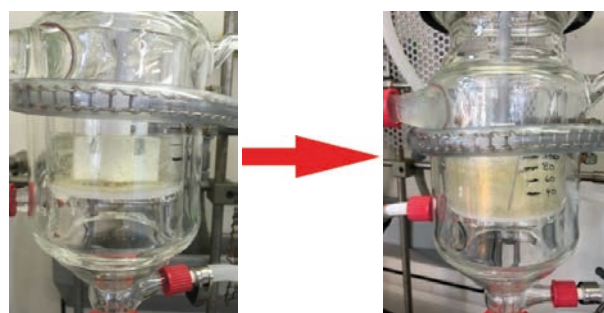


Figure 2: Reaction mixture before, Figure 3: Reaction mixture after crystallization.

The hydroformylation/ hydrogenation reaction was operated with two different catalysts, whereas the hydroformylation was catalyzed by a rhodium/ Biphephos complex and the subsequent hydrogenation was catalyzed by a ruthenium/ tetracyclone complex. This reaction system resulted in high *n*-selectivity (82 %). The yield of the isolated linear alcohol after crystallization was 82 %. By crystallization of the product most of the catalyst remained in the reaction solution and was recycled for further reactions.

Publications:

[1] T. Seidensticker, H. Busch, C. Diederichs, J. J. von Dincklage, A. J. Vorholt: *ChemCatChem* 2016, 8, 2890–2893.

[2] M. Furst, V. Korkmaz, T. Gaide, T. Seidensticker, B. Arno, A. J. Vorholt: *ChemCatChem* 2017, 9, 4319–4323.

Contact:

thomas.seidensticker@tu-dortmund.de

Micelle-Like Polymer Particles – Phase Transfer Agents in Aqueous Hydroformylation of 1-octene

Daniel Peral, D. Stehl, B. Bibouche, H. Yu, J. Mardoukh, R. Schomäcker, R. von Klitzing, Dieter Vogt

For the industrial application of homogeneous catalysts efficient separation and recycling are important issues. The use of water soluble catalysts in aqueous biphasic catalysis is a proven concept for catalyst recovery in the Ruhrchemie-RhônePoulenc hydroformylation process. However, this is only applicable for water soluble substrates. In order to apply the concept also for higher alkenes, micelle-like polymer particles have been used as phase transfer agents and catalyst carriers for anionic ligands in aqueous multiphase hydroformylation reactions. High reaction rates and efficient catalyst recycling were demonstrated, showing the high potential of this approach.

Colloidal, micelle-like polymer particles have been synthesized - constituting a non-polar cross-linked polystyrene core, a polyethylene glycol shell (making them water soluble) and are functionalized with cationic ammonium salts which can attract anionic ligands.

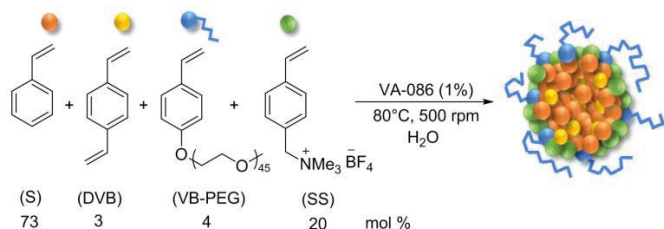


Figure 1: Molar composition and reaction conditions for the synthesis of the polymer particle suspensions by emulsion polymerization.

The particles were characterised by dynamic light scattering (DLS), atomic force microscopy (AFM), transmission electron microscopy (TEM), scanning electron microscopy (SEM) and zeta potential (ζ) measurements.

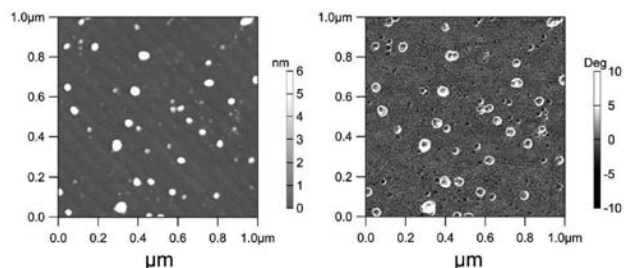
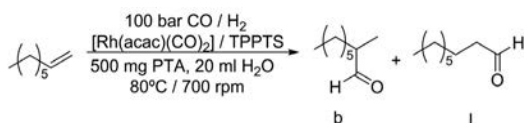


Figure 2: AFM images of polymer particles. Height image (left) and phase image (right).

These polymer particles were designed to act as microreactors in aqueous biphasic catalytic reactions. The particles are suspended in the aqueous catalyst phase where they electrostatically attract any ionic ligands (e.g. the common TPPTS-ligand). The particles were applied as phase transfer agents in aqueous multiphase rhodium-catalysed hydroformylation of 1-octene (scheme 1 below).



Scheme 1: Multiphase hydroformylation of 1-octene.

The reactions were performed in high pressure autoclaves fitted with mechanical gas-inlet stirrers, temperature control, dropping funnels and mass flow control units. Only branched and linear aldehydes were detected in the GC analysis after the reaction, obtaining around 72 % linear aldehydes. The organic phase was further analyzed by ICP-OES showing the amount of rhodium to be below 0.5 ppm. Recycling experiments of the aqueous catalyst/particle phase was then performed three times (Table 1 below).

Run	Conversion (%)	Chemoselect. (%)	l: b	TOF at 10% conv. (h ⁻¹)
1	74.6	>99	2.6	272
2	91.9	96.4	2.5	476
3	92.7	82.7	2.5	462
4	98.5	85.9	1.7	381

Reaction conditions: 0.03 mmol [Rh(acac)(CO)₂], 0.18 mmol TPPTS, 150 mmol 1-octene, [C]:[L]:[S] = 1:6:5000, 15 mmol *n*-dodecane as standard. 500 mg of LX5, 20 ml H₂O. 80 °C, 700 rpm, 100 bar CO:H₂ (1:1), 22 h.

Table 1: Recycling experiments of the multiphase hydroformylation of 1-octene using latex particles.

The reaction progress of the recycling experiments is shown in Figure 3 below.

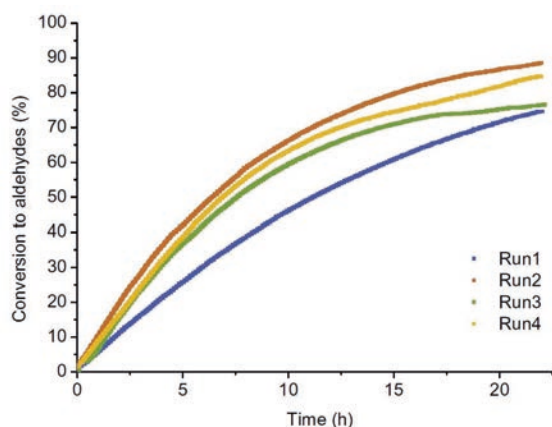


Figure 3: Yield of aldehyde vs. time in the aqueous multiphase hydroformylation of different alkenes.

Further work to optimize the system is underway, with particular focus on recyclability, conversion and selectivity – parameters which are important for industrial application of a process.

Continuously Operated Hydroamination – Toward High Catalytic Performance *via* Organic Solvent Nanofiltration in a Membrane Reactor

Implementation of a stable polymeric membrane for *in-situ* separation of the homogeneous catalyst

Dennis Vogelsang, Jens M. Dreimann, D. Wenzel, Andreas J. Vorholt

The continuous operation of the palladium catalysed hydroamination is still a challenging task. Herein, we present the high performance of a membrane reactor by the implementation of ambitious hydroamination reaction of β -myrcene with morpholine. Via application of a proper poly ether-ether-ketone (PEEK) membrane, operation at elevated temperatures was possible in an integrated reaction/separation unit. By application of model-based predicted reaction conditions, a drastic increase of the turnover number from 460 to 5135 compared to a batch process was achieved. The desired geranyl amines as target products were obtained in very good yields higher than 80%, while an excellent conversion of β -myrcene above 93% was reached in a long-time stable process.

The palladium-catalysed hydroamination of β -myrcene with morpholine is a value adding well-studied reaction to form allylic amines in a 100% atom economic way (Figure 1). The industrial relevant terpenyl amines¹ can be applied as intermediates in Takasago process to produce (-)-menthol.

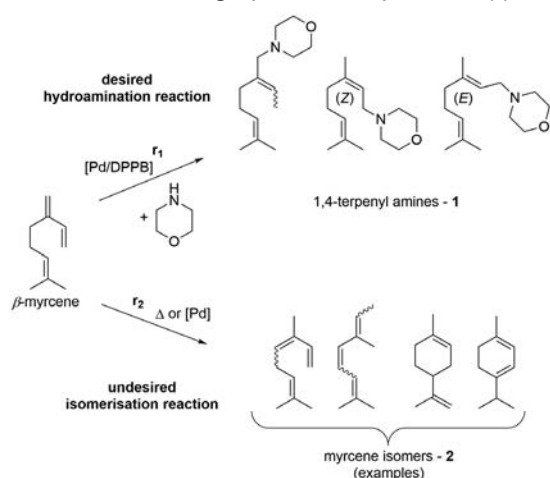


Figure 1: Reaction pathways of the hydroamination reaction of β -myrcene and morpholine. (r_1 =hydroamination, r_2 =isomerisation); For simplification only examples of double bond isomers are shown.

Still, the continuous operation of the hydroamination is a challenging task. The applied palladium catalyst is prone to precipitation by changing the reaction conditions, which limits the number of suitable catalyst recovery methods.

One concept to increase the productivity of the homogeneous transition metal without having a strong influence on the reaction conditions is the usage of organophilic solvent nanofiltration (OSN).

In the present study, a polymeric poly-ether-ether-ketone-membrane was applied in a dead-end filtration membrane reactor. To evaluate the optimal process conditions, the continuous operation was implemented in three steps. First, the kinetics of the hydroamination reaction and relevant membrane characteristics were determined under optimized reaction conditions. Afterwards, these results were incorporated in a reactor/separator model to predict the process behavior. With this, catalyst replenishment was adjusted resulting in stable continuous operation (Figure 2).

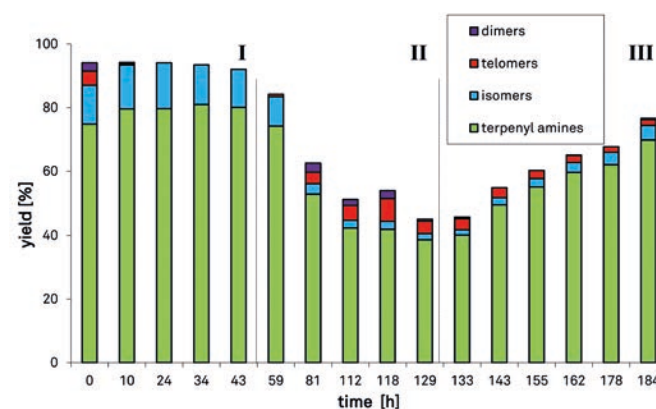


Figure 2: Interval I: (predicted optimal conditions): $c(\beta\text{-myrcene}) = c(\text{morpholine}) = 0.17 \text{ mol/L}$, $c(\text{Pd}(\text{tfa})_2) = 6.86 \cdot 10^{-5} \text{ mol/L}$, $c(\text{DPPB}) = 5.56 \cdot 10^{-4} \text{ mol/L}$, $T = 100 \text{ }^\circ\text{C}$, 500 rpm, feed = 9.9 g/h; interval II ligand omitted): $c(\beta\text{-myrcene}) = c(\text{morpholine}) = 0.17 \text{ mol/L}$, $T = 100 \text{ }^\circ\text{C}$, 500 rpm, feed = 9.9 g/h; III = I; all results were determined via GC-FID-analysis.

The desired geranyl amines were obtained in yields and selectivities higher than 90% over a time period of one week. Via utilization of Organic Solvent Nanofiltration the turn-over-number (TON) of the catalyst could be drastically increased to 5135 compared to the batch process with 460. By this process intensification, the continuous hydroamination could be more feasible for industrial application.

Publications:

D. Vogelsang, J. M. Dreimann, D. Wenzel, L. Peeva, J. da Silva Bursal, A. G. Livingston, A. J. Vorholt, Ind. Eng. Chem. Res. 56, 13634-13641 (2017).

Contact:

dennis.vogelsang@tu-dortmund.de
andreas-j.vorholt@cec.mpg.de

Publications 2017 - 2015

2017

- A. Behr, Z. Bayrak, G. Samli, D. Yildiz, V. Korkmaz, S. Peitz, G. Stochniol
Recycling and Oligomerization Activity of Ni/Al Catalyst in a Biphasic System with Ionic Liquids
Chemical Engineering and Technology 40 (1), 196–204 (2017)
- A. Behr, M. Halama, L. Domke
High throughput screening of homogeneously catalyzed hydrogenations in a continuously perfused membrane reactor
Chem. Eng. Res. Des. 123, 23–34 (2017)
- Behr, Arno; Agar, David W.; Jörisen, Jakob; Vorholt, Andreas J. (2016)
Einführung in die Technische Chemie
Berlin, Heidelberg: Springer Berlin Heidelberg
- J. M. Dreimann, T. A. Faßbach, S. Fuchs, M. R. L. Fürst, T. Gaide, R. Kuhlmann et al.
Vom Laborkuriosum zum kontinuierlichen Prozess
Chem. Ing. Tech. 89 (3), 252–262 (2017)
- J. M. Dreimann, F. Hoffmann, M. Skiborowski, A. Behr, A. J. Vorholt
Merging Thermomorphic Solvent Systems and Organic Solvent Nanofiltration for Hybrid Catalyst Recovery in a Hydroformylation Process
Ind. Eng. Chem. Res. 56 (5), 1354–1359 (2017)
- T. Färber, A. Behr, N. Fink, J. Koop
A Continuous Process for the Purification of Terpenyl Amines Using a Reversible Acid-Base Reaction
Chemical Engineering and Technology 40 (10), 1916–1922 (2017)
- T. A. Faßbach, T. Gaide, M. Terhorst, A. Behr, A. J. Vorholt
Renewable Surfactants through the Hydroaminomethylation of Terpenes
ChemCatChem 9 (8), 1359–1362 (2017)
- T. A. Faßbach, N. Gösser, F. O. Sommer, A. Behr, X. Guo, S. Romanski et al.
Palladium-catalyzed hydroamination of farnesene – Long chain amines as building blocks for surfactants based on a renewable feedstock
Appl. Catal., A 543, 173–179 (2017)
- T. A. Faßbach, R. Kirchmann, A. Behr, A. J. Vorholt
Recycling of homogeneous catalysts in reactive ionic liquid – solvent-free aminofunctionalizations of alkenes
Green Chem 19 (21), 5243–5249 (2017)
- T. A. Faßbach, F. O. Sommer, A. Behr, S. Romanski, D. Leinweber, A. J. Vorholt
Non-ionic surfactants from renewables – amphiphilic ligands in biphasic reactions
Catal. Sci. Technol. 7 (8), 1650–1653 (2017)
- S. Fuchs, D. Lichte, M. Dittmar, G. Meier, H. Strutz, A. Behr, A. J. Vorholt
Tertiary Amines as Ligands in a Four-Step Tandem Reaction of Hydroformylation and Hydrogenation
ChemCatChem 9 (8), 1436–1441 (2017)
- S. Fuchs, M. Steffen, A. Dobrowolski, T. Rösler, L. Johnen, G. Meier et al.
Secondary diamines as a monomer from bis-hydroaminomethylation of industrial cyclic dienes
Catal. Sci. Technol. 7 (21), 5120–5127 (2017)
- M. R. L. Furst, V. Korkmaz, T. Gaide, T. Seidensticker, A. Behr, A. J. Vorholt
Tandem Reductive Hydroformylation of Castor Oil Derived Substrates and Catalyst Recycling by Selective Product Crystallization
ChemCatChem 9 (23), 4319–4323 (2017)
- T. Gaide, J. Bianga, K. Schlipköter, A. Behr, A. J. Vorholt
Linear Selective Isomerization/Hydroformylation of Unsaturated Fatty Acid Methyl Esters
ACS Catal. 7 (6), 4163–4171 (2017)
- T. Gaide, A. Jörke, K. E. Schlipköter, C. Hamel, A. Seidel-Morgenstern, A. Behr, A. J. Vorholt
Isomerization/hydroformylation tandem reaction of a decene isomeric mixture with subsequent catalyst recycling in thermomorphic solvent systems
Appl. Catal., A 532, 50–56 (2017)
- A. Jörke, T. Gaide, A. Behr, A. Vorholt, A. Seidel-Morgenstern, C. Hamel
Hydroformylation and tandem isomerization – hydroformylation of n-decenes using a rhodium-BiPhePhos catalyst
Chem. Eng. J. 313, 382–397 (2017)
- R. Kuhlmann, A. Prüllage, K. Künnemann, A. Behr, A. J. Vorholt
Process development of the continuously operated synthesis of N,N-dimethylformamide based on carbon dioxide
Journal of CO2 Utilization 22, 184–190 (2017)
- R. Kuhlmann, S. Schmitz, K. Haßmann, A. Prüllage, A. Behr
Synthesis of N,N-dimethylformamide from carbon dioxide in aqueous biphasic solvent systems
Appl. Catal., A 539, 90–96 (2017)
- D. Peral, D. Stehl, B. Bibouche, H. Yu, J. Mardoukh, R. Schomäcker et al.
Colloidal polymer particles as catalyst carriers and phase transfer agents in multiphasic hydroformylation reactions
Journal of colloid and interface science 513, 638–646 (2017)
- N. Piens, K. van Hecke, D. Vogt, M. D'hooghe
Cobalt carbonyl-catalyzed carbonylation of functionalized aziridines to versatile β -lactam building blocks
Organic & biomolecular chemistry 15 (22), 4816–4821 (2017)
- D. Vogelsang, J. M. Dreimann, D. Wenzel, L. Peeva, J. da Silva Burgal, A. G. Livingston et al.
Continuously Operated Hydroamination – Toward High Catalytic Performance via Organic Solvent Nanofiltration in a Membrane Reactor
Ind. Eng. Chem. Res. 56 (46), 13634–13641 (2017)
- A. J. Vorholt, S. Immohr, K. A. Ostrowski, S. Fuchs, A. Behr
Catalyst recycling in the hydroaminomethylation of methyl oleate
Eur. J. Lipid Sci. Technol. 119 (5), 1600211 (2017)
- H. Warmeling, D. Hafki, T. von Söhnen, A. J. Vorholt
Kinetic investigation of lean aqueous hydroformylation – An engineer's view on homogeneous catalysis
Chem. Eng. J. 326, 298–307 (2017)
- H. Warmeling, D. Janz, M. Peters, A. J. Vorholt
Acceleration of lean aqueous hydroformylation in an innovative jet loop reactor concept
Chem. Eng. J. 330, 585–595 (2017)

- H. Warmeling, R. Koske, A.J. Vorholt
Procedural Rate Enhancement of Lean Aqueous Hydroformylation of 1-Octene without Additives
Chem. Eng. Technol. 40 (1), 186–195 (2017)

Books and Bookarticles

- P.C.J. Kamer, D. Vogt, J. Thybaut (Eds.)
Contemporary Catalysis; Science, Technology and Applications
RSC 2017
- A. Behr, A.J. Vorholt (Eds.)
Homogeneous Catalysis with Renewables
Springer International Publishing 2017

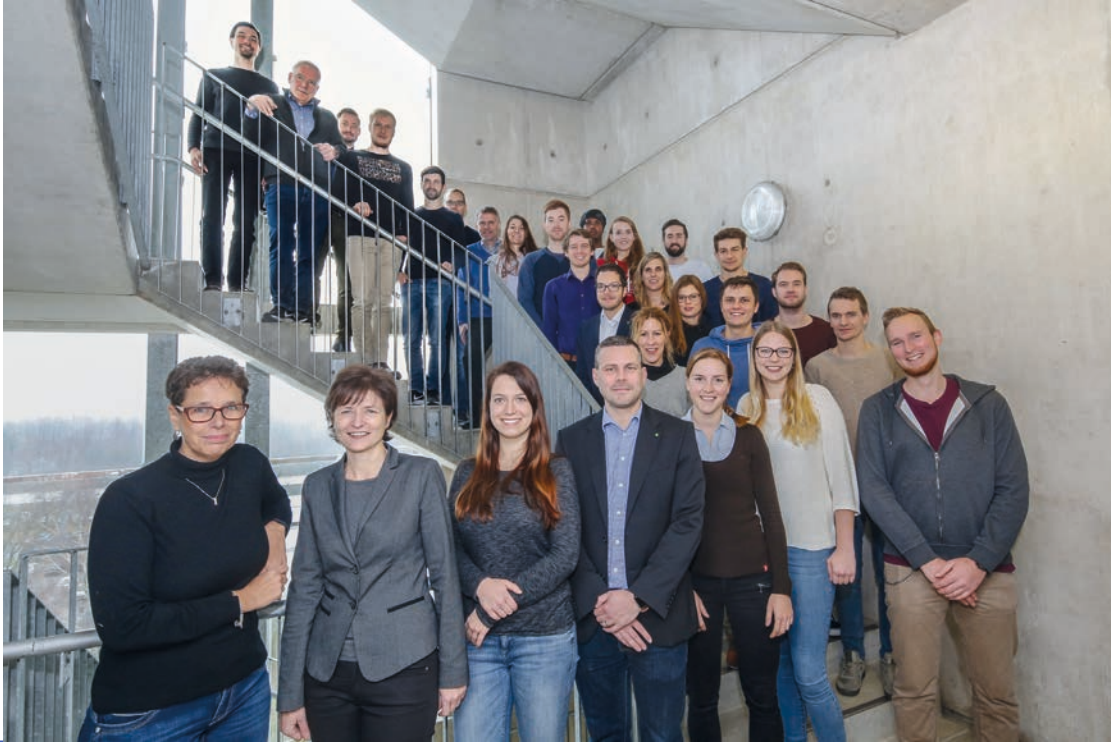
2016

- A. Kämper, P. Kucmierczyk, T. Seidensticker, A.J. Vorholt, R. Franke, A. Behr
Ruthenium-Catalyzed Hydroformylation: From Laboratory to Continuous Miniplant Scale
Catal. Sci. Technol., 2016, 6, 8072–8079, DOI: 10.1039/C6CY01374K
- J. M. Dreimann, M. Skiborowski, A. Behr, A.J. Vorholt
Recycling homogeneous catalysts simply via organic solvent nanofiltration: New ways to efficient catalysis
ChemCatChem, 2016, 8 (21), 3330–3333, DOI: 10.1002/cctc.201601018
- A.J. Vorholt, S. Immohr, K.A. Ostrowski, S. Fuchs, A. Behr
Catalyst Recycling in the Hydroaminomethylation of Methyl Oleate: A Route to Novel Polyamide Monomers
Eur. J. Lipid Sci. Technol., 2016, accepted, DOI: 10.1002/ejlt.201600211
- T. Seidensticker, H. Busch, C. Diederichs, J.J. von Dincklage, A.J. Vorholt
From Oleo Chemicals to Polymer: Bis-Hydroaminomethylation as a Tool for the Preparation of a Synthetic Polymer from Renewables
Chemcatchem, 2016, 8 (18), 2890–2893, DOI: 10.1002/cctc.201600629
- J.M. Dreimann, H. Warmeling, J.N. Weimann, K. Künnemann, A. Behr, A.J. Vorholt
Increasing selectivity of the hydroformylation in a miniplant catalyst, solvent and olefin recycle in two loops
AIChE J., 2016, DOI: 10.1002/aic.15345
- T. Färber, O. Riechert, T. Zeiner, G. Sadowski, A. Behr, A.J. Vorholt
Homogeneously Catalyzed Hydroamination in a Taylor-Couette Reactor using a Thermomorphic Multicomponent Solvent System
Chem. Eng. Res. Des., 2016, 112, 263–273; DOI: 10.1016/j.cherd.2016.06.022
- J. Dreimann, A.J. Vorholt, M. Skiborowski, A. Behr
Removal of homogeneous precious metal catalysts via organic solvent nanofiltration, Chemical Engineering Transactions
Chem. Eng. Trans., 2016, 47, 343–348; DOI:10.3303/CET1647058
- T.A. Faßbach, R. Kirchmann, A. Behr, S. Romanski, D. Leinweber, A.J. Vorholt
Telomerization of 1,3-Butadiene with highly substituted Alcohols Using Pd/NHC-Catalysts – Structure-Reactivity-Relationship of the O-Nucleophile
J. Mol. Catal. A: Chem. 2016, accepted; DOI:10.1016/j.molcata.2016.05.002
- H. Warmeling, A. Behr, A.J. Vorholt
Jet loop reactors as a versatile reactor set up - Intensifying catalytic reactions: A review
Chem. Eng. Sci., 2016, 149, 229–248; DOI:10.1016/j.ces.2016.04.032
- P. Neubert, I. Meier, T. Gaide, A. Behr
Additive-Free Palladium-Catalysed Hydroamination of Piperylene with Morpholine
Synthesis 48 (2016), A–G
- A. Behr, L. Johnen, A. Wintzer, A. G. Cetin, P. Neubert, L. Domke
Ruthenium-Catalyzed Cross Metathesis of β -Myrcene and its Derivatives with Methyl Acrylate
ChemCatChem 8 (2016), 515–522
- A. Kämper, S.J. Warrelmann, K. Reisch, R. Kuhlmann, R. Franke, A. Behr
First iridium-catalyzed hydroformylation in a continuously operated miniplant
Chem. Eng. Sci. 144 (2016), 364–371
- P. Neubert, I. Meier, T. Gaide, R. Kuhlmann, A. Behr
First telomerisation of piperylene with morpholine using palladium-carbene catalysts
Catalysis Comm. 77 (2016), 70–74
- J. Haßelberg, A. Behr, C. Weiser, J.B. Bially, I. Sinev
Process development for the synthesis of saturated branched fatty derivatives: Combination of homogeneous and heterogeneous catalysis in miniplant scale
Chem. Eng. Sci. 143 (2016), 256–269
- J. Haßelberg, A. Behr
Saturated branched fatty compounds Proven industrial processes and new alternatives
Eur. J. Lipid Sci. Technol. 118 (2016) 36–46
- A. Behr, Z. Bayrak, G. Samli, D. Yildiz, S. Peitz, G. Stochniol
Oligomerization of n-butenes in a two phase reaction system with homogeneous Ni/Al-catalysts
Chem. Eng. Technol. 39 (2016), 263–270
- M. Zagajewski, J. Dreimann, M. Thönes, A. Behr
Rhodium catalyzed hydroformylation of 1-dodecene using an advanced solvent system: Towards highly efficient catalyst recycling
Chem. Eng Process. 99 (2016), 115–123
- K.A. Ostrowski, D. Vogelsang, A.J. Vorholt
A general and efficient method for the palladium-catalysed conversion of allylic alcohols into their corresponding dienes
Catal. Sci. Technol., 2016, accepted. DOI: 10.1039/C5CY02096D
- T. Gaide, J. Dreimann, A. Behr, A.J. Vorholt
Overcoming Phase-Transfer Limitations in the Conversion of Lipophilic Oleo Compounds in Aqueous Media-A Thermomorphic Approach
Angew. Chem. Int. Ed., 2016, 55, 2924–2928, DOI: 10.1002/anie.201510738
- T. Seidensticker, J. M. Vosberg, K.A. Ostrowski, A.J. Vorholt
Rhodium-Catalyzed Bis-Hydroaminomethylation of Linear Aliphatic Alkenes with Piperazine
Adv. Synth. Catal., 2016, 358, 610–621, DOI: 10.1002/adsc.201500896
- K.A. Ostrowski, D. Vogelsang, T. Seidensticker, A.J. Vorholt
Direct Synthesis of an α,ω -Diester from 2,7-Octadienol as Bulk Feedstock in Three Tandem Catalytic Steps
Chem. Eur. J. 2016, 22, 1840–1846. DOI: 10.1002/chem.201503785
- T. Seidensticker, D. Möller, A.J. Vorholt
Merger of Johnson–Claisen rearrangement and alkoxycarbonylation for atom efficient diester synthesis
Tetrahedron Lett., 2016, 57, 371–374. DOI: 10.1016/j.tetlet.2015.12.032
- K.A. Ostrowski, D. Lichte, M. Stuck, A.J. Vorholt
A comprehensive investigation and optimisation on the proteinogenic amino acid catalysed homo aldol condensation
Tetrahedron, 2016, 72, 592–598. DOI: 10.1016/j.tet.2015.11.069
- T. Gaide, A. Behr, M. Terhorst, A. Arns, F. Benski, A.J. Vorholt
Katalysatorvergleich bei der Hydroesterifizierung von 10-Undecensäuremethylester in thermomorphen Lösungsmittelsystemen
Chem. Ing. Tech., 2016, 88, 158–167. DOI: 10.1002/cite.201500096

- D.L.L. Pingen, C. Altintas, M. Schaller, D. Vogt
A Ruthenium Racemisation Catalyst for Synthesis of Primary Amines from Secondary Amines
Dalton Trans. 2016, 45, 11765-11771. <http://dx.doi.org/10.1039/C6DT01525E>, first published on the web 10 June, 2016

2015

- A. Behr, A. Wintzer
Hydroaminomethylation of the Renewable Limonene with Ammonia in an Aqueous Biphasic Solvent System
Chem. Eng. Technol. 12 (2015), 2299-2304
- T. Färber, R. Schulz, O. Riechert, T. Zeiner, A. Górak, G. Sadowski, A. Behr
Different recycling concepts in the homogeneously catalysed synthesis of terpenyl amines
Chem. Eng. Process. 98 (2015), 22-31
- A. Behr, A. Kämper, M. Nickel, R. Franke
Crucial role of additives in iridium-catalyzed hydroformylation
Appl. Catal. A: General 505 (2015), 243-248
- A. Behr, D. Levikov, E. Nürenberg
Rhodium-catalyzed hydroaminomethylation of cyclopentadiene
RSC Adv. 5 (2015), 60667-60673
- P. Neubert, M. Steffen, A. Behr
Three step auto-tandem catalysed hydroesterification: Access to linear fruity esters from piperylene
J. Mol. Catal. A: Chem. 407 (2015), 122-127
- P. Neubert, S. Fuchs, A. Behr
Hydroformylation of piperylene and efficient catalyst recycling in propylene carbonate
Green Chem. 17 (2015), 4045-4052
- A. Behr, D. Levikov, D. Vogelsang
First rhodium-catalyzed hydroformylation of cyclopentadiene
J. Mol. Catal. A: Chem. 406 (2015), 114-117
- A. Behr, T. Färber
Application of a Taylor-Couette Reactor in Homogeneous Catalysis
Chem. Ing. Trans. 43 (2015), 835-840
- A. Behr, K.A. Irawadi
Glycerin-Oxidation mit magnetisch abtrennbaren Nanokatalysatoren
Chem. Ing. Tech. 87 (2015)
- A. Behr, Z. Bayrak, S. Peitz, G. Stochniol, D. Maschmeyer
Oligomerization of 1-butene with a homogeneous catalyst system based on allylic nickel complexes
RSC Adv. 5 (2015), 41372-41376
- A. Behr, A. Wintzer, C. Lübke, M. Müller
Synthesis of primary amines from the renewable compound citronellal via biphasic reductive amination
Journal of Molecular Catalysis A: Chemical 404 (2015), 74-82
- A. Behr, D. Levikov, E. Nürenberg
Rhodium catalyzed one-step hydroamidation of cyclopentadiene and dicyclopentadiene
Catal. Sci. Technol. 5 (2015), 2783-2787
- A. Behr, S. Toepell
Comparison of Reactivity in the Cross Metathesis of Allyl Acetate-Derivates with Oleochemical Compounds
J Am Oil Chem Soc 92 (2015), 603-611
- K. A. Ostrowski, D. Lichte, M. Terhorst, A.J. Vorholt
Two sides of the same amino acid-development of a tandem aldol condensation/epoxidation by using the synergy of different catalytic centres in amino acids
Appl. Catal., A, 2015, 509, 1-7. DOI: 10.1016/j.apcata.2015.10.018
- T. Seidensticker, M. R. L. Furst, R. Frauenlob, J. Vondran, E. Paetzold, U. Kragl, A.J. Vorholt
Palladium-Catalyzed Aminocarbonylation of Aliphatic Alkenes with N,N-Dimethylformamide as an In Situ Source of CO
ChemCatChem, 2015, 7, 4085-4090. DOI: 10.1002/cctc.201500824.
- A. Behr, A. Kämper, R. Kuhlmann, A.J. Vorholt, R. Franke
First efficient catalyst recycling for the iridium-catalysed hydroformylation of 1-octene
Catal. Sci. Technol., 2015, 6, 208-214. DOI: 10.1039/C5CY01018G
- T. Seidensticker, A.J. Vorholt, A. Behr
The mission of addition and fission – catalytic functionalization of oleochemicals
Eur. J. Lipid Sci. Technol., 2016, 118, 3-25. DOI: 10.1002/ejlt.201500190
- K.A. Ostrowski, T.A. Faßbach, D. Vogelsang, A.J. Vorholt
The Quest for Decreasing Side Products and Increasing Selectivity in Tandem Hydroformylation/Acyloin Reaction
ChemCatChem, 2015, 7, 2607-2613. DOI: 10.1002/cctc.201500727
- J. Dreimann, P. Lutze, M. Zagajewski, A. Behr, A. Górak, A.J. Vorholt
Chemical Engineering and Processing, Highly Integrated Reactor-Separator Systems for the Recycling of Homogeneous Catalysts
Chem. Eng. Proc. 2016, 99, 124-131. DOI:10.1016/j.cep.2015.07.019
- K. McBride, T. Gaide, A.J. Vorholt, A. Behr, K. Sundmacher
Chemical Engineering and Processing, Thermomorphic Solvent Selection for Homogeneous Catalyst Recovery based on COSMO-RS
Chem. Eng. Proc. 2015, 99, 97-106. DOI:10.1016/j.cep.2015.07.004
- T. Gaide, A. Behr, A. Arns, F. Benski, A.J. Vorholt
Chemical Engineering and Processing, Hydroesterification of methyl 10-undecenoate in thermomorphic multicomponent solvent systems-Process development for the synthesis of sustainable polymer precursors
Chem. Eng. Proc., 2015, 99, 197-204. DOI: 10.1016/j.cep.2015.07.009
- K.A. Ostrowski, T.A. Faßbach, A.J. Vorholt
Tandem Hydroformylation/Acyloin Reaction – The Synergy of Metal Catalysis and Organocatalysis Yielding Acyloins Directly from Olefins
Adv. Synth. Catal., 2015, 357, 1374-1380. DOI: 10.1002/adsc.201401031
- A. Behr, A.J. Vorholt, T. Seidensticker
An Old Friend in a New Guise-Recent Trends in Homogeneous Transition Metal Catalysis
ChemBioEng Rev. 2015, 2, 6-21. DOI: 10.1002/cben.201400034
- A. Falk, A. Cavalieri, D. Vogt, H.-G. Schmalz
Enantioselective Nickel-Catalyzed Hydrocyanation using Chiral Phosphine-Phosphite Ligands: Recent Improvements and Insights
Adv. Synth. Catal. 2015, 357, 3317-3320. <http://dx.doi.org/10.1002/adsc.201500644>, first published on the web 14 Oct, 2015
- E.H. Boymans, P.T. Witte, D. Vogt
Study on the Selective Hydrogenation of Nitroaromatics to N-aryl hydroxylamines using a Supported Pt Nanoparticle Catalyst
Catal. Sci. Technol. 2015, 5, 176-183. <http://dx.doi.org/10.1039/C4CY00790E>, first published on the web 29 Aug, 2014



Thermodynamics (TH)

Modeling Mixtures of Long-Chain Hydrocarbons and Water Using PC-SAFT

Niklas Haarmann^a, Sabine Enders^b, Gabriele Sadowski^a

^aLaboratory of Thermodynamics, TU Dortmund

^bInstitute for Technical Thermodynamics and Refrigeration, Karlsruhe Institute of Technology

Modeling and measuring the very low mutual solubility in binary n -alkane + water mixtures is very challenging. Consequently, experimental data regarding mutual solubilities of these components scatter remarkably. In this work, the PC-SAFT equation of state has been applied to successfully model liquid-liquid equilibria of binary n -alkane + water mixtures. Excellent agreement between modeling results and available experimental data has been achieved for the liquid-liquid equilibria even describing the minimum of n -alkane solubility in water as a function of temperature. These results could further be used to predict mutual solubilities in binary methyl ester + water mixtures.

In petrochemical plants like refineries and steam crackers, process water or steam inevitably gets in contact with crude oil or hydrocarbons. If water exceeds its solubility limit in hydrocarbons, e.g. n -alkanes, corrosion of plant equipment can be caused. Furthermore, wastewater streams are polluted with n -alkanes which need to be removed for environmental reasons. Hence, knowledge of the mutual solubility in n -alkane + water mixtures is indispensable.

In the past, several thermodynamic models have already been applied to model the mutual solubility in these systems without achieving a satisfying description of the phase behavior. In this work, the homo-segmental Perturbed-Chain Statistical Associating Fluid Theory (PC-SAFT) was applied for the modeling. The results are depicted in Figure 1 along with experimental data from literature. It can be seen that the solubility of water in the organic phase monotonically increases with temperature and only slightly depends on the chain length of the n -alkane. In contrast, the solubility of the n -alkanes in the aqueous phase exhibits a minimum as function of temperature and significantly varies with the chain length of the n -alkane.

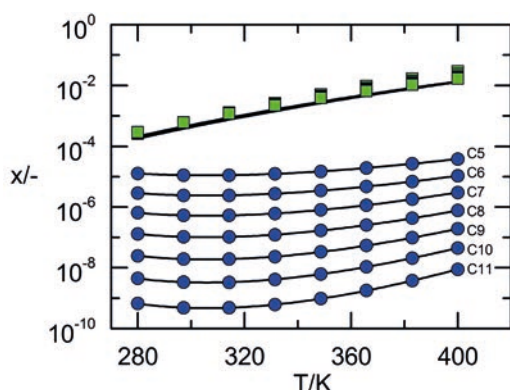


Figure 1: Mutual solubilities of water and n -alkanes (n -pentane to n -undecane). Lines: modeling results with PC-SAFT. Symbols: experimental data where squares represent the solubility of water in the organic phase and circles show the solubility of the n -alkanes in the aqueous phase (J. Phys. Chem. Ref. Data 33 (2004) 549-577).

PC-SAFT achieves a remarkably good description of the solubility of the n -alkane in the aqueous phase for all n -alkanes from n -pentane to n -undecane including describing the minimum as function of temperature, whereas the models used in the literature so far predict a continuous decrease in solubility for decreasing temperature. Beyond that, the solubility of water in the organic phase is also predicted very well. These modeling results could also be used within a new hetero-segmental approach of PC-SAFT to predict the mutual solubilities in binary methyl ester + water mixtures. For this, the long-chain ester was modeled as comprising a universal functional head domain and an n -alkylic residue modeled as an n -alkane. Hence, the interactions between water and the n -alkylic residue were described using the aforementioned modeling approach of n -alkane + water mixtures. As an example, the mutual solubility in the binary methyl hexanoate + water mixture could be predicted without any parameter fitting as shown in Figure 2.

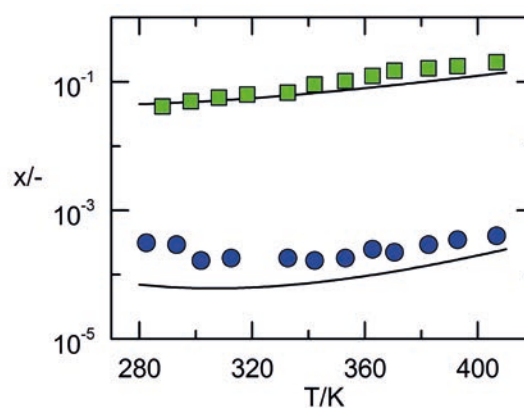


Figure 2: Mutual solubilities of water and methyl hexanoate. Lines: predictions with PC-SAFT. Symbols: experimental data where squares represent the solubility of water in the organic phase and circles show the solubility of methyl hexanoate in the aqueous phase.

Contact:

niklas.haarmann@tu-dortmund.de

gabriele.sadowski@tu-dortmund.de

Publications:

N. Haarmann, S. Enders, G. Sadowski; Modeling binary mixtures of n -alkanes and water using PC-SAFT, Fluid Phase Equilibria 2018, <https://doi.org/10.1016/j.fluid.2017.11.015>.

Selecting Best Polymeric Excipients for Amorphous Solid Dispersions

Kristin Lehmkemper^{1,2}, Samuel Kyeremateng¹, Matthias Degenhardt¹, Gabriele Sadowski²

¹AbbVie Deutschland GmbH & Co. KG, ²Laboratory of Thermodynamics, BCI, TU Dortmund

The formulation of so-called amorphous solid dispersions (ASDs) is an established technique to improve the oral bioavailability of poorly-water-soluble active pharmaceutical ingredients (APIs). In an ASD, an amorphous API which usually shows a higher solubility than its crystalline form is embedded in excipient(s) (e.g. amorphous polymers) to inhibit API crystallization. The excipient selection for long-term physically-stable, crystal-free ASD formulations usually requires time- and resource-consuming stability studies at relevant storage temperatures and relative humidities (RHs). This work shows that thermodynamic modeling can be used to determine suitable excipients and excipient compositions therewith reducing cost-intensive stability studies to a minimum.

The low water solubility of many active pharmaceutical ingredients (APIs) is a main bottleneck in the development of oral solid dosage forms. The aim of dissolving the API in amorphous excipients by generating so-called amorphous solid dispersions (ASDs) is to stabilize the higher-soluble amorphous form of the API. ASDs are thermodynamically stable if the API content is lower than the API solubility in the excipients. Supersaturated ASDs are kinetically stabilized as long as the storage temperature is sufficiently lower than the glass-transition temperature (T_g) of the ASD. Thus, the physical stability of ASDs in terms of API-crystallization inhibition can be concluded from the phase diagram which contains solubility curve and T_g curve.

In this work, the Perturbed-Chain Statistical Associating Fluid Theory (PC-SAFT), and the Kwei equation were applied to model the solubility curve and the T_g curve, respectively, of naproxen and paracetamol ASDs at 0 %, 60 % and 75 % RH. Hydroxypropyl methylcellulose acetate succinate (HPMCAS), poly(vinylpyrrolidone-co-vinyl acetate) (PVPVA 64) and poly(vinylpyrrolidone) (PVP) as well as blends of these polymers were considered as excipients. For validation of the modeling results, ASD formulations were prepared via hot-melt extrusion or spray drying and stored for up to 24 months at standard conditions (25 °C/0 % RH; 25 °C/60 % RH; 40 °C/75 % RH). The samples were monitored periodically for API crystallization by polarized-light microscopy and powder X-ray diffraction.

At 0 % RH, the modeling revealed decreasing solubilizing and kinetically-stabilizing abilities of the applied polymers in the order PVP > PVPVA64 > HPMCAS. The physical stability was also predicted to decrease with increasing HPMCAS content in the API/polymer-blend ASDs. The predicted impact of RH generally correlates with the hydrophilicity of the polymers: PVP > PVPVA64 > HPMCAS.

Figure 1 shows as an example the predicted phase diagrams for paracetamol/polymer ASDs at 75 % RH.

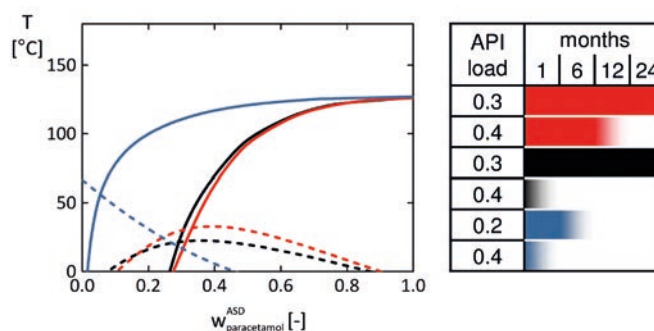


Figure 1: Physical stability of paracetamol ASDs with PVP (red), PVPVA64 (black) and HPMCAS (blue). left: Phase diagrams at 75 % RH. The full lines represent the solubility lines calculated using PC-SAFT. The dashed lines represent the T_g calculated using the Kwei equation. The x-axis refers to the API content in the water-free ASDs. right: Experimental results of stability studies at 40 °C/75 % RH. The lengths of the bars indicate the number of months after which first crystals were observed. Full bar indicates the ASD was still crystal-free at the end of the studies.

As to be seen, PVP and PVPVA64 ASDs with 30 wt% paracetamol remained stable at 40 °C/75 % RH for 24 months, while the PVP and PVPVA64 ASDs with higher paracetamol loads (≥ 40 wt%) and the HPMCAS ASDs (≥ 20 wt % paracetamol) crystallized within one to twelve months. This agrees with the predicted phase diagrams; at 40 °C the 30 wt% PVP and PVPVA64 samples are located to the left of the solubility lines, while all other samples are supersaturated (to the right of the solubility line).

Same as the presented example, stability results of all investigated systems agreed very well with the modeled phase diagrams. Thus, PC-SAFT and the Kwei equation can be applied as an early tool for excipient selection in the design of ASD formulations.

Disclosure: This study was funded by AbbVie. AbbVie participated in the study design, research, data collection, analysis and interpretation of data, as well as writing, reviewing, and approving the publication. S.K., M.D., and K.L. are AbbVie employees and may own AbbVie stock/options. G.S. is an employee at the Department for Biochemical and Chemical Engineering of the TU Dortmund and has no conflict of interest to report.

Contact:

kristin.lehmkemper@abbvie.com
gabriele.sadowski@tu-dortmund.de

Publications:

K. Lehmkemper, S.O. Kyeremateng, O. Heinzerling, M. Degenhardt, G. Sadowski, Mol. Pharm. 14, 4374–4386, 2017.

K. Lehmkemper, S.O. Kyeremateng, M. Bartels, M. Degenhardt, G. Sadowski, Eur. J. Pharm. Biopharm. 124, 147–157, 2018.

Crystallization Kinetics in Pharmaceutical Formulations

Christian Luebbert, Gabriele Sadowski

Most recently marketed polymer-based pharmaceutical formulations are thermodynamically instable; their long-term stability is basically impaired by crystallization of the incorporated active pharmaceutical ingredient. Robust detection and quantification of crystal formation- especially at temperatures and humidities relevant for long-term storage tests - are essential for understanding the crystallization phenomena. In this work, the moisture-induced crystallization kinetics was investigated just by measuring the kinetics of water-sorption from humid air. By combining these experiments with thermodynamic predictions of the water sorption in amorphous versus crystallized formulations, the amount of crystallized nifedipine could be in-situ determined as function of time just by weighing the ASD samples and without any calibration.

The bioavailability of poorly water-soluble active pharmaceutical ingredients (APIs) is significantly improved by dissolving the amorphous API in a suitable polymer. Several formulations based on this approach have been marketed recently. In most of these formulations, the API loading exceeds the equilibrium solubility of the API in the polymer. The API will therefore crystallize as function of time, meaning the end of shelf life of the formulation. Knowledge of the API crystallization kinetics in such systems is essential to find suitable polymeric excipients and sufficiently long-term-stable API/polymer compositions. Time-dependent water sorption measurements in nifedipine/poly (vinyl acetate) formulations revealed that the water content in the formulation changes even during storage at constant storage conditions (40 °C/75% relative humidity (RH)). Results of sorption measurements in formulations with different nifedipine loadings are shown in Figure 1.

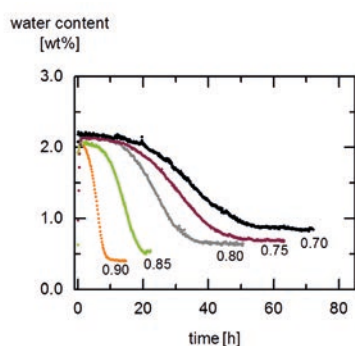


Figure 1: Measured water sorption as function of time in nifedipine/ poly (vinyl acetate) formulations with indicated nifedipine loadings stored at 40 °C / 75% RH.

As can be seen in Figure 1, the water content increased almost instantaneously upon exposure to RH to a value of approximately 2.1 wt% followed by a decrease after a few hours finally reaching a second plateau. X-ray measurements confirmed that initially amorphous formulations crystallized during these sorption measurements.

Contact:
christian.luebbert@tu-dortmund.de
gabriele.sadowski@tu-dortmund.de

Using Perturbed-Chain Statistical Associating Fluid Theory (PC-SAFT) the observed water-sorption behavior of the amorphous (at the beginning) and crystallized (at the end) formulations was predicted almost quantitatively. Thus, the amount of nifedipine crystals could be directly obtained by combining the experimental results from Figure 1 with PC SAFT water-sorption predictions (Figure 2).

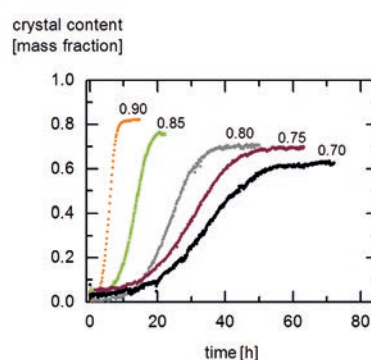


Figure 2: Nifedipine crystallization kinetics in nifedipine/ poly (vinyl acetate) formulations with different nifedipine loadings calculated from the measured water-sorption data (Figure 1) combined with PC-SAFT water-sorption predictions.

Figure 2 shows that the crystal content was predicted to be zero at the beginning of the experiment and increased sigmoidally upon further storage. Obviously, a high API content in a formulation accelerates the crystallization kinetics (12 hours in formulations containing 90 wt % nifedipine vs. 60 hours in those containing 70 wt %).

This robust new approach allows for easy, reliable and in-situ determining the crystallization kinetics in pharmaceutical formulations and thus estimating their shelf life.

Publications:
C. Luebbert, M. Wessner, G. Sadowski, Mol. Pharm. 15, 669-678, 2018.
C. Luebbert, G. Sadowski, Eur. J. Pharm. Biopharm. 127, 183-193, 2018.

Excipients for High-Concentration Biopharmaceutical Formulations

How thermodynamics can aid in the choice for the right excipients

Miko Schleinitz, Gabriele Sadowski, Christoph Brandenbusch

Biopharmaceuticals, especially therapeutic proteins such as monoclonal antibodies (mAbs) are the fastest growing segment in the pharmaceutical industry. However, most of these proteins show a poor aqueous solubility limiting their application to intravenous administration over several hours to deliver the required dosage (> 100 mg). “High Concentration Protein Formulations” (HCPFs) can solve this problem and lead to formulations with concentrations allowing for delivery of the required dosage in a single injection (self-administration). However, identification of these HCPFs is commonly based on heuristic decisions and “trial-and-error” screening approaches. Within this work, we developed a physical sound method to identify HCPFs with the aid of thermodynamic modeling.

HCPFs are commonly achieved by addition of suitable excipients (e.g. salts, sugars, amino acids, surfactants), which are approved by the Food and Drug Administration (FDA), to aqueous protein solutions. Even though many excipients described in recent literature fulfill the requirements of enhanced solubility and solubility of the biopharmaceutical in solution, no general approach exists to identify suitable excipients. Furthermore, the “state-of-the-art” development of HCPFs and the selection of excipients are almost solely based on heuristic approaches hindering transferability of the results to other biopharmaceuticals or formulations. Furthermore consideration of negative influences induced by the excipients (e.g. protein agglomeration) upon excipient selection is so far not possible in advance. To solve this challenge, we developed a physically-sound method (using both, experiments and thermodynamic modelling) to identify suitable excipients based on intermolecular interactions.

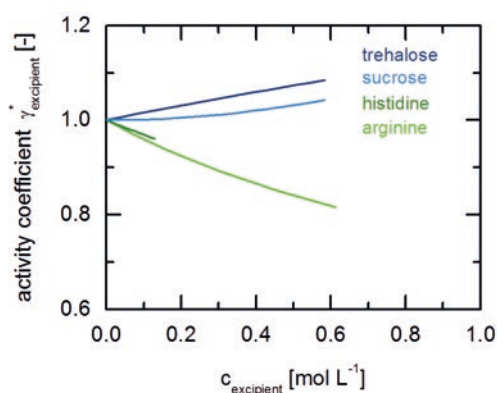


Figure 1: Activity coefficients of sugars and amino acids as a function of excipient concentration.

The suitability of an excipient was first predicted based on its thermodynamic behavior in aqueous buffer solution expressed by its activity coefficient.

If the latter is below 1, the excipient prefers to be surrounded by other excipients (instead of water molecules) thus

leaving more water molecules for the hydration of the biopharmaceutical (see Figure 1) which is beneficial.

Thus, an initial excipient screening can already be performed without the knowledge on the biopharmaceutical itself, and limited amount of experimental data. Afterwards, osmotic virial coefficients were taken into account to access the protein-protein interactions in the presence of the excipients (second osmotic virial coefficient, B_{22}) as well as the protein-excipient interactions (cross virial coefficient, B_{23}).

Based on these values, which can be measured by light-scattering experiments as well as predicted using an in-house model, the aggregation propensity of the biopharmaceutical was accessible (Fig. 2).

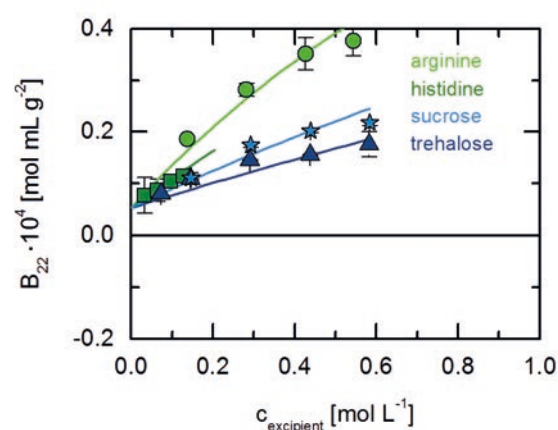


Figure 2: Second osmotic virial coefficients B_{22} of a monoclonal antibody as a function of sugar or amino acid concentration.

Results on optimal formulations were then evaluated by long-term stability studies. Critical parameters are both aggregate formation / loss in monomer content as well as solubility of the biopharmaceutical.

This method will simplify the future of biologics formulation development and increase the understanding of the mechanisms behind the stabilization of biopharmaceuticals by excipients and excipient mixtures.

Publications:

M. Schleinitz, G. Sadowski, C. Brandenbusch, Prospects for the identification of excipient mixtures and novel excipients, PEP Talk 2018, San Diego (CA).

Contact:

miko.schleinitz@tu-dortmund.de
christoph.brandenbusch@tu-dortmund.de

Reaction Equilibria and Reaction Kinetics of an Enzyme-Catalyzed Reaction

Experimental and Theoretical Study on the Influence of Additives on Reaction Equilibrium and Reaction Kinetics

Anton Wangler, Gabriele Sadowski, Christoph Held

Reaction equilibrium and reaction kinetics are two key parameters in biotechnological process design. While reaction conditions (T , pH , concentrations) usually only moderately influence the equilibrium position and reaction kinetics, the influence of additives such as PEG or salts (e.g. Na_3Cit) is known to be much stronger. In this work, the influence of the additives PEG and Na_3Cit on the reaction equilibrium and reaction kinetics of the acetophenone reduction catalyzed by ADH 270 was studied. The experimental results showed a very beneficial effect of the additives on reaction kinetics while the reaction equilibrium was shifted to the reactant side. The observed effects were explained by molecular interactions between the reacting agents and the reaction medium. These were expressed and quantified via activity coefficients of the reacting agents, which allowed even predicting the additive influence on reaction kinetics and reaction equilibrium.

New developments in downstream processing, e.g. the addition of possible phase formers (inert additives) for in situ product removal from aqueous broth constantly improve the process design in biotechnology. While leading to more efficient product purification, the presence of additives also affects reaction yield and reaction kinetics. This was addressed in the present work for an alcohol dehydrogenase (ADH 270) – catalyzed reaction:

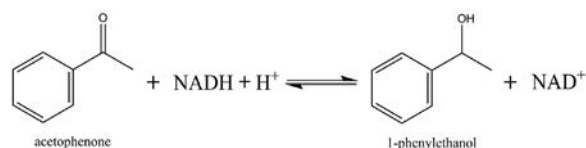


Figure 1: Reaction scheme of the reduction of acetophenone to 1-phenylethanol by a modified alcohol dehydrogenase ADH 270.

The reaction yield is connected to the thermodynamic equilibrium constant K_{th} , that only depends on temperature and pressure as:

$$K_{th} = K_{exp} K_{\gamma} = \frac{x_{\text{NAD}^+} \cdot x_{\text{1-PE}}}{x_{\text{NADH}} \cdot x_{\text{ACP}} \cdot x_{\text{H}^+}} \frac{\gamma_{\text{NAD}^+} \cdot \gamma_{\text{1-PE}}}{\gamma_{\text{NADH}} \cdot \gamma_{\text{ACP}} \cdot \gamma_{\text{H}^+}} \quad (1)$$

In Eq. (1), x and γ are the mole fractions and activity coefficients of the reacting agents at equilibrium. The kinetics of an enzyme-catalyzed reaction is characterized by the maximum reaction velocity r_{max} and the Michaelis constant K_M , which is an important factor for determining substrate affinity to the enzyme. The Michaelis-Menten equation for a two-substrate reaction based on substrate activities a_i is:

$$r = \frac{r_{max} \cdot a_{\text{NADH}} \cdot a_{\text{ACP}}}{K_{IA} \cdot K_{M,ACP}^a + a_{\text{NADH}} \cdot K_{M,ACP}^a + a_{\text{ACP}} \cdot K_{M,NADH}^a + a_{\text{NADH}} \cdot a_{\text{ACP}}} \quad (2)$$

where K_{IA} and K_M^a are the inhibition constant and the activity-based Michaelis constants of ACP and NADH, respectively.

Addition of inert additives to the reaction mixture will impact the activity coefficients and thus the equilibrium position and the reaction kinetics, while K_{th} and K_M^a remain constant,

as long as the stability of the enzyme upon addition of the additives is still ensured. The tremendous influence of the considered additives (PEG and Na_3Cit) on equilibrium position and reaction kinetics is illustrated in Figures 2 and 3. For both additives the reaction equilibrium was significantly shifted to the reactant side (Figure 2 left). Regarding reaction kinetics, K_M of acetophenone increased, while K_M of NADH decreased upon addition of PEG to the neat reaction mixtures (Figure 2 right). This behavior could be explained by molecular interactions between reacting agents and the reaction medium. For quantification, the activity coefficients of the reacting agents were predicted using ePCSAFT, which allowed for accurately predicting the equilibrium position and the Michaelis constants. This further shows that activity-based constants are general and additive-independent values that are crucial for process design in biotechnology.

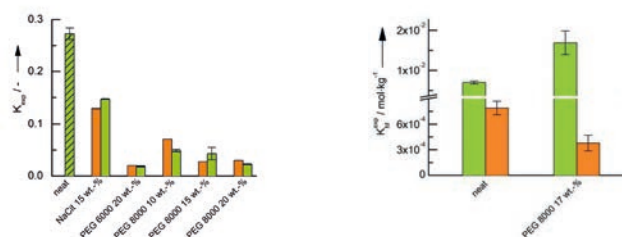


Figure 2 left: Comparison between predicted equilibrium compositions K_{exp} (orange) and the respective experimental values (green) of the acetophenone reduction; $T = 303 \text{ K}$, $pH = 8$.

Figure 2 right: Comparison of between experimental Michaelis constants K_M of acetophenone (green) and NADH (orange); $T = 303 \text{ K}$, $pH = 8$.

Contact:

anton.wangler@tu-dortmund.de
christoph.held@tu-dortmund.de
gabriele.sadowski@tu-dortmund.de

Publications:

A. Wangler, R. Loll, T. Greinert, G. Sadowski, C. Held; J. Chem. Thermodynamics 128, 275–282, 2019.

A. Wangler, D. Boettcher, A. Hueser, G. Sadowski, C. Held; Prediction and validation of co-solvent influence on Michaelis constants: A thermodynamic activity-based approach; Eur. J. Chem., accepted, 2018.

New Experimental Melting Properties for Predicting Amino-Acid Solubility

The combination of new experimental melting properties and the modeling using PC-SAFT allows quantitative predictions of amino-acid solubility in water

Yeong Zen Chua, Hoang Tam Do, Christoph Schick, Dzmitry Zaitsau, Christoph Held

Predicting the solubility of solid compounds requires their melting properties. Measuring the melting temperature and the enthalpy of fusion of biological compounds by calorimetry is often not possible due to the decomposition during heating. To overcome this problem, fast scanning calorimetry (FSC) was used to measure the melting properties of glycine and L-alanine. These new melting properties were used to predict the solubility of an amino acid in water by using the modeling framework PC-SAFT. At first, the solubility-independent thermodynamic properties such as osmotic coefficients and mixture densities of these amino acids in water were used to fit the pure-component PC-SAFT parameters and one binary parameter. The predicted solubility of amino-acid in water was found to be in quantitative agreement over a broad temperature range. The combination of FSC and PC-SAFT provides access for predicting solubility of biomolecules which decompose before melting.

The production and purification of amino acids is still realized through crystallization which is the state-of-the-art unit operation. The solubility of amino-acid is essential for crystallization because it determines the product yield and purity as well as the choice of the solvent in the process. The experimental measurement of solubility is time-consuming and expensive, especially according to the high number of influences on solubility (temperature, pH-value, type and concentration of co-solutes and co-solvents). The prediction of solubility using thermodynamic models is therefore desired and can be realized by

$$x_i^{L,sat} = \frac{1}{\gamma_i^{sat}} \cdot \exp \left\{ -\frac{\Delta_{fus}H_m}{R} \left(\frac{1}{T} - \frac{1}{T_{fus}} \right) \right\} \quad (1)$$

where $x_i^{L,sat}$ the solubility, γ_i^{sat} the activity coefficient of component i at its solubility, T_{fus} and $\Delta_{fus}H_m$ the melting temperature and molar fusion enthalpy, respectively. The PC-SAFT parameters for the amino acids were taken from the literature. The binary interaction parameter k_{ij} was fitted to experimental osmotic-coefficient data at $T = 298.15$ K and $p = 1$ atm (Figure 1).

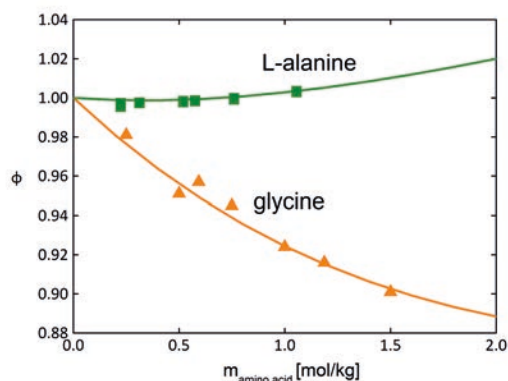


Figure 1: Osmotic coefficients Φ of glycine + water and L-alanine + water solutions at $T = 298.15$ K and $p = 1$ atm. Symbols are experimental data (glycine: triangles and L-alanine: squares) and lines are PC-SAFT modeling results.

The melting properties of L-alanine and glycine were determined using fast scanning calorimetry (FSC) to $\Delta_{fus}H_m = (21 \pm 4)$ kJ·mol⁻¹ and $T_{fus} = (569 \pm 7)$ K for glycine, and $\Delta_{fus}H_m = (22 \pm 5)$ kJ·mol⁻¹ and $T_{fus} = (608 \pm 9)$ K for L-alanine. Based on these melting properties, amino-acid solubility was predicted with PC-SAFT (Figure 2) and validated with experimental data from different authors.

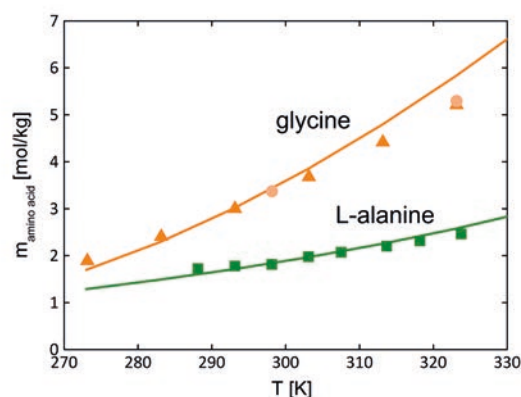


Figure 2: Solubility of glycine and L-alanine in water vs. temperature. Symbols represent experimental data (glycine: triangles, circles and L-alanine: squares). Lines represent PC-SAFT predictions.

As to be seen, the prediction and experiments are in agreement over a wide temperature range. The combination of FSC and PC-SAFT allows an accurate prediction of amino-acid solubility in water which opens the door for the future for predicting solubility of molecules which decompose before melting.

Publications 2017 - 2015

2017

- J. Sauer, H.-D. Kuehl
Numerical model for Stirling cycle machines including a differential simulation of the appendix gap
Applied Thermal Engineering 111, 819-833 (2017)
- J. Sauer, H.-D. Kuehl
Analysis of unsteady gas temperature measurements in the appendix gap of a Stirling engine
Proc. 15th IECEC, AIAA Propulsion and Energy Forum, AIAA 2017-4795 (2017)
- C. Kress, G. Sadowski, C. Brandenbusch
Solubilization of proteins in aqueous two-phase extraction through combinations of phase-formers and displacement agents
European Journal of Pharmaceutics and Biopharmaceutics 112, 38-44 (2017)
- J. Gorden, E. Geiser, N. Wierckx, L.M. Blank, T. Zeiner, C. Brandenbusch
Integrated process development of a reactive extraction concept for itaconic acid and application to a real fermentation broth
Engineering in Life Science 17 (7), 809-816 (2017)
- Y. Ji, M. Lemberg, A. Prudic, R. Paus, G. Sadowski
Modeling and analysis of dissolution of paracetamol/Eudragit® formulations
Chemical Engineering Research and Design 121, 22-31 (2017)
- M. Lemberg, G. Sadowski, M. Gerlach, E. Kohls, M. Stein, C. Hamel, A. Seidel-Morgenstern
Predicting solvent effects on the 1-dodecene hydroformylation reaction equilibrium
AIChE Journal 63, 4576-4585 (2017)
- M. Lemberg, G. Sadowski
Predicting the Solvent Effect on Esterification Kinetics
ChemPhysChem 18, 1977-1980 (2017)
- K. Lehmkemper, S.O. Kyeremateng, O. Heinzerling, M. Degenhardt, G. Sadowski
Long-Term Physical Stability of PVP- and PVPVA-Amorphous Solid Dispersions
Molecular Pharmaceutics 14, 157-171 (2017)
- K. Lehmkemper, S.O. Kyeremateng, O. Heinzerling, M. Degenhardt, G. Sadowski
Impact of polymer type and relative humidity on the long-term physical stability of amorphous solid dispersions
Molecular Pharmaceutics 14, 4374-4386 (2017)
- C. Luebbert, G. Sadowski
Moisture-induced phase separation and recrystallization in amorphous solid dispersions
International Journal of Pharmaceutics 532, 635-646 (2017)
- C. Luebbert, F. Huxoll, G. Sadowski
Amorphous-Amorphous Phase Separation in API/Polymer Formulations
Molecules 22, 296 (2017)
- M. Voges M, I.V. Prikhodko, S. Prill, M. Hübner, G. Sadowski, C. Held
Influence of pH Value and Ionic Liquids on the Solubility of L-Alanine and L-Glutamic Acid in Aqueous Solutions at 30 °C
Journal of Chemical & Engineering Data 62, 52-61 (2017)
- F. Meurer, H.T. Do, G. Sadowski, C. Held
Standard Gibbs energy of metabolic reactions: II. Glucose-6-phosphatase reaction and ATP hydrolysis
Biophysical Chemistry 223, 30-38 (2017)
- M. Voges, F. Fischer, M. Neuhaus, G. Sadowski, C. Held
Measuring and Predicting Thermodynamic Limitation of an Alcohol Dehydrogenase Reaction
Industrial & Engineering Chemistry Research 56, 5535-5546 (2017)
- E. Altuntepe, T. Greinert, F. Hartmann, A. Reinhardt, G. Sadowski, C. Held
Thermodynamics of enzyme-catalyzed esterifications: I. Succinic acid esterification with ethanol
Applied Microbiology and Biotechnology 101, 5973-5984 (2017)
- P. Pontes, E.A. Crespo, M.A.R. Martins, L.P. Silva, C.M.M.S. Neves, G.J. Máximo, M.D. Hubinger, E.A.C. Batista, S.P. Pinho, J.A.P. Coutinho, G. Sadowski, C. Held
Measurement and PC-SAFT Modeling of Solid-Liquid Equilibrium of Deep Eutectic Solvents of Quaternary Ammonium Chlorides and Carboxylic Acids
Fluid Phase Equilibria 448, 69-80 (2017)
- E. Altuntepe, A. Reinhardt, J. Brinkmann, T. Briesemann, G. Sadowski, C. Held
Phase behaviour of binary mixtures containing succinic acid or its esters
Journal of Chemical & Engineering Data 62, 1983-1993 (2017)
- C.H.J.T. Dietz, D.J.G.P van Osch, M.C. Kroon, G. Sadowski, M. van Sint Annaland, F. Gallucci, L.F. Zubeir, C. Held
PC-SAFT modeling of CO₂ solubilities in hydrophobic deep eutectic solvents
Fluid Phase Equilibria 448, 94-80 (2017)
- M. Voges, R. Abu, M.T. Gundersen, C. Held, J.M. Woodley, G. Sadowski
Reaction equilibrium of the ω -transamination of (S)-phenylethylamine: Experiments and ePC-SAFT modeling
Organic Process Research & Development 21, 976-986 (2017)
- M. Voges, C. Fischer, D. Wolff, C. Held
Influence of Natural Solutes and Ionic Liquids on Yield of Enzyme-catalyzed Reactions: Measurements and Predictions
Organic Process Research & Development 21, 1059-1068 (2017)
- M. Gao, C. Held, S. Patra, C. Held, G. Sadowski, R. Winter
Crowders and Cosolvents—Major Contributors to the Cellular Milieu and Efficient Means to Counteract Environmental Stresses
ChemPhysChem 18, 2951-2972 (2017)
- E.A. Crespo, L.P. Silva, M.A.R. Martins, C. Held, S.P. Pinho, J.A.P. Coutinho
Characterization and Modeling of the Liquid Phase of Deep Eutectic Solvents Based on Fatty Acids/Alcohols and Choline Chloride
Industrial and Engineering Chemistry Research 56, 12192-12202 (2017)
- E. Altuntepe, V.N. Emel'yanenko, M. Forster-Rotgers, S.P. Verevkin, C. Held
Thermodynamics of enzyme-catalyzed esterifications: II. Levulinic acid esterification with short-chain alcohols
Applied Microbiology and Biotechnology 101, 7509-7521 (2017)
- R.I. Canales, C. Held, M.J. Lubben, J.F. Brennecke, G. Sadowski
Predicting the Solubility of CO₂ in Toluene + Ionic Liquid Mixtures with PC-SAFT
Industrial and Engineering Chemistry Research 56, 9885-9894 (2017)

2016

- I. Domínguez, B. Gonzalez, B. Orge, C. Held, M. Voges, E.A. Macedo
Activity coefficients at infinite dilution for different alcohols and ketones in [EMpy][ESO4]: Experimental data and modeling with PC-SAFT
Fluid Phase Equilibria, 424, 32-40 (2016)
- J. Gorden, T. Zeiner, G. Sadowski, C. Brandenbusch
Recovery of cis,cis-Muconic Acid from Organic Phase after Reactive Extraction
Separation and Purification Technology, 169, 1-8 (2016)
- J. Pfeiffer, H.-D. Kühl
New Analytical Model for Appendix Gap Losses in Stirling Cycle Machines
Journal of Thermophysics and Heat Transfer, 30, 288-300 (2016)
- J. Pfeiffer, H.-D. Kühl
Optimization of the Appendix Gap Design in Stirling Engines
Journal of Thermophysics and Heat Transfer, 30, 831-842 (2016)
- L. Lange, S. Heisel, G. Sadowski
Predicting the Solubility of Pharmaceutical Cocrystals in Solvent/Anti-Solvent Mixtures
Molecules, 21, 593 (2016)
- M. Herhut, C. Brandenbusch, G. Sadowski
Modeling and prediction of protein solubility using the second osmotic virial coefficient
Fluid Phase Equilibria, 422, 32-42 (2016)
- M. Voges, F. Schmidt, D. Wolff, G. Sadowski, C. Held
Thermo-dynamics of the alanine aminotransferase reaction
Fluid Phase Equilibria, 422, 87-98 (2016)
- V.N. Emelyanenko, A.V. Yermalayeu, M. Voges, C. Held, G. Sadowski, S.P. Verevkin
Thermodynamics of a model biological reaction: A comprehensive combined experimental and theoretical study
Fluid Phase Equilibria, 422, 99-110 (2016)
- S. Glonke, G. Sadowski, C. Brandenbusch
Applied catastrophic phase inversion: a continuous non-centrifugal phase separation step in biphasic whole-cell biocatalysis
Journal of Industrial Microbiology & Biotechnology, 43, 1527-1535 (2016)
- S. Mohammad, C. Held, E. Altuntepe, T. Köse, T. Gerlach, I. Smirnova, G. Sadowski
Salt influence on MIBK/water liquid-liquid equilibrium: Measuring and modeling with ePC-SAFT and COSMO-RS
Fluid Phase Equilibria, 416, 83-93 (2016)
- S. Mohammad, G. Grundl, R. Müller, W. Kunz, G. Sadowski, C. Held
Influence of electrolytes on liquid-liquid equilibria of water/1-butanol and on the partitioning of 5-hydroxymethylfurfural in water/1-butanol
Fluid Phase Equilibria, 428, 102-111 (2016)
- T. Färber, O. Riechert, T. Zeiner, G. Sadowski, A. Behr, J. Vorholt A.
Homogeneously catalyzed hydroamination in a Taylor-Couette reactor using a thermomorphic multicomponent solvent system
Chemical Engineering Research and Design, 112, 263-273 (2016)
- T. Reschke, V. Zherikova K., P. Verevkin S., C. Held
Benzoic Acid and Chlorobenzoic Acids: Thermodynamic Study of the Pure Compounds and Binary Mixtures With Water, J
Pharm Sci-U.S., 105, 1050-1058 (2016)
- K.V. Zherikova, A. Svetlov, M. Varfolomeev, S.P. Verevkin, C. Held
Thermochemistry of halogenobenzoic acids as an access to PC-SAFT solubility modeling
Fluid Phase Equilibria, 409, 399-407 (2016)
- X. Ji, C. Held
Modeling the density of ionic liquids with ePC-SAFT
Fluid Phase Equilibria 410, 9-22 (2016)
- Y. Ji, K. Lesniak A., A. Prudic, R. Paus, G. Sadowski
Drug Release Kinetics and Mechanism from PLGA Formulations
AIChE Journal, 62, 4055-4065 (2016)
- C. Held, G. Sadowski
Thermodynamics of Bioreactions
Annual Review of Chemical and Biomolecular Engineering, 7, 395-414 (2016)
- C. Kress, G. Sadowski, C. Brandenbusch
Protein partition coefficients can be estimated efficiently by hybrid shortcut calculations
Journal of Biotechnology, 233, 151-159 (2016)
- C. Kress, G. Sadowski, C. Brandenbusch
Novel Displacement Agents for Aqueous 2-Phase Extraction Can Be Estimated Based on Hybrid Shortcut Calculations, J
Journal of Pharmaceutical Sciences, 105, 3030-3038 (2016)
- C. Held, G. Sadowski: Compatible solutes
Thermodynamic properties relevant for effective protection against osmotic stress
Fluid Phase Equilibria, 407, 224-235 (2016)
- L.F. Zubeir, C. Held, G. Sadowski, M.C. Kroon
PC-SAFT Modeling of CO₂ Solubilities in Deep Eutectic Solvents
The Journal of Physical Chemistry B, 120, 2300-2310 (2016)
- S. Mohammad, C. Held, E. Altuntepe, T. Köse, G. Sadowski
Influence of Salts on the Partitioning of 5-Hydroxymethylfurfural in Water/MIBK
The Journal of Physical Chemistry B, 120, 3797-3808 (2016)
- L. Lange, K. Lehmkemper, G. Sadowski
Predicting the Aqueous Solubility of Pharmaceutical Cocrystals As a Function of pH and Temperature
Crystal Growth & Design, 16, 2726-2740 (2016)
- L. Lange, M. Schleinitz, G. Sadowski
Predicting the Effect of pH on Stability and Solubility of Polymorphs, Hydrates, and Cocrystals
Crystal Growth & Design, 16, 4136-4147 (2016)
- N. Gushterov, F. Doghieri, D. Quitmann, E. Niesing, F. Katzenberg, C. Tiller J., G. Sadowski
VOC Sorption in Stretched Cross-Linked Natural Rubber
Industrial & Engineering Chemistry Research, 55, 7191-7200 (2016)
- C. Held, N. Tsurko E., R. Neueder, G. Sadowski, W. Kunz
Cation Effect on the Water Activity of Ternary (S)-Aminobutanedioic Acid Magnesium Salt Solutions at 298.15 and 310.15 K
Journal of Chemical & Engineering Data, 61, 3190-3199 (2016)
- L. Lange, G. Sadowski
Polymorphs, Hydrates, Cocrystals, and Cocrystal Hydrates: Thermodynamic Modeling of Theophylline Systems
Crystal Growth & Design, 16, 4439-4449 (2016)
- F. Meurer, M. Bobrownik, G. Sadowski, C. Held
Standard Gibbs Energy of Metabolic Reactions: I. Hexokinase Reaction
Biochemistry, 55, 5665-5674 (2016)

- M. Herhut, C. Brandenbusch, G. Sadowski
Non-monotonic course of protein solubility in aqueous polymer-salt solutions can be modeled using the sol-mxDLVO model
Biotechnology Journal, 11, 282-9 (2016)
- M. Herhut, C. Brandenbusch, G. Sadowski
Inclusion of mPRISM potential for polymer-induced protein interactions enables modeling of second osmotic virial coefficients in aqueous polymer-salt solutions
Biotechnology Journal, 11, 146-54 (2016)
- H. Ji Y., R. Paus, A. Prudic, C. Lubbert, G. Sadowski
A Novel Approach for Analyzing the Dissolution Mechanism of Solid Dispersions
Pharmaceutical Research, 32, 2559-2578 (2015)
- R. Paus, E. Hart, H. Ji Y., G. Sadowski
Solubility and Caloric Properties of Cinnarizine
Journal of Chemical & Engineering Data, 60, 2256-2261 (2015)
- Y. Ji, R. Paus, A. Prudic, C. Lubbert, G. Sadowski
A Novel Approach for Analyzing the Dissolution Mechanism of Solid Dispersions
Pharmaceutical Research, 32, 2559-78 (2015)

2015

- M. Uyan, G. Sieder, T. Ingram, C. Held
Predicting CO₂ solubility in aqueous N-methyldiethanolamine solutions with ePC-SAFT
Fluid Phase Equilibria, 393, 91-100 (2015)
- I. Rodriguez-Palmeiro, O. Rodriguez, A. Soto, C. Held
Measurement and PC-SAFT modelling of three-phase behaviour
Physical Chemistry Chemical Physics, 17, 1800-1810 (2015)
- R. Paus, A. Prudic, Y. Ji
Influence of excipients on solubility and dissolution of pharmaceuticals
International Journal of Pharmaceutics, 485, 277-287 (2015)
- T. Färber, R. Schulz, O. Riechert, T. Zeiner, A. Górak, G. Sadowski, A. Behr
Different recycling concepts in the homogeneously catalysed synthesis of terpenyl amines
Chemical Engineering and Processing: Process Intensification, 98, 22-31 (2015)
- C.M.S.S. Neves, C. Held, S. Mohammad, M. Schleinitz, L.A.P. Coutinho, M.G. Freire
Effect of salts on the solubility of ionic liquids in water: experimental and electrolyte Perturbed-Chain Statistical Associating Fluid Theory
Physical Chemistry Chemical Physics, 17, 32044-32052 (2015)
- R. Paus, Y. Ji, F. Braak, G. Sadowski
Dissolution of Crystalline Pharmaceuticals: Experimental Investigation and Thermodynamic Modeling
Industrial & Engineering Chemistry Research, 54, 731-742 (2015)
- J. Gorden, T. Zeiner, C. Brandenbusch
Reactive extraction of cis,cis-muconic acid
Fluid Phase Equilibria, 393, 78-84 (2015)
- V.N. Emel'yanenko, D.H. Zaitsau, E. Shoifet, F. Meurer, S.P. Verevkin, C. Schick, C. Held
Benchmark Thermochemistry for Biologically Relevant Adenine and Cytosine. A Combined Experimental and Theoretical Study
The Journal of Physical Chemistry A, 119, 9680-9691 (2015)
- S.P. Verevkin, A.Y. Sazonova, A.K. Frolkova, D.H. Zaitsau, I.V. Prikhodko, C. Held
Separation Performance of BioRenewable Deep Eutectic Solvents
Industrial & Engineering Chemistry Research, 54, 3498-3504 (2015)
- F. Laube, T. Klein, G. Sadowski
Partition Coefficients of Pharmaceuticals as Functions of Temperature and pH
Industrial & Engineering Chemistry Research, 54, 3968-3975 (2015)
- R. Paus, Y. Ji, L. Vahle, G. Sadowski
Predicting the Solubility Advantage of Amorphous Pharmaceuticals: A Novel Thermodynamic Approach
Molecular Pharmaceutics, 12, 2823-2833 (2015)
- T. Reschke, C. Brandenbusch, G. Sadowski
Modeling aqueous two-phase systems: III. Polymers and organic salts as ATPS former
Fluid Phase Equilibria, 387, 178-189 (2015)
- O. Riechert, T. Zeiner, G. Sadowski
Measurement and Modeling of Phase Equilibria in Systems of Acetonitrile, n-Alkanes and beta-Myrcene
Industrial & Engineering Chemistry Research, 54, 1153-1160 (2015)
- O. Riechert, T. Zeiner, G. Sadowski
Phase Equilibria in Systems of Morpholine, Acetonitrile and n-Alkanes
Journal of Chemical & Engineering Data, 60, 2098-2103 (2015)
- J. Collins, M. Grund, C. Brandenbusch, G. Sadowski, A. Schmid, B. Buehler
The dynamic influence of cells on the formation of stable emulsions in organic-aqueous biotransformations
Journal of Industrial Microbiology & Biotechnology, 42, 1011-1026 (2015)
- A. Prudic, A.K. Lesniak, Y. Ji, G. Sadowski
Thermodynamic phase behaviour of indomethacin/PLGA formulations
European Journal of Pharmaceutics and Biopharmaceutics, 93, 88-94 (2015).
- C. Kress, C. Brandenbusch
Osmotic Virial Coefficients as Access to the Protein Partitioning in Aqueous Two-Phase Systems
J Pharm Sci-U.S., 104, 3703-3709 (2015)
- C. Brandenbusch, S. Glonke, J. Collins, R. Hoffrogge, K. Grunwald, B. Buehler, A. Schmid, G. Sadowski
Process boundaries of irreversible scCO₂-assisted phase separation in biphasic whole-cell biocatalysis
Biotechnology and Bioengineering, 112, 2316-2323 (2015)
- G.L. Shen, C. Held, X.H. Lu, X.Y. Ji
Modeling thermodynamic derivative properties of ionic liquids with ePC-SAFT
Fluid Phase Equilibria, 405, 73-82 (2015)
- L. Lange, G. Sadowski
Thermodynamic Modeling for Efficient Cocrystal Formation
Crystal Growth & Design, 15, 4406-4416 (2015)
- O. Riechert, M. Husham, G. Sadowski, T. Zeiner
Solvent effects on esterification equilibria
AIChE Journal, 61, 3000-3011 (2015)

Proceedings

- H.-D. Kühl, J. Pfeiffer, J. Sauer
Operating Characteristics of a Laboratory-Scale, Convertible Stirling-Vuilleumier-Hybrid CHP System Including a Reversed-Rotation Stirling Mode
Proc. 16th International Stirling Engine Conference, 294-304, Bilbao, Spain, Sep 24-26, 2014. ISSN 2409-0387
- J. Pfeiffer, H.-D. Kühl
Analytical Modeling of Appendix Gap Losses in Stirling Cycle Machines
Proc. 16th International Stirling Engine Conference, 451-463, Bilbao, Spain, Sep 24-26, 2014. ISSN 2409-0387
- J. Pfeiffer, H.-D. Kühl
New Analytical Model for Appendix Gap Losses in Stirling Cycle Machines
Proc. 12th International Energy Conversion Engineering Conference, AIAA 2014-3856, Cleveland, OH, Jul 28-30, 2014. <http://dx.doi.org/10.2514/6.2014-3856>
- J. Pfeiffer, H.-D. Kühl
Optimization of the Appendix Gap Design in Stirling Engines
Proc. 13th International Energy Conversion Engineering Conference, AIAA 2015-3902, Orlando, FL, Jul 27-29, 2015. <http://dx.doi.org/10.2514/6.2015-3902>

Impressum

Fakultät Bio- und Chemieingenieurwesen

TU Dortmund

www.bci.tu-dortmund.de

Redaktion: Prof. Joerg C. Tiller

Publication date: September 2018

Printed by: Lensing Druck GmbH & Co. KG